AD_____

Award Number: DAMD17-99-1-9481

TITLE: Protein Kinase Pathways that Regulate Neuronal Survival and Death

PRINCIPAL INVESTIGATOR: Kim A. Heidenreich, Ph.D.

CONTRACTING ORGANIZATION: University of Colorado Health Sciences Center
Denver, Colorado 80291-0238

REPORT DATE: August 2000

TYPE OF REPORT: Annual

PREPARED FOR: U.S. Army Medical Research and Materiel Command
Fort Detrick, Maryland 21702-5012

REPORT DOCUMENTATION PAGE

Form Approved
OMB No. 074-0188

1. AGENCY USE ONLY (Leave blank)	2. REPORT DATE	3. REPORT TYPE AND DATES COVERED
	August 2000	Annual (1 Aug 99 – 31 Jul 00)

4. TITLE AND SUBTITLE
Protein Kinase Pathways that Regulate Neuronal Survival and Death

5. FUNDING NUMBERS
DAMD17-99-1-9481

6. AUTHOR(S)
Kim A. Heidenreich, Ph.D.

7. PERFORMING ORGANIZATION NAME(S) AND ADDRESS(ES)
University of Colorado Health Sciences Center
Denver, Colorado 80291-0238

E-MAIL:
Kim.Heidenreich@UCHSC.edu

8. PERFORMING ORGANIZATION REPORT NUMBER

9. SPONSORING / MONITORING AGENCY NAME(S) AND ADDRESS(ES)
U.S. Army Medical Research and Materiel Command
Fort Detrick, Maryland 21702-5012

10. SPONSORING / MONITORING AGENCY REPORT NUMBER

11. SUPPLEMENTARY NOTES
Report contains color graphics.

12a. DISTRIBUTION / AVAILABILITY STATEMENT
Approved for public release; Distribution unlimited

12b. DISTRIBUTION CODE

13. ABSTRACT ***(Maximum 200 Words)***

Loss of post-mitotic neurons from the adult brain underlies the pathology of neurodegenerative diseases and neurotoxin exposure. Neuronal cell death occurs by two mechanisms; necrosis and apoptosis. Apoptosis is a process whereby developmental cues and environmental stimuli activate a genetic program to implement a series of steps that culminate in cell death. An important aspect of apoptosis is that it can be halted and such interventions may rescue dying neurons. The overall goal of this project is to identify key protein kinases involved in regulating neuronal survival and apoptosis. The aims for the first year of funding, as described in the Statement of Work, were to: 1) Define key protein kinase cascades regulated by neurotrophic factors in neurons, and 2) Modulate the protein kinase cascades regulated by neurotrophic factors and determine the consequence on neuronal survival and death. In the last year, we have identified 3 different protein kinases that regulate neuronal survival and a few of the downstream targets of these kinases. We have also shown that treatment of brain grafts with neurotrophic factors or inhibitors of stress-activated protein kinases increase survival of transplanted dopaminergic neurons in hemi-parkinsonian rats. These studies have resulted in 6 published manuscripts and 4 abstracts presented at national scientific meetings.

14. SUBJECT TERMS
Neurodegeneration, apoptosis, neurons, p38 MAP kinase, JNK, Akt kinase, ERK

15. NUMBER OF PAGES
132

16. PRICE CODE

17. SECURITY CLASSIFICATION OF REPORT	18. SECURITY CLASSIFICATION OF THIS PAGE	19. SECURITY CLASSIFICATION OF ABSTRACT	20. LIMITATION OF ABSTRACT
Unclassified	Unclassified	Unclassified	Unlimited

NSN 7540-01-280-5500

Standard Form 298 (Rev. 2-89)
Prescribed by ANSI Std. Z39-18
298-102

Table of Contents

Introduction

Loss of post-mitotic neurons from the adult brain underlies the pathology of neurodegenerative diseases and neurotoxin exposure. Neuronal cell death occurs by two mechanisms; necrosis and apoptosis. Apoptosis is a process whereby developmental cues and environmental stimuli activate a genetic program to implement a series of steps that culminate in cell death. An important aspect of apoptosis is that it can be halted and such interventions may rescue dying neurons. The overall goal of this project is to identify key protein kinases involved in regulating neuronal survival and apoptosis. The aims for the first year of funding as described in the Statement of Work were to: 1) Define key protein kinase cascades regulated by neurotrophic factors in neurons, and 2) Modulate the protein kinase cascades regulated by neurotrophic factors and determine the consequence on neuronal survival and death. The progress made in these 2 areas, described below, has resulted in 6 published manuscripts and 4 abstracts presented at national scientific meetings (Appendices 1-10).

Task #1. The first task was to identify protein kinase cascades that are regulated by neurotrophic factors known to support the survival of neurons.

a) PI 3kinase/ Akt kinase/ GSK-3 pathway promotes survival of rat cerebellar granule neurons. Previous studies have established a key role for phosphatidylinositol (PI) 3-kinase in regulating trophic factor-dependent survival of neurons (1-2). The Akt protein kinase (also termed protein kinase B and Rac) has been implicated as the transducer of PI 3-kinase dependent survival signals generated by serum and certain growth factors (3-5). In response to PI 3-kinase activation, Akt binds to phosphorylated membrane lipids via its pleckstrin homology domain and is phosphorylated at threonine 308 and serine 473 (6). Phosphorylation of Akt at these two sites leads to its activation and propagation of an anti-apoptotic signal. One of the downstream targets of Akt implicated in cell survival is glycogen synthase kinase-3 (GSK-3). Although GSK-3 was originally identified as a kinase that phosphorylates glycogen synthase, subsequent studies have revealed that GSK-3 has a broader role in the cell (7-10). It phosphorylates a number of substrates not involved in glycogen metabolism including the initiation factor eIF2B (11), the microtubule-associated protein tau (12), and the transcription factors, CREB (13), c-myc (14), c-jun (15), and β -

catenin (16). GSK-3 β has been shown by complementation to be the mammalian homologue of the *shaggy* gene from *Drosophila melanogaster* that regulates cell-fate decisions during axial patterning and neurogenesis (9). GSK-3 β homologues in Dictyostelium (17) and Xenopus (18,19) also appear to regulate cell fate in development. The role of GSK-3 β in mammalian cell development is less clear. Recent studies in our laboratory indicate that IGF-I and agents that elevate cAMP phosphorylate and inhibit GSK-3 β at the same concentrations that these survival factors decrease apoptosis in rat cerebellar granule neurons. Interestingly, inhibition of PI-3 kinase completely blocked the phosphorylation of GSK-3 β induced by IGF-I and the survival effects of IGF-I, but had no effect on cAMP-mediated survival. Likewise, a dominant-negative Akt blocked survival mediated by IGF-I but not by cAMP . These data suggested that cAMP promotes neuronal survival by another mechanism independent of PI-3 kinase/Akt activation. Further studies in our laboratory, recently accepted for publication in Molecular and Cellular Biology (**Appendix 1**), demonstrate that elevation of intracellular cAMP in rat cerebellar granule neurons leads to phosphorylation of GSK-3 β. The increased phosphorylation of GSK-3β by PKA occurs at serine 9, the same site phosphorylated by Akt. Purified PKA is able to phosphorylate recombinant GSK-3 β *in vitro*. Inhibitors of GSK-3 block apoptosis in these neurons and transfection of neurons with a GSK-3 β mutant that cannot be phosphorylated interferes with the pro-survival effects of cAMP. These data indicate that activated PKA can directly phosphorylate GSK-3 β and inhibits its proapoptotic activity in neurons.

b) IGF-I activation of CREB in PC12 cells. In other studies, we collaborated with Dr. Jane Reusch to examine the potential role of CREB in mediating the trophic effects of IGF-I in neuronal cells. Activation of the nuclear transcription factor cAMP response element-binding protein (CREB) has emerged as a central determinant in neuronal functions. We examined whether IGF-I regulated the phosphorylation and transcriptional activation of CREB in rat pheochromocytoma (PC12) cells, a cellular model for neuronal differentiation. We found that CREB phosphorylation at serine 133 and its transcriptional activation as measured by a CREB-specific Gal4-CREB reporter and the neuroendocrine-specific gene chromogranin A was induced 2-3.3-fold by insulin-like growth factor (IGF)-I. This activation was significantly blocked ($p > 0.001$) by the dominant negative K-CREB or by mutation of the CRE site. IGF-I stimulated chromogranin A gene expression by Northern

blot analysis 3.7-fold. Inhibition of MAPK kinase with PD98059, PI 3-kinase with wortmannin, and p38 MAPK with SB203580 blocked IGF-I-mediated phosphorylation and transcriptional activation of CREB by 30-50% ($p < 0.001$). Constitutively active and dominant negative regulators of the Ras and PI 3-kinase pathways confirmed the contribution of these pathways for CREB regulation by IGF-I. Cotransfection of PC12 cells with p38 β MAP kinase and constitutively active MAPK kinase 6 resulted in enhanced basal as well as IGF-I-stimulated chromogranin A promoter. IGF-I activated p38 β, which was blocked by the inhibitor SB203580. This is the first description of a p38 β -mediated nuclear signaling pathway for IGF-I leading to CREB-dependent neuronal specific gene expression. These studies also indicated that p38 β and p38 α have very distinct functions in neurons since p38 α is proapoptotic in PC12 cells. This work was published in the Journal of Biological Chemistry (**Appendix 2**).

c) Akt up-regulates Bcl-2 expression through CREB. To determine potential anti-apoptotic genes that are regulated by IGF-I via CREB in PC12 cells, we examined the role of Akt on Bcl-2 expression in PC12 cells. A series of transient transfections using a luciferase reporter gene driven by the promoter region of Bcl-2 containing a CRE were carried out. Pharmacological inhibition of phosphatidylinositol (PI) 3-kinase, the upstream kinase of Akt, with LY294002 led to a 45% decrease in Bcl-2 promoter activity. The reporter activity was enhanced 2.3-fold by overexpression of active p110 subunit of PI 3-kinase and inhibited 44% by the dominant negative p85 subunit of PI 3-kinase. Cotransfection with 3-phosphoinositide-dependent kinase (PDK1), which is required for the full activation of Akt, resulted in enhanced luciferase activity. Insulin-like growth factor I mediated induction of the bcl-2 promoter activity was decreased significantly by the dominate negative forms of p85 subunit of PI-3 kinase, PDK1, and Akt. These data indicate that the regulation of Bcl-2 expression by IGF-I involves a signaling cascade mediated by PI 3-kinase/PDK1/Akt/CREB. Furthermore, we measured the Bcl-2 mRNA in PC12 cells overexpressing Akt by real-time quantitative reverse transcription PCR using the TaqMan fluorogenic probe system. We observed a 2.1-fold increase in Bcl-2 mRNA levels in the Akt cell line compared with control PC12 cells, supporting the observation that enhanced CREB activity by Akt signaling leads to increased Bcl-2 promoter activity and cell survival. These results were published in the Journal of Biological Chemistry (**Appendix 3**).

d) Growth arrest-specific gene 6 (Gas6)/adhesion related kinase (Ark) signaling promotes gonadotropin-releasing hormone neuronal survival via ERK and Akt. In collaboration with Dr. Maggie Wierman's laboratory, we identified Ark, the mouse homolog of the receptor tyrosine kinase Axl (Ufo, Tyro7), in a screen for novel factors involved in GnRH neuronal migration and survival by using differential-display PCR on cell lines derived at two windows during GnRH neuronal development. Ark is expressed in Gn10 GnRH cells, developed from a tumor in the olfactory area when GnRH neurons are migrating, but not in GT1-7 cells, derived form a tumor in the forebrain when GnRH neurons are postmigratory. Since Ark (Axl) signaling protects from programmed cell death in fibroblasts, we hypothesized that it may play an antiapoptotic role in GnRH neurons. Gn10 (Ark positive) GnRH cells were more resistant to serum withdrawal-induced apoptosis than Gt1-7 (Ark negative) cells, and this effect was augmented with the addition of Gas6, the Ark (Axl) ligand. Gas6/Ark stimulated the extracellular signal-regulated kinase, ERK, and the serine-threonine kinase, Akt, a downstream component of the phosphoinositide 3-kinase (P13-K) pathway. To determine whether ERK or Akt activation is required for the antiapoptotic effects of Gas6/Ark in GnRH neurons, cells were serum starved in the absence or presence of Gas6, with or without inhibitors of ERK and P13-K signaling cascades. Gas6 rescued Gn10 cells from apoptosis, and this effect was blocked by coincubation of the cells with the mitogen-activated protein/ERK kinase (MEK) inhibitor, PD98059, or wortmannin (but not rapamycin). These data support an important role for Gas6/Ark signaling via the ERK and P13-K (via Akt) pathways in the protection of GnRH neurons from programmed cell death across neuronal migration. (Molecular Endocrinology 13:191-201, 1999, **Appendix 4**).

e) The transcription factors MEF2-A and -D regulate survival of rat cerebellar neurons. MEF2 transcription factors have been shown to regulate the development of skeletal, cardiac, and smooth muscle. MEF2 factors are present in the brain, but less in known about their function in nervous tissue. The MEF2 factors, MEF2-A,-B, -C, and-D, bind to DNA as homo- or hetero- dimers to regulate gene expression. In recent and ongoing studies, we have shown that all four MEF2s are present in rat cerebellar granule neurons, and MEF2D was the prominent species. Gel shift mobility assays (EMSA) indicated that MEF2D and MEF2A were the major MEF2s bound to DNA in healthy neurons. When neurons were induced to undergo apoptosis by lowering extracellular potassium to 5mM, MEF2D and MEF2A were

phosphorylated and a decrease in the MEF2/DNA binding complex was observed. Transfection of neurons with a dominant-inactive mutant of MEF2A induced apoptosis, whereas, the dominant-active MEF2 mutant blocked apoptosis. Thus, MEF2D and 2A are critical factors for survival of cerebellar granule neurons. Ongoing studies are directed at identifying the protein kinase that phosphorylates the MEF2s and defining the neuronal genes that are regulated by MEF2s. **(Appendix 5)**.

Task #2 The second task was to determine whether activation or inhibition of the neurotrophin- regulated kinases is necessary or sufficient to influence neuronal survival.

a) Inhibitors of p38 MAP kinase block apoptosis of dopamine neurons *in vitro* **(Appendix 6).**
The survival of dopaminergic neurons in embryonic rat ventral mesencephalic cultures is dependent on the presence of trophic factors contained in serum and withdrawal of serum results in apoptosis. This model system was used in the present studies to examine factors that rescue dopaminergic neurons from apoptotic cell death. In each experiment, primary neurons from ventral mesencephalon were grown in the presence of 5% human placental serum for 24 hours. At that time, medium was replaced with identical medium or medium lacking serum in the presence or absence of increasing concentrations of the p38 MAP kinase inhibitors PD169316, SB203580, and SB202190. Twenty hours after the media change, the cultures were fixed and stained with antibodies against tyrosine hydroxylase (TH) to identify surviving dopamine neurons. In control cultures fed with medium containing serum, there were 856 ± 30 surviving TH^+ neurons/cm^2. Serum withdrawal (20hr) reduced the number of surviving TH^+ neurons/cm^2 to 283 ± 32. All of the pyridinyl imidazole compounds, when added at the time of serum withdrawal, improved the survival of TH^+ neurons at concentrations shown to be effective in blocking p38 MAP kinase activity. The survival effects of SB203580 and SB202190 reached their maximum at 1μM nearly doubling the number of surviving TH^+ neurons. Application of SB203580 and SB202190 resulted in survival of 523 ± 34 and 537 ± 37 TH^+ neurons/cm^2, respectively. The highest dose (10 μM) of the SB compounds did not further improve survival of dopamine neurons and at concentrations higher than 10μM the compounds became toxic. In contrast, 10 μM PD169316 protected all of the TH^+ neurons, supporting the survival of 857 ± 39 TH^+ neurons/cm^2. These experiment revealed that, in respect to neurotrophic support, PD169316 has a unique ability to act as serum replacement.

The morphology of TH^+ neurons grown in the absence and presence of serum was also examined. Twenty hours after the media change, dopamine neurons cultured in medium containing serum, in the absence or presence of PD169316 (10 μM), appeared healthy and contained long neurites and highly ramified growth cones. In contrast, dopamine neurons from which serum was withdrawn were fewer in number, had truncated neurites and lacked growth cones. Supplementation of the serum-withdrawn cultures with 10 μM PD169316 rescued the TH^+ neurons and their morphology was indistinguishable from that of the serum-fed neurons.

To determine if PD169316 exerted its survival effects on dopamine neurons by reducing the rate of apoptosis, we co-stained rat ventral mesencephalic cultures with TH antibodies to identify surviving dopamine neurons and Hoechst 33258 dye to examine nuclear morphology. Apoptotic dopamine neurons were defined as TH^+ cells that contained one or more lobes of condensed nuclear chromatin. In the presence of serum, greater than 90% of TH^+ neurons (FITC-positive) showed normal nuclear morphology with the chromatin (stained blue) uniformly distributed throughout the nucleus. The apoptotic dopamine neurons showed marked nuclear condensation and had degenerating neurites. Maintenance of the cell membrane integrity in the apoptotic dopamine neurons, another characteristic of apoptosis, was evidenced by retention of TH enzyme within the apoptotic bodies. Removal of serum increased the number of adherent apoptotic cells by over 3-fold. PD169316 reduced the rate of apoptosis of dopamine neurons to control levels and SB203580 partially reduced the amount of apoptosis seen after serum withdrawal.

b) Inhibitors of p38 MAP kinase increase the survival of transplanted dopamine neurons. Fetal cell transplantation therapies are being developed for the treatment of a number of neurodegenerative disorders including Parkinson's disease. Massive apoptotic cell death is a major limiting factor for the success of neurotransplantation. Having demonstrated that p38 MAP kinase inhibitor are effective in blocking apoptosis of dopamine neurons *in vitro*, we examined whether they could block apoptosis of dopamine neurons after transplantation. We discovered that inhibitors of p38 MAP kinase (the pyridinyl imidazole compounds: PD169316, SB203580, and SB202190) improve survival of rat dopamine neurons after transplantation into hemiparkinsonian rats. In the hemiparkinsonian rat, preincubation of ventral mesencephalic tissue with PD169316 prior to transplantation accelerated behavioral recovery and doubled the survival of transplanted dopamine neurons (details are provided in **Appendix 6**, a manuscript in press, Brain Research). We conclude that inhibitors of stress-activated protein kinases may improve the outcome of cell transplantation

by preventing apoptosis of neurons after grafting. These inhibitors offer advantages over other approaches to block neuronal apoptosis because they are small organic molecules that are orally active and cross the blood-brain barrier.

c) IGF-I and bFGF improve dopamine neuron survival and behavioral outcome in Parkinsonian rats receiving cultured human fetal tissue strands

In collaboration with Dr. Curt Freed, we investigated the effects of growth factors on survival of human dopamine neurons transplanted into Parkinsonian rats. To promote dopamine cell survival in human fetal tissue strands transplanted into immunosuppressed 6-OHDA lesioned rats, we preincubated tissue in insulin-like growth factor-I (IGF-I, 150 ng/ml) and basic fibroblast growth factor (bFGF, 15 ng/ml) in vitro for two weeks. Growth factor treatment did not affect the rate of homovanillic acid production in vitro but increased overall dopamine neuron survival in animals after transplant from 1240 + 250 to 2380 + 440 neurons ($p<0.05$). Animals in the growth factor-treated group had a significantly greater reduction in methamphetamine-induced rotation (66%) compared to control transplants (30%, $p<0.05$). We conclude that *in vitro* preincubation of human fetal tissue strands with IGF-I and bFGF improves dopamine cell survival and the behavioral outcome of transplants (additional details are provided in **Appendix 7**).

Key Research Accomplishments

Our key research accomplishments lie in 2 areas. One is defining molecular mechanisms that regulate neuronal survival and death. These studies require the use of tissue culture model systems such as primary cultures of rat cerebellar neurons or rat ventral mesencephalic neurons, and cultured differentiated PC12 cells. Using these model systems, we have identified new cellular protein kinase pathways that suppress and activate neuronal apoptosis, and are in the process of identifying the transcription factors and genes regulated by these protein kinase pathways. We predict that targeted delivery of specific protein kinase inhibitors and/or targeted expression of various transcription factors or genes will prove to be effective therapies for preventing neuronal cell death in the future. The other exciting area of accomplishment has been to link our *in vitro* findings with translational research. We have shown that treatment of dopamine neurons with either growth factors or inhibitors of p38 MAP kinase increases the survival of transplanted dopamine neurons. The advantages that the p38 MAP kinase inhibitors

(pyridinyl compounds) have over growth factors and caspase inhibitors for preventing apoptosis include their small size, organic nature, and ability to cross the blood-brain barrier. These characteristics make the pyridinyl imidazole compounds promising candidate drugs for improving survival of dopamine neurons following transplantation into Parkinson's patients.

Reportable Outcomes

Manuscripts

Pugazhenthi S, T Boras, MK Meintzer, **KA Heidenreich**, JE-B Reusch: Insulin-like growth factor I-mediated phosphorylation and activation of CREB in PC12 cells. Multiple signaling pathways are involved. J Biol Chem 274: 2829-2837, 1999.

Allen MP, C Zeng, K Schneider, MK Meintzer, C Basilico, B Varnum, **KA Heidenreich**, ME Wierman. Growth arrest specific gene (Gas 6)/adhesion related kinase (ARK) signaling promotes gonadotropin releasing hormone (GnRH) neuronal survival via ERK and Akt. Mol. Endocrinology 13: 191-201, 1999.

Pugazhenthi S, E Miller, C Sable, P Young, **KA Heidenreich**, LM Boxer, J E-B Reusch. Insulin-like growth factor-I induces bcl-2 promoter through the transcription factor cAMP response element binding protein. J. Biol. Chem. 274: 27529-27535, 1999.

Zawada WM, MK Meintzer, C Sable, CR Freed, and **KA Heidenreich**. Inhibitors of p38 MAP kinase improve survival of dopamine neurons both in culture and after neurotransplantation in parkinsonian rats. (in press, Brain Res.)

Pugazhenthi S, A Nesterova, C Sable, **KA Heidenreich**, LM Boxer, LE Heasley, J E-B Reusch. Akt/ Protein kinase B mediated cell survival involves transcriptional upregulation of bcl-2 (J. Biol. Chem. 275: 10761-10766, 2000.

Li MT, X Wang, MK Meintzer, and **KA Heidenreich**. CAMP protects neurons from apoptosis by inhibiting GSK-3B activity in rat cerebellar granule neurons (in press, Mol. Cell Biol.).

Clarkson, ED, WM Zawada, KP Bell, JE Esplen, PK Choi, **KA Heidenreich**, and CR Freed. IGF-I and bFGF improve dopamine neuron survival and behavioral outcome in parkinsonian rats receiving cultured human feat tissue strands. (in press, Exp. Neurology).

Abstracts

Sable CL, MK Meintzer, **KA Heidenreich**: Regulation of apoptosis in rat cerebellar granule neurons. The Endocrine Society 1999.

Pugazhenthi S, E Miller, C Sable, **KA Heidenreich**, L Boxer, J E-B Reusch: Induction of the Bcl-2 promoter by p38 β MAPK-mediated signaling pathway. The Endocrine Society 1999.

Zawada WM, MK Meintzer, C Sable, CR Freed, and **KA Heidenreich**. Pyridinyl imidazole compounds rescue dopaminergic neurons from apoptotic cell death. Soc. Neuroscience 1999.

Wierman ME, MP Allen, Z Fang, M Xu, C Zeng, **KA Heidenreich**, and S Tobet. Factors Regulating GnRH neurons. Invited speaker symposium, The Endocrine Society 2000

Zawada, WM, MK Meintzer, P Rao, J Marotti, X Wang, JE Esplen, ED Clark, CR Freed, and **KA Heidenreich**. Inhibitors of p38 MAP kinase increase survival of transplanted dopamine neurons. Soc. Neuroscience 2000.

Li, M, MP Allen, T Laessig, X Wang, ME Wierman, and **KA Heidenreich**. Myocyte enhancer factor-2 (MEF2) –A and –D regulate survival of rat cerebellar granule neurons. Soc. Neuroscience 2000.

Invited talks

1999	Neuroscience Program, UCHSC, Denver, CO
1999	Plenary talk, American Federation for Medical Research, Carmel, CA
2000	Neuroscience Program, UCHSC, Denver, CO
2000	Division of Endocrinology, UCHSC, Denver, CO
2000	Program of Molecular and Cellular Pathology, University of Alabama, GA
2000	Joslin Diabetes Center and Harvard Medical School, Signaling mechanisms that regulate neuronal survival, Boston, MA
2000	Michael J. Fox Foundation for Parkinson's Research, Public Policy Forum, Washington, D.C.
2000	Danish Society for Neuroscience and Danish Society for Biochemistry and Molecular Biology, Symposium on Molecular Mechanisms in Neuronal Degeneration, Copenhagen, Denmark

Conclusions

The scope of research over the last year has been to carry out Task#1 and Task#2 of our research proposal. Towards this goal, we have identified a number protein kinase cascades and some of the effectors that regulate neuronal survival. In cultured rat cerebellar granule neurons, a good model for studying apoptosis in primary differentiated neurons, we have studied various aspects of 3 different pathways that regulate neuronal survival, a neurotrophic factor –regulated protein kinase pathway involving PI-3 kinase and Akt, a PKA pathway regulating GSK-3 β activity, and a Ca++ sensitive pathway regulating the activity of a family of transcription factors that signal survival. The major contribution of these studies is the discovery of a unique PKA pathway that inhibits apoptosis by a mechanism that does not require the Akt protein kinase. Another

important finding from these studies is the demonstration that multiple anti-apoptotic kinase pathways converge at the level of GSK-3 β to inhibit its activity. Identifying the proapoptotic effectors of GSK-3β is an important study for the future. Also, the discovery that the MEF2 transcription fators regulate neuronal survival is important for identifying genes that promote neuronal survival. Experiments are planned to continue studying the regulation of MEF2s in neurons and identify the genes that are transcriptionally modified by this family of transcription factors. In differentiated PC12 cells , another common model system for studying neuronal apoptosis, we've discovered in collaboration with Dr. Jane Reusch that IGF-I regulates CREB phosphorylation and transcriptional activity which, in turn, regulates the levels of Bcl-2 in PC12 cells. Thus, at least part of the antiapoptotic effects of IGF-I is mediated by upregulation of the antiapoptotic protein Bcl-2. Bcl-2 plays a role in inhibiting caspase activation and subsequent proteolysis of vital cellular substrates. We would like to repeat these experiments in primary rat cerebellar granule neurons to establish the generality of this mechanism. Finally, as indicated in the Key Accomplishments, we have been able to translate some of findings from our *in vitro* studies to more clinically relavent research. We have shown that treatment of dopamine neurons with either growth factors or inhibitors of p38 MAP kinase increases the survival of transplanted dopamine neurons. Although other laboratories have shown that inhibitors of apoptosis (i.e. peptide caspase inhibitors) improve transplantation, the practicality of using peptide inhibitors clinically is hampered by their poor entry into brain. The advantages that the p38 MAP kinase inhibitors (pyridinyl compounds) have over growth factors and caspase inhibitors for preventing apoptosis include their small size, organic nature, and ability to cross the blood-brain barrier. These characteristics make the pyridinyl imidazole compounds promising candidate drugs for improving survival of dopamine neurons following transplantation into Parkinson's patients.

References

1. **Dudek, H., Datta, S. R., Franke, T. F., Birnbaum, M. J., Yao, R., Cooper, G. M., Segal, R. A., Kaplan, D. R., and M. E. Greenberg.** 1997. Regulation of neuronal survival by the serine-threonine protein kinase Akt. Science **275:**661-665.
2. **Fruman, D. A., Meyers, R. E., and C. C. Cantley.** 1998. Phosphoinositide kinases. Annual Rev. Biochem. **67:**481-507.

3. **Franke, T. F., Yang, S., Chan, T. O., Datta, K., Kazlauskas, A., Morrison, D. K., Kaplan, D. R., and P. N. Tsichlis.** 1995. The protein kinase encoded by the Akt proto-oncogene is a target of the PDGF-activated phosphatidylinositol 3-kinase. Cell **81:**727-736.
4. **Burgering, B. M. T., and P. J. Coffer.** 1995. Protein kinase B (cAkt) in phosphatidylinositol-3-OH kinase signal transduction. Nature **376:**599-602.
5. **Jones, P. F., Jakubowicz, T., Pitossi, F. J., Maurer, F., and B. A. Hemmings.** 1991. Molecular cloning and identification of a serine threonine protein kinase of the second-messenger subfamily. Proc. Natl. Acad. Sci. USA. **88:**4171-4175.
6. **Downward, J.** 1998. Mechanisms and consequences of activation of protein kinase B/Akt. Curr. Opin. Cell. Biol. **10:**262-267.
7. **Woodgett, J. R.** 1991. A common denominator linking glycogen metabolism, nuclear oncogenes and development. TIBS. **16:**177-181.
8. **Woodgett, J.R., Plyte, S.E., Pulverer, B.J., Mitchell, J.A., and K. Hughes.** 1993. Roles of glycogen synthase kinase-3 in signal transduction. Biochem Soc Trans. **21**:905-7
9. **Welsh, G. I., Wilson, C., and C. G. Proud.** 1996. GSK3: a SHAGGY frog story. Trends in Cell Biol. **6:** 274-279.
10. **Cross, D. A. E., Alessi, D. R., Cohen, P., Andjelkovich, M., and B. A. Hemmings.** 1995. Inhibition of glycogen synthase kinase-3 by insulin mediated by protein kinase B. Nature **378:**785-789.
11. **Welsh, G. I., and C. G. Proud.** 1993. Glycogen synthase kinase-3 is rapidly inactivated in response to insulin and phosphorylates eukaryotic initiation factor elF-2B. Biochem. J **294:**625-629.
12. **Hong, M., and V. M.-Y. Lee.** 1997. Insulin and insulin-like growth factor-1 regulate tau phosphorylation in cultured human neurons. J. Biol. Chem. **272:**19547-19553.
13. **Foil, C. J., Williams, J. S., Chou, C.-H., Wang, Q. M., Roach, P. J., and O. M. Andrisani.** 1994. A secondary phosphorylation of $CREB^{341}$ at Ser^{129} is required for the cAMP-mediated control of gene expression. J. Biol. Chem. **269:**32187-32193.
14. **Plyte, S. E., Hughes, K., Nikolakaki, E., Pulverer, B. J., and J. R. Woodgett.** 1992. Glycogen synthase kinase-3: functions in oncogenesis and development. Biochim. Biophys. Acta **1114:**147-162.

15. **Boyle, W. J., Smeal, T., Defize, L. H., Angel, P., Woodgett, J. R., Karin, M., and T. Hunter.** 1991. Activation of protein kinase C decreases phosphorylation of c-Jun at sites that negatively regulate its DNA-binding activity. Cell **64:**573-584.

16. **Seeling, J. M., Miller, J. R., Gil, R., Moon, R. T., White, R., and D. M. Virshup.** 1999. Regulation of beta-catenin signaling by the B56 subunit of protein phosphatase 2A. Science **283:**2089-2091.

17. **Harwood, A. J., Plyte, S. E., Woodgett, J., Strutt, H., and R. R. Kay.** 1995. Glycogen synthase kinase 3 regulates cell fate in dictyostelium. Cell **80:**139-148.

18. **Dominguez, I., Itoh, K., and S. Y. Sokol.** 1995. Role of glycogen synthase kinase 3 B as a negative regulator of dorsoventral axis formation in Xenopus embryos. Proc. Natl. Acad . Sci. USA **92:**8498-8502.

19. **Itoh, K., Tang, T. L., Neel, B. G., and S. Y. Sokol.** 1995. Specific modulation of ectodermal cell fates in Xenopus embryos by glycogen synthase kinase. Development **121:**3979

Appendices: 6 MANUSCRIPTS attached

4 ABSTRACTS attached

Appendix 1

Revised
M.C.B.
Molecular and
Cellular Biology
July 2000
In press

Cyclic AMP promotes neuronal survival by phosphorylation of glycogen synthase kinase-3 β

Mingtao Li, Xiaomin Wang, Mary Kay Meintzer, Tracey Laessig, Morris J. Birnbaum [ϵ], and Kim A. Heidenreich*

Department of Pharmacology, University of Colorado Health Sciences Center, and the Denver Veterans Affairs Medical Center, Denver, CO 80262 and the Howard Hughes Medical Institute, University of Pennsylvania, Philadelphia, PA[ϵ]

*Corresponding Author. Mailing address: Denver VAMC, 1055 Clermont Street, Denver, CO, 80220, Phone: 303-399-8020 (3891), Fax: 303-393-5271, E-mail: kim.heidenreich@uchsc.edu

ABSTRACT

Agents that elevate intracellular cyclic AMP (cAMP) promote neuronal survival in a manner independent of neurotrophic factors. Inhibitors of phosphatidylinositol (PI) 3-kinase and dominant-inactive mutants of the protein kinase Akt do not block the survival effects of cAMP suggesting that another signaling pathway is involved. In this report, we demonstrate that elevation of intracellular cAMP in rat cerebellar granule neurons leads to phosphorylation and inhibition of GSK-3β. The increased phosphorylation of GSK-3β by PKA occurs at serine 9, the same site phosphorylated by Akt. Purified PKA is able to phosphorylate recombinant GSK-3β *in vitro*. Inhibitors of GSK-3 block apoptosis in these neurons and transfection of neurons with a GSK-3 β mutant that cannot be phosphorylated interferes with the pro-survival effects of cAMP. These data suggest that activated PKA directly phosphorylates GSK-3 β and inhibits its apoptotic activity in neurons.

INTRODUCTION

Neurons require continuous exposure to extracellular trophic factors for survival and those that fail to receive sufficient trophic factor support undergo apoptotic cell death (1). Among the extracellular factors shown to influence neuronal survival are the neurotrophins which include nerve growth factor, brain-derived neurotrophic factor, neurotrophin 3, and neurotrophin 4, the fibroblast growth factors, ciliary growth factor, insulin, and insulin-like growth factors (2,3). Agents that elevate intracellular cyclic AMP (cAMP) also promote neuronal survival in a manner independent of neurotrophic factors (4,5). Substantial progress has been made over the last several years in delineating signal transduction pathways that mediate trophic factor-induced cell survival. Less is known about the survival pathways activated by cAMP in neurons.

Recent reports have established a key role for phosphatidylinositol (PI) 3-kinase in regulating trophic factor-dependent survival of neurons (6-7). The Akt protein kinase (also termed protein kinase B and Rac) has been implicated as the transducer of PI 3-kinase dependent survival signals generated by serum and certain growth factors (8-10). In response to PI 3-kinase activation, Akt binds to phosphorylated membrane lipids via its pleckstrin homology domain and is phosphorylated at threonine 308 and serine 473 (11). Phosphorylation of Akt at these two sites leads to its activation and propagation of an anti-apoptotic signal. Several downstream targets of Akt implicated in cell survival include the Bcl-2 family member BAD (12), caspase 9 (13), and FKHRL1, a member of the Forkhead family of transcription factors (14). Another Akt substrate recently implicated in cell fate decisions is glycogen synthase kinase-3 (GSK-3). Mammalian GSK-3 exists as two isoforms termed α (51 kDa) and β (47 kDa), each encoded by a distinct gene (15-17). The GSK-3 isoforms share 85% homology at the amino acid level and are ubiquitously expressed (15-17). Although GSK-3 was originally identified as a kinase that phosphorylates glycogen synthase, subsequent studies have revealed that GSK-3 has a broader role in the cell (15-18). It phosphorylates a number of substrates not involved in glycogen metabolism including the initiation factor eIF2B (19), the microtubule-associated protein tau (20), and the transcription factors CREB (21), c-myc (22), c-jun (23), and β -catenin (24). Recently, GSK-3 β was shown by complementation to be the mammalian homologue of the *shaggy* gene from *Drosophila melanogaster* that regulates cell-fate decisions during axial

patterning and neurogenesis (17). GSK-3 β homologues in Dictyostelium (25) and Xenopus (26,27) also appear to regulate cell fate in development. The role of GSK-3 β in mammalian cell development is less clear, although recent evidence suggests that it may be a downstream target of the PI3-kinase/Akt anti-apoptotic signaling pathway. Overexpression of a dominant-negative mutant of GSK-3 β prevents apoptosis following inhibition of PI-3 kinase, whereas, catalytically active GSK-3 β induces apoptosis of both rat-1 and PC12 cells (28).

One possible mechanism by which cAMP could promote survival is by activating the PI-3 kinase/Akt pathway. Indeed, agents that elevate intracellular cAMP stimulate the activity of Akt when the enzyme is overexpressed in 292 cells (29,30). The activation of Akt by cAMP is independent of PI-3 kinase activity, does not require the PH domain of Akt, and is dependent on T308 phosphorylation but not S473 phosphorylation. In cerebellar granule neurons, inhibition of PI-3 kinase completely blocked the survival effects of IGF-I but had no effect on cAMP-mediated survival (31). Likewise, in sympathetic ganglion neurons, expression of either a dominant-negative PI-3 kinase or a dominant-negative Akt blocked survival mediated by depolarization but not by cAMP (32). The inability of PI-3 kinase inhibitors or dominant-negative Akt mutants to block the pro-survival effects of cAMP in both neuronal types suggests that cAMP promotes neuronal survival by another mechanism independent of PI-3 kinase/Akt activation. In this report, we show that elevation of intracellular cAMP in rat cerebellar granule neurons leads to phosphorylation and inhibition of GSK-3β independent of Akt activation. The increased phosphorylation of GSK-3β by PKA occurs at serine 9, the same site phosphorylated by Akt. Inhibitors of GSK-3 block apoptosis in these cells and transfection of neurons with a GSK-3 mutant that cannot be phosphorylated interferes with the pro-survival effects of cAMP.

MATERIALS AND METHODS

Antibodies. The monoclonal anti-GSK-3 β antibody was from Transduction Laboratories (Lexington, KY). The polyclonal phosphorus-specific GSK-3β (Ser9) antibody was obtained from Calbiochem (La Jolla, CA). The polyclonal phosphorus-specific antibodies for Akt (Ser 473 and Thr 308), p90 RSK(Ser381), GSK-3α/β (Ser21/9), GSK-3 β (ser9)and MAPK (Thr202/Tyr204), the polyclonal phospho-independent Akt antibody, the immobilized Akt

antibody, and ERK antibodies were from New England BioLabs (Beverly, MA). The polyclonal anti-β-galactosidase (β-gal) antibody was purchased from 5'-3' Prime Inc.(Boulder, CO). Cy3-conjugated goat antibody to rabbit IgG and fluoroscein-conjugated goat antibody to mouse IgG were purchased from Chemicon International, Inc. (Temecula, CA). The monoclonal antibody (clone 12CA5) against the HA epitope was obtained from Boehringer Mannheim (Indianopolis, IN).

Materials. The PKA inhibitor H-89 dihydrochloride, the cell-permeable, myristoylated PKI inhibitor, the cAMP-elevating agents forskolin and chlorophenylthiol (CPT)-cAMP, the PKC inhibitor bisindolylmaleimide, the PI-3 kinase inhibitor wortmannin, and the MEK inhibitor PD98059 were from Calbiochem (La Jolla, CA). The recombinant GSK-3α and GSK-3β proteins were from New England BioLabs. The PKA catalytic subunit purified from bovine heart was from Promega. Valproic acid and lithium chloride were purchased from Sigma (St. Louis, MO). Plasmid purification kits were from Qiagen (Valencia, CA) and calcium-phosphate transfection kits were from Promega (Madison, WI). The Akt kinase assay kit was from New England Biolabs (Beverly, MA). [γ-32P]-ATP (3000 Ci/mmol) was purchased from Amersham Pharmacia Biotechnology and L-pyruvate kinase was purchased from Sigma. The phosphoglycogen synthase peptide-2 was obtained from Upstate Biotechnology.

Neuronal culture and induction of apoptosis. Rat cerebellar granule neurons were prepared from 7-8-day-old Sprague-Dawley rat pups (15-19g) as described previously (33). Briefly, neurons were dissociated from freshly dissected cerebella by mechanical disruption in the presence of trypsin and DNase and were then plated on poly-L-lysine-coated Nunc culture plates (Fisher, Pittsburgh, PA). Cells were seeded at a density of 2.0×10^6 cells/ml in basal modified Eagle (BME) medium containing 10% fetal bovine serum, 25 mM KCl, 2 mM glutamine, and penicillin (10 units/ml) -streptomycin (10 μg/ml). Cytosine arabinoside (10 μM) was added to the culture medium 24 hr after plating to limit the growth of non-neuronal cells. Using this protocol, 95-99 % of the cultured cells were granule neurons. After 7 or 8 days in culture, apoptosis was induced by removing serum and reducing the extracellular potassium concentration from 25mM to 5 mM. Neurons were rinsed two times in serum-free BME containing 5 mM KCl and then maintained in the same medium in the presence or presence of

various drugs. Control cultures were treated identically, but were maintained in serum-free medium supplemented with 25 mM KCl. When inhibitors were used for signaling assays, cells were treated with the inhibitor 30 min before addition of the stimulus. Cells that did not receive drugs received control vehicle (dimethyl sulfoxide for forskolin, H-89 dihydrochloride, wortmannin, and PD98059; water for CPT-cAMP, valproic acid and lithium chloride). The final concentration of dimethyl sulfoxide was less than 0.1%.

Immunoblotting assay. Cerebellar granule neurons were cultured on poly-L-lysine-coated 35 mm plates for 7 or 8 days. After stimulation with drugs (the times are indicated in the text), neurons were lysed by adding SDS sample buffer (62.5 mM Tris-HCl [pH6.8], 2% [wt/vol] SDS, 10 % glycerol, 50 mM DTT, 0.1 % [wt/vol] bromphenol blue) and immediately scraped off the plate. Samples were resolved by SDS-10% PAGE and transferred to Hybond-P membranes (polyvinylidene difluoride, Amersham, Arlington Heights, IL). Membranes were incubated for an hour in a blocking buffer containing 5% (wt/vol) non-fat dry milk in TBST (10 mM Tris-HCl, 140 mM NaCl [pH7.4], 0.1% Tween 20) and then incubated overnight at 4 °C with appropriate primary antibody diluted (1:1000) in the TBST containing 5% BSA. The membranes were washed 15 min in TBST and then incubated at room temperature for 60 min with horseradish peroxidase (HRP)-conjugated anti-rabbit or anti-mouse antibody diluted 1:2000 in TBST containing 5% non-fat dry milk. After washing extensively for 30 min in TBST, membranes were processed for 1 min using the ECL chemiluminescent substrate kit (Amersham, Arlington Heights, IL) and exposed to autoradiographic film (Kodak, Rochester, NY). Quantitation was performed using the Biorad Quantity One software.

Calcium phosphate transfection of neurons.

Cerebellar granule neurons were transfected using a calcium phosphate co-precipitation method (34). All plasmids were prepared and purified with Qiagen Plasmid Maxi Kit (Cat # 12163) according to the manufacture's instructions. Briefly, neurons were cultured for 5-6 day in 24-well plates or 35 mm dishes. The DNA-calcium-phosphate precipitate was prepared by mixing one volume of DNA in 250 mM $CaCl_2$ with an equal volume of 2 × HBS (50mM Hepes, 280 mM NaCl, 1.5 mM Na_2HPO_4, pH 7.1). Plasmids pcDNA3, pCMV5, pAkt (K179M), pcDNA3 GSK-3 β (wt), pcDNA3 GSK-3 β (S9A) or pcDNA GSK-3β (KI) contained in the precipitate

were at a final concentration of 40 μg /ml together with 8 μg /ml of an expression vector encoding β-galactosidase (pCMV lacZ) to allow detection of the transfected cells. The calcium phosphate-DNA precipitate was incubated at room temperature for 30 min before addition to the cultures. The conditioned culture media was removed and saved. The cultures were washed two times with BME, and then 1.5 ml of transfection media (BME, no addition of glutamine and antibiotics, 37°C, pH 7.4) was added to cultures, immediately followed by the addition of the calcium phosphate-DNA precipitate. Plasmids were added to the transfection media at a final concentration of 4-5 μg/ml. Plates were incubated (37°C, 5 % CO_2) for 30 min and then the transfection media was aspirated. After washing twice with fresh transfection media, the saved conditioned media was added back to the cultures. Transfection efficiency was assessed by determining the percentage of cells expressing β-galactosidase by X-gal staining or immunostaining (24-48 h later). Glycerol or DMSO shock did not increase transfection efficiency but did result in cell damage. Experimental treatments were initiated 24h after transfection.

Immunostaining. Neurons were stained 2 days after transfection to identify cells expressing the proteins encoded by the transgenes. Cultures were fixed in 4% paraformaldehyde in PBS for 20 min at room temperature and permeabilized with 0.1 % Triton X-100. The fixed cells were incubated at room temperature for 15 min in 5 % goat serum in TBST (10 mM Tris-HCl, 140 mM NaCl [pH7.4], 0.1% Triton X-100) to block nonspecific interactions of the antibodies and then incubated with the appropriate primary antibody diluted in 3% BSA in TBS overnight at 4° C. After washing 3 times with TBST for 15 min, the cells were incubated at room temperature for 60 min with Cy3- or fluoroscein-conjugated secondary antibodies in TBS containing 3% BSA. Expression of β-galactosidase was detected by immunostaining with a polyclonal antibody to β-galactosidase (1:500 dilution) followed by a Cy3-conjugated goat antibody to rabbit IgG (1:500). Neurons transfected with the HA-epitope-tagged GSK-3β were immunostained with monoclonal antibody to HA (1: 500) followed by a fluorescein-conjugated goat antibody to mouse IgG (1:500). Stained cells were visualized by digital deconvolution fluorescence microscopy to confirm that β-galactosidase was co-expressed with GSK-3β (wt), GSK-3β (S9A), GSK-3β (KI). To visualize the nuclei of transfected neurons, we included the DNA dye Hoechst 33258 (5.0 μg /ml) in the wash after the secondary antibody incubation.

In vitro phosphorylation of GSK-3 by PKA. The phosphorylation reaction was performed in 50 µl of kinase buffer (50 mM Tris [pH 7.2], 10 mM $MgCl_2$, 1mM dithiothreitol) containing 4 units of PKA catalytic subunit(bovine heart, Promega), 0.3 µg GSK-3β protein, and 100 µM ATP. Reactions were carried out in the absence and presence of the PKA inhibitor H-89 (5 µM) or PKI (2.5 µM). The phosphorylation reaction was allowed to proceed for 30 min at 30 °C and stopped by adding 3 × SDS sample buffer. The phosphorylation of GSK-3β was measured by Western blotting using GSK-3β (Ser9) antibody. In experiments where the Km and Vmax were determined, 50 µM [γ-^{32}P]ATP (5 µCi/nmol) was added to the kinase reaction. At the end of the phosphorylation reactions, these samples were solubilized in Laemmli's sample buffer and analyzed by SDS-polyacrylamide gel electrophoresis. Gels were dried and subjected to autoradiography. The incorporation of phosphate into GSK-3β and l-pyruvate kinase (a known substrate of GSK-3) was determined by Cerenkov counting of excised SDS-polyacrylamide gel slices.

Assay of GSK-3β

After stimulation with the reagents indicated, neurons were washed with cold phosphate-buffered saline and neuronal extracts were prepared in cell lysis buffer (20 mM Tris-HCl [pH7.4], 150 mM NaCl, 1 mM EDTA, 1 mM EGTA, 1% Triton X-100, 2.5 mM sodium pyrophosphate, 5 mM β-glycerolphosphate, 1 mM Na_3VO_4, 1 µg/ml leupeptin, 1 mM phenylmethylsulfonyl fluoride, 1 µM microcystin) for 15 min at 4 °C. After sonicating briefly, the lysates were clarified by centrifugation at 15,000 × *g* for 10 min at 4 °C and GSK-3β from 200 µg of cell extract was immunoprecipitated with 1.0 µg of GSK-3β antibody for 2 h at 4 °C with rotation. Protein G Plus/ protein A Agarose (20 µl of a 50% suspension) was then added, and the incubation was continued for 1 h at 4 °C with rotation. Immune complexes were recovered by centrifugation at 4 °C and washed three times with extraction buffer and twice with kinase buffer. Kinase activity of the immunoprecipitated GSK-3 was assayed in a total volume of 40 µl containing 25 mM sodium glycerophosphate, 20 mM Tris-HCl, pH 7.4, 10 mM $MgCl_2$, 5 mM dithiothreitol, 20 µM phosphoglycogen synthase peptide-2, and 50 µM [γ-^{32}P]ATP (1 µCi). After 10 min of incubation at 30 °C, reaction mixtures were centrifuged for 1 min, and 20 µl of the

supernatant was spotted onto Whatman P81 phosphocellulose paper. Filters were washed in four changes of 175 mM phosphoric acid for a total of 20 min, rinsed in acetone, dried, and the radioactivity was determined by Cerenkov counting. Background values obtained from reactions lacking cell lysate were subtracted from all values.

In vitro Akt kinase assay. After stimulation with the reagents indicated, neuronal extracts were prepared by solubilizing the neurons in cell lysis buffer (20 mM Tris-HCl [pH7.4], 150 mM NaCl, 1 mM EDTA, 1 mM EGTA, 1% Triton X-100, 2.5 mM sodium pyrophosphate, 5 mM β-glycerolphosphate, 1 mM Na_3VO_4, 1 μg/ml leupeptin, 1 mM phenylmethylsulfonyl fluoride, 1 μM microcystin) for 15 min at 4 °C. After sonicating briefly, the lysates were clarified by centrifugation at 15,000 × *g* for 10 min at 4 °C and Akt from 200 μl cell extract was immunoprecipitated with 20 μl of immobilized Akt antibody crosslinked to agarose hydrazide beads. After washing the beads three times with cell lysis buffer and three times with kinase buffer (25 mM Tris-HCl, 10 mM $MgCl_2$, 1 mM dithiothreitol, pH 7.4), kinase activity was assayed with GSK-3α fusion protein as a substrate (1μg) in kinase buffer containing 100 μM ATP and 2.5 μM PKI. The phosphorylation reaction was allowed to proceed for 30 min at 30 °C and stopped by adding 3 × SDS sample buffer. Phosphorylation of GSK-3α was measured by Western blotting using phospho-GSK-3α/β(Ser21/9) antibody.

Quantitation of Apoptosis by Nuclear Morphological Changes. Cerebellar granule neurons were cultured in 35-mm culture dishes and 24-wells plates as described above. After removal of the medium, the neurons were rinsed once with cold PBS, pH7.2, fixed for 10 min with 4% paraformaldehyde in PBS at 4 °C, washed with distilled water, and dried at room temperature. Cells were stained with Hoechst 33258 (5 μg/ml) for 5 min, washed, and dried. Apoptosis was quantified by scoring the percentage of cells in the adherent cell population with condensed or fragmented nuclei. To obtain unbiased counting, cells were scored blind without knowledge of their prior treatment.

RESULTS

Forskolin and cpt-cAMP stimulate GSK-3 β phosphorylation.

Cultures of newborn rat cerebellar granule neurons, the interneurons of the cerebellum, provide a good model for investigating signaling pathways that regulate neuronal apoptosis because of the high degree of cellular homogeneity. These neurons survive and differentiate *in vitro* in the presence of serum and depolarizing concentrations of KCl (25 mM). If the medium is changed to serum-free medium containing 5 mM KCl, the neurons undergo apoptotic cell death. Previous studies have shown that apoptosis of cerebellar granule neurons is inhibited by a variety of molecules which raise cAMP (31, 36-38). To investigate the potential role of GSK-3β in mediating the protective effects of cAMP, we examined whether agents that elevate cAMP regulate the phosphorylation state of GSK-3β. After 7 days in culture, rat cerebellar granule neurons were incubated in serum-free medium containing 5 mM KCl for 4 hr and then incubated with forskolin (10 μM), an activator of adenylate cyclase, to elevate intracellular cAMP. The neurons were then solubilized and the phosphorylation state of GSK-3 β was measured by Western blotting using phospho-specific GSK-3 β (Ser9) antibodies. Forskolin rapidly increased the phosphorylation of GSK-3 β (47 kDa) on serine 9 (Fig. 1A). The extent of GSK-3 β phosphorylation by forskolin was similar to that obtained with a maximal concentration of IGF-I (50 ng/ml). The phosphorylation of GSK-3 β by forskolin was completely blocked when neurons were preincubated for 30 min with the cell-permeable myristoylated PKI inhibitor (25 μM) and with H89 (10 μM), a selective inhibitor of PKA (Fig. 1B and 1C). Preincubation of neurons with PD98059, a MEK kinase inhibitor that blocks the ERK pathway, had no significant effect on the phosphorylation of GSK-3 β by forskolin. The ability of forskolin to stimulate phosphorylation of GSK-3 β was mimicked by incubating the neurons with a cell permeable cAMP analog (cpt-cAMP) (Fig.1C). As seen with forskolin, the phosphorylation of GSK-3 β by cpt-cAMP was blocked by the PKI inhibitor and H89 but not by PD98059 (Fig. 1C).

Phosphorylation of GSK-3 β at serine 9 is known to inhibit enzyme activity. To confirm this, *in vitro* kinase assays were carried out following immunoprecipitation of GSK-3β using phosphoglgogen synthase peptide 2 as the substrate (Fig. 1D). Treatment of neurons with

forskolin lead to about a 50 % decrease in GSK-3β activity, similar to the decrease in activity observed with IGF-I. The cell-permeable PKI inhibitor and H89 blocked the forskolin-induced decrease in GSK-3 β activity.

The phosphorylation of GSK-3 β by forskolin is not mediated by the ERK pathway.

The inability of the MEK inhibitor PD98059 to block phosphorylation of GSK-3 β by forskolin suggested that the ERK pathway was not involved in the phosphorylation event. However, cAMP has been previously shown to activate the ERK pathway (39) and recent data has indicated that RSK can directly phosphorylate GSK-3 β (40). To examine the potential relationship between activation of the ERK pathway and phosphorylation of GSK-3 β by forskolin, we first determined whether forskolin activates the ERK pathway in RCG neurons. Incubation of neurons with forskolin (10 μM) for 30 min lead to increased phosphorylation of ERK on threonine 202 and tyrosine 204 (Fig, 2, top panel) and RSK on serine 381 (Fig. 2, middle panel). The phosphorylation of ERK and RSK by forskolin was completely inhibited by the MEK inhibitor PD98059 (Fig. 2A, top and middle panels). However, although PD98059 completely blocked the activation of ERK and RSK by forskolin it had no effect on the phosphorylation of GSK-3β by forskolin (Fig. 2, bottom panel). As expected, H89 inhibited the phosphorylation of ERK and GSK-3β by forskolin. Thus, although the activation of PKA stimulates the ERK pathway in neurons, this pathway does not lead to GSK-3β phosphorylation in cerebellar granule neurons.

The phosphorylation of GSK-3 β by forskolin is not mediated by the Akt pathway.

To investigate the potential role of the Akt pathway in the regulation of GSK-3β by forskolin, we examined whether forskolin could activate Akt in the cerebellar granule neurons. Neurons were incubated with forskolin and the phosphorylation state of Akt was determined using phospho-specific (ser473) antibodies (Fig.3A). Forskolin had no effect on Akt phosphorylation at site serine 473. In constrast, IGF-I (50 ng/ml) stimulated Akt phosphorylation at this site and the increased phosphorylation of Akt by IGF-I was blocked by wortmannin. Similar results were obtained when phospho-specific (ser 308) antibodies were used (Fig.3A) indicating that forskolin was unable to phosphorylate Akt at the 2 critical residues that activate the kinase. The activity of Akt was directly measured after immunoprecipitation with phosphorylation-independent Akt

antibodies using a GSK-3 α fusion protein as the substrate. Phosphorylation of GSK-3α was then detected by Western blotting using phospho-specific GSK-3 α /β(ser21/9) antibodies (Fig. 2B). Consistent with the data obtained with phospho-specific Akt antibodies, forskolin had no effect on Akt activity. However, in the control samples, IGF-I markedly increased the activity of Akt.

Additional experiments were done to examine whether a dominant-inactive Akt construct, pAkt (K179M), could block the protective effects of cAMP on cell survival (Fig. 3C). As previously reported, dominant-inactive Akt had no effect on the ability of forskolin or cpt-cAMP to protect rat cerebellar granule neurons from apoptosis induced by lowering extracellular potassium. On the other hand, dominant-inactive Akt significantly blocked the ability of IGF-I to protect these neurons from the same apoptotic stimulus.

Purified PKA can phosphorylate GSK-3β in vitro.

Since forskolin did not appear to phosphorylate GSK-3β through the protein kinases known to directly phosphorylate GSK-3, we questioned whether PKA itself could directly phosphorylate GSK-3β. To address this question, an *in vitro* kinase assay was performed using purified PKA and recombinant GSK-3 β. Phosphorylation of GSK-3 β and was detected by Western blotting with phospho-specific antibodies (Fig.4). In the presence of ATP, purified PKA catalytic subunit phosphorylated GSK-3 β. The site phosphorylated by PKA in GSK-3 β (ser 9) resides in the PKB (or Akt) consensus site. These data suggest that the PKB consensus site in GSK-3 β (RTT**S**F) is similar enough to the PKA consensus site (RRX**S**F) for PKA phosphorylation. There was no detectable phosphorylation in the absence of purified PKA. The H89 PKA inhibitor and the PKI inhibitor significantly blocked the *in vitro* phosphorylation of recombinant GSK-3 β. Assays were carried out to determine the Km and Vmax for human recombinant GSK-3β and a known substrate, l-pyruvate kinase. The Km and Vmax values for GSK-3β and l-pyruvate kinase were 7.24 μM and 7.23 μM/min/mg protein and 19.18 μM and 30.48 μM/min/mg protein, respectively. These values were determined by non-linear regression analysis of data plotted by Michealis-Menton. The relatively low Km for the in vitro phosphorylation of GSK-3 β raise the possibility that PKA directly phosphorylates GSK-3β *in vivo.* To date, we have been unable to demonstrate direct interaction of PKA and GSK-3β in neurons by co-immunoprecipitation (data not shown). This implies that the interaction between

PKA and GSK-3β is not strong enough to detect by immunoprecipitation or that they do not interact *in vivo* because there is another kinase downstream of PKA that directly phosphorylates GSK-3 β.

Inhibitors of GSK-3 β protect neurons from apoptosis.

To determine the role of GSK-3 β in the neuroprotective effects of cAMP we first examined the effects of various inhibitors of GSK-3β on apoptosis in rat cerebellar granule neurons. In agreement with previous studies, forskolin and cpt-cAMP markedly inhibited apoptosis induced by withdrawal of serum and lowering of KCl (Fig. 5). If cells are preincubated with a PKA inhibitor H89 prior to the addition of forskolin or cpt-cAMP, the protective effects are blocked. Consistent with results demonstrating that the ERK pathway does not mediate the phosphorylation of GSK-3 β by forskolin or cpt-cAMP, the MEK inhibitor PD98059 did not influence the ability of forskolin and cpt-cAMP to protect neurons from apoptosis. Lithium and valproate, two direct inhibitors of GSK-3β (41,42), blocked apoptosis to the same extent as forskolin and cpt-cAMP. These data suggest that GSK-3 β mediates the apoptotic effects induced by serum withdrawal and that inhibition of GSK-3 β by phosphorylation protects neurons from apoptosis.

Transfection of cerebellar granule neurons with WT-GSK-3β, kinase-inactiveGSK-3β mutant, and ser9-ala-9GSK-3β mutant.

To confirm results from the inhibitor studies described above, neurons were transfected with GSK-3 β plasmids to determine whether a kinase-dead mutant of GSK-3 β would block apoptosis induced in this model system. Transfections were also carried out with wild-type GSK-3 β and a mutant of GSK-3β that cannot be phosphorylated on serine 9 position. In all of the transfection experiments, neurons were cotransfected with β–galactosidase as an indicator of transfection. The cultures were co-immunostained with rabbit antibodies against β–galactosidase (secondary Ab conjugated to Cy3) and mouse antibodies against HA, the epitope tag on the GSK constructs (secondary Ab conjugated to FITC). DAPI stain was included in the final wash of the cultures to determine nuclear morphology (Fig.6A). Co-stained neurons were scored as apoptotic if they had one or more lobes of condensed chromatin. Seven hundred

to 1200 neurons were counted in each experimental group. The results from these experiments are shown in Figure 6B. In cells transfected with the control vector, 18 +/- 3 % of the total neurons were apoptotic in the presence of serum. Serum withdrawal and lowering KCl lead to a 3-fold increase in the percentage of apoptotic neurons (51 +/- 3%). Incubation of the neurons with cpt-cAMP or forskolin at the time of serum withdrawal prevented the increase in apoptosis. Similar data were obtained when neurons were transfected with WT-GSK-3 β. By constrast, transfection of neurons with a kinase-inactive GSK-3 β blunted the increase in apoptosis induced by serum and KCl withdrawal (27 +/- 4% vs. 51 +/- 3%) but had no effect on basal apoptosis or the ability of cpt-cAMP and forskolin to protect from apoptosis. On the other hand, transfection of neurons with a GSK-3 β mutant that cannot be phosphorylated on serine 9 interfered with the ability of cAMP and forskolin to protect neurons from apoptosis but had little effect on basal apoptosis.

Discussion

Agents that elevate intracellular cAMP levels, such as forskolin (a direct activator of adenylate cyclase), cholera toxin (an activator of Gs), IBMX (a phosphodiesterase inhibitor), and pituitary adenylate cyclase-activation polypeptide (PACAP-38), protect neurons from a variety of apoptotic signals (4,5,31,32,36-39,43-46). The anti-apoptotic effects of cAMP are seen in many types of neuronal systems including cerebellar granule neurons (4,5,31,36-38), dopamine neurons (44), septal cholinergic neurons (45), and sympathetic and sensory neurons (32,47,48). The mechanisms underlying the anti-apoptotic effects of cAMP are not well understood. In previous studies, two signaling pathways that could mediate the neuroprotective effect of cAMP have been explored: the ERK pathway and the PI-3 kinase/Akt pathway. The ERK pathway has been implicated in the survival of sympathetic neurons exposed to cytosine arabinoside (47) and in PC12 cells induced to undergo apoptosis by NGF withdrawal (49). However, other studies in sympathetic neurons (46,48) indicate that cAMP promotes neuronal survival through an ERK-independent pathway. In our studies, cAMP stimulated phosphorylation of both ERK and RSK in the cerebellar granule neurons, but activation of this pathway did not lead to protection against apoptosis since the MEK inhibitors blocked phosphorylation but not the ability of cAMP to

protect the neurons from apoptosis. These results concur with the finding of Creedon et al. (46) and indicate that, in rat cerebellar granule neurons, the ERK pathway does not mediate the survival effects of cAMP. As previously discussed, most studies examining the role of PI-3 kinase/Akt in mediating the neuroprotective effects of cAMP have demonstrated that the Akt pathway is not involved. The potential involvement of the Akt pathway was re-examined in our cells since GSK-3β is known to be downstream of Akt. The results from western blotting with T308 and S473 phospho-specific Akt antibodies and direct Akt kinase assays showed that cAMP had no effect on Akt phosphorylation or activity in cerebellar granule neurons. Consistent with these findings, wortmannin and transfection of cerebellar granule neurons with a dominant-negative Akt mutant failed to diminish the protective effect of cAMP in our cells. Thus, Akt does not mediate the survival effects of cAMP in rat cerebellar granule neurons.

Our data suggest a novel signaling pathway by which cAMP promotes neuronal survival, a PKA pathway that leads to inhibition of GSK-3 β. Forskolin and cpt-AMP phosphorylate and inactivate GSK-3 β in cerebellar granule neurons. As expected, the phosphorylation of GSK-3 β by forskolin and pt-cAMP is blocked by specific inhibitors of PKA. PKA phosphorylates GSK-3 β *in vitro* at a site known to inhibit its activity, and indeed, forskolin inhibited the kinase activity of GSK-3β. If neurons are transfected with a GSK-3 β mutant that cannot be phosphorylated, cAMP is unable to fully protect neurons from apoptosis. Furthermore, direct inhibitors of GSK-3β , valproate and lithium, and a dominant-negative mutant of GSK-3 β protect cerebellar granule neurons from apoptosis. These data strongly support the hypothesis that cAMP activates PKA and leads to the phosphorylation and inactivation of GSK-3 β, a pro-apoptotic kinase in cerebellar granule neurons.

The ability of PKA to phosphorylate GSK-3 β *in vitro* supports that notion that PKA directly phosphorylates GSK-3β *in vivo*. These data suggest that PKA and PKB (Akt) share a phosphorylation target in cells. Cell localization of PKA, Akt, and GSK-3 β may be an important factor in determining which kinase has access to GSK-3 β in response to a given stimulus. In addition to PKA and Akt, the protein kinases RSK and integrin-linked kinase (ILK) also phosphorylate and inactivate GSK-3 (40,50). Inactivation of GSK-3 by RSK is a proposed mechanism by which the NMDA activated- ERK pathway opposes apoptosis. Inactivation of

GSK-3 by ILK is thought to mediate the anti-apoptotic effects of cell attachment (50). Thus GSK-3 β appears to represent a convergence site of multiple signaling pathways involved in cell fate decisions.

ACKNOWLEDGEMENTS

We would like to thank Dr. Paula Hoffman and Dr. Sanjiv Bhave for their assistance in establishing cultures of rat cerebellar granule neurons and Dr. Marc Montminy for providing the Akt expression plasmid. We also thank Dr. Jenifer Monks for her assistance with digital deconvolution fluorescent microscopy.

REFERENCES

1. **Narayanan, V.** 1997. Apoptosis in development and disease of the nervous system: 1. Naturally occurring cell death in the developing nervous system. Pediatric. Neurol. **16:**9-13.
2. **Levi-Monalcini, R.** 1987. The nerve growth factor:thirty-five years later. EMBO J **6:**1145-1154.
3. **Barde, Y. A.** 1989. Trophic factors and neuronal survival. Neuron **2:**1525-1534.
4. **Rydel, R. E. , and L.A. Greene.** 1988. cAMP analogs promote survival and neurite outgrowth in cultures of rat sympathetic and sensory neurons independently of nerve growth factor. Proc. Natl. Acad. Sci. U S A.. **85:**1257-61
5. **Hanson, M. G., Jr, Shen, S., Wiemelt, A. P., McMorris, F. A., and B.A. Barres.** 1998. Cyclic AMP elevation is sufficient to promote the survival of spinal motor neurons in vitro. J. Neurosci. **18:**7361-71.
6. **Dudek, H., Datta, S. R., Franke, T. F., Birnbaum, M. J., Yao, R., Cooper, G. M., Segal, R. A., Kaplan, D. R., and M. E. Greenberg.** 1997. Regulation of neuronal survival by the serine-threonine protein kinase Akt. Science **275:**661-665.
7. **Fruman, D. A., Meyers, R. E., and C. C. Cantley.** 1998. Phosphoinositide kinases. Annual Rev. Biochem. **67:**481-507.
8. **Franke, T. F., Yang, S., Chan, T. O., Datta, K., Kazlauskas, A., Morrison, D. K., Kaplan, D. R., and P. N. Tsichlis.** 1995. The protein kinase encoded by the Akt proto-oncogene is a target of the PDGF-activated phosphatidylinosital 3-kinase. Cell **81:**727-736.

9. **Burgering, B. M. T., and P. J. Coffer.** 1995. Protein kinase B (cAkt) in phosphatidylinositol-3-OH kinase signal transduction. Nature **376:**599-602.
10. **Jones, P. F., Jakubowicz, T., Pitossi, F. J., Maurer, F., and B. A. Hemmings.** 1991. Molecular cloning and identification of a serine threonine protein kinase of the second-messenger subfamily. Proc. Natl. Acad. Sci. USA. **88:**4171-4175.
11. **Downward, J.** 1998. Mechanisms and consequences of activation of protein kinase B/Akt. Curr. Opin. Cell. Biol. **10:**262-267.
12. **Datta, S. R., Dudek, H., Tao, X., Masters, S., Fu, H., Gotoh, Y., and M. E. Greenberg.** 1997. Akt phosphorylation of BAD couples survival signals to the cell-intrinsic death machinery. Cell **91:**231-241.
13. **Cardone, M. H., Roy, M., Stennicke, H. R., Salvesen, G. S., Franke, T. F., Stanbridge, E., Frisch, S.,** and J. C. Reed. 1998. Regulation of cell death protease caspase-9 by phosphorylation. Science 282:1318-1321.
14. **Brunet, A., Bonni, A., Zigmond, M. J., Lin, M. Z., Juo, P., Hu, L. S., Anderson, M. J., Arden, K. C., Blenis, J., and M. E. Greenberg.** 1999. Akt promotes cell survival by phosphorylating and inhibiting a forkhead transcription factor. Cell. **96**:857-68.
15. **Woodgett, J. R.** 1991. A common denominator linking glycogen metabolism, nuclear oncogenes and development. TIBS. **16:**177-181.
16. **Woodgett, J.R., Plyte, S.E., Pulverer, B.J., Mitchell, J.A., and K. Hughes.** 1993. Roles of glycogen synthase kinase-3 in signal transduction. Biochem Soc Trans. **21**:905-7
17. **Welsh, G. I., Wilson, C., and C. G. Proud.** 1996. GSK3: a SHAGGY frog story. Trends in Cell Biol. **6:** 274-279.
18. **Cross, D. A. E., Alessi, D. R., Cohen, P., Andjelkovich, M., and B. A. Hemmings.** 1995. Inhibition of glycogen synthase kinase-3 by insulin mediated by protein kinase B. Nature **378:**785-789.
19. **Welsh, G. I., and C. G. Proud.** 1993. Glycogen synthase kinase-3 is rapidly inactivated in response to insulin and phosphorylates eukaryotic initiation factor elF-2B. Biochem. J **294:**625-629.
20. **Hong, M., and V. M.-Y. Lee.** 1997. Insulin and insulin-like growth factor-1 regulate tau phosphorylation in cultured human neurons. J. Biol. Chem. **272:**19547-19553.

21. **Foil, C. J., Williams, J. S., Chou, C.-H., Wang, Q. M., Roach, P. J., and O. M. Andrisani.** 1994. A secondary phosphorylation of $CREB^{341}$ at Ser^{129} is required for the cAMP-mediated control of gene expression. J. Biol. Chem. **269:**32187-32193.

22. **Plyte, S. E., Hughes, K., Nikolakaki, E., Pulverer, B. J., and J. R. Woodgett.** 1992. Glycogen synthase kinase-3: functions in oncogenesis and development. Biochim. Biophys. Acta **1114:**147-162.

23. **Boyle, W. J., Smeal, T., Defize, L. H., Angel, P., Woodgett, J. R., Karin, M., and T. Hunter.** 1991. Activation of protein kinase C decreases phosphorylation of c-Jun at sites that negatively regulate its DNA-binding activity. Cell **64:**573-584.

24. **Yost, C. Torres, M., Miller, J.R., Huang, E., Kimelman, D., and Moon, R.T.** 1996. The axis-inducing activity, stability, and subcellular distribution of beta-catenin is regulated in Xenopus embryos by glycogen synthase kinase 3. Genes Dev. **10**: 1443-1454.

25. **Harwood, A. J., Plyte, S. E., Woodgett, J., Strutt, H., and R. R. Kay.** 1995. Glycogen synthase kinase 3 regulates cell fate in dictyostelium. Cell **80:**139-148.

26. **Dominguez, I., Itoh, K., and S. Y. Sokol.** 1995. Role of glycogen synthase kinase 3 β as a negative regulator of dorsoventral axis formation in Xenopus embryos. Proc. Natl. Acad . Sci. USA **92:**8498-8502.

27. **Itoh, K., Tang, T. L., Neel, B. G., and S. Y. Sokol.** 1995. Specific modulation of ectodermal cell fates in Xenopus embryos by glycogen synthase kinase. Development **121:**3979-3988.

28. **Pap, M., and G. M. Cooper.** 1998. Role of glycogen synthase kinase-3 in the phosphatidylinositol 3-Kinase/Akt cell survival pathway. J. Biol. Chem. **273:**19929-19932.

29. **Sable, C.L., N. Filippa, B. Hemmings, and E. Van Obberghen**. 1997 cAMP stimulates protein kinase B in a Wortmannin-insensitive manner. FEBS Lett. **409**, 253-257.

30. **Filippa, M., Sable, C. L., Filloux, C., Hemmings, B., and E. V. Obberghen** 1999. Mechanism of protein kinase B activation by cyclic AMP-dependent protein kinase. Mol. Cell. Biol. **19**:4989-5000.

31. **Miller, T.M., M.G. Tansey, E.M. Johnson, Jr., and D.J. Creedon.** 1997 Inhibition of phosphatidylinositol 3-kinase activity blocks depolarization and insulin-like growth factor I-mediated survival of cerebellar granule cells. J. Biol. Chem. **272**, 9847-9853.

32. **Crowder, R.J. and R.S. Freeman**. 1999 The survival of sympathetic neurons promoted by potassium depolarization, but not cAMP, requires phosphatidylinositol 3-kinase and Akt. J. Neurochem. **73**, 466-475.

33. **Novelli, A., Reilly, J. A., Lysio, P.G., and R.C. Henneberry.** 1988. Glutamate becomes neurotoxic via the *N*-methyl-D-aspartate receptor when intracellular energy levels are reduced. Brain Res. **451**:205-212.

34. **Xia Z, Dudek H, Miranti CK, Greenberg ME** 1996. Calcium influx via the NMDA receptor induces immediate early gene transcription by a MAP kinase/ERK-dependent mechanism. J Neurosci **16**:5425-36.

35. **Beavo, J.A., Bechtel, P.J., and Kreb, E.G**. 1974. Preparation of homogeneous cAMP-dependent protein kinases(s) from rat skeletal muscle. Methods in Enzymology **38**: 299-308.

36. **Campard, P.K., Crochemore, C., Rene, F., Monnier, D., Koch, B., and J. P. Loeffler.** 1997. PACAP type I receptor activation promotes cerebellar neuron survival through the cAMP/PKA signaling pathway. DNA Cell Biol **16:**323-33.

37. **Villalba, M., Bockaert, J., and L, Journot.** 1997. Pituitary adenylate cyclase-activating polypeptide (PACAP-38) protects cerebellar granule neurons from apoptosis by activating the mitogen-activated protein kinase (MAP kinase) pathway. J Neurosci **17:**83-90.

38. **D'Mello, S.R., Galli, C., Ciotti, T., and P. Calissano.** 1993. Induction of apoptosis in cerebellar granule neurons by low potassium: inhibition of death by insulin-like growth factor I and cAMP. Proc Natl Acad Sci U S A . **23**:10989-93.

39. **Dugan, L.L., J.S. Kim, Y. Zhang, R.D. Bart, Y. Sun, D.M. Holtzman, and D.H. Gutmann**. 1999 Differential effects of cAMP in neurons and astrocytes. Role of B-raf. J. Biol. Chem. **36**, 25842-25848.

40. **Torres, M. A., Eldar-Finkelman, H., Krebs, E.G., and R.T. Moon.** 1999. Regulation of ribosomal S6 protein kinase-p90(rsk), glycogen synthase kinase 3, and beta-catenin in early Xenopus development. Mol. Cell. Biol. **19:**1427-37.

41. **Klein, P. S., and D. A.. Melton.** 1996. A molecular mechanism for the effect of lithium on development. Proc. Natl. Acad. USA. 93:8455-8459.

42. **Chen, G., Huang, L-D., Jiang, Y-M., and H. K. Manji.** 1999. The mood-stabilizing agent valproate inhibits the activity of glycogen synthase kinase-3 β. J. Neurochem. **72**:1327-1330.

43. **Yan, G.M., Lin, S.Z., Irwin, R.P., and S.M. Paul.** 1995. Activation of G proteins bidirectionally affects apoptosis of cultured cerebellar granule neurons. J Neurochem. **65**:2425-31.

44. **Mena, M.A., Casarejos, M.J., Bonin, A., Ramos. J.A, and J. Garcia Yebenes.** 1995. Effects of dibutyryl cyclic AMP and retinoic acid on the differentiation of dopamine neurons: prevention of cell death by dibutyryl cyclic AMP. J Neurochem **65**:2612-20.

45. **Kew, J. N, Smith, D.W., and M.V. Sofroniew.** 1996. Nerve growth factor withdrawal induces the apoptotic death of developing septal cholinergic neurons in vitro: protection by cyclic AMP analogue and high potassium. Neuroscience **70**:329-39.

46. **Creedon, D. J., Johnson, E. M., and J. C. Lawrence.** 1996. Mitogen-activated protein kinase-independent pathways mediate the effects of nerve growth factor and cAMP on neuronal survival. J. Biol. Chem. **271:**20713-8

47. **Anderson, C.N.G., and A.M. Tolkovsky.** 1999. A role for MAPK/ERK in sympathetic neuron survival: protection against a p53-dependent, JNK-independent induction of apoptosis by cytosine arabinoside. J Neurosci **19**:664-73.

48. **Virdee, K., and A. M. Tolkovsky.** 1995. Activation of p44 and p42 MAP kinases is not essential for the survival of rat sympathetic neurons. Eur J Neurosci **7**:2159-69

49. **Xia, Z., Dickens, M., Raingeaud, J., Davis, R.J., and M.E. Greenberg** 1995. Opposing effects of ERK and JNK-p38 MAP kinases on apoptosis. Science **270**:1326-31

50. **Delcommenne, M., Tan, C., Gray, V., Rue, L., Woodgett, J., and Dedhar, S.** 1998. Phosphoinositide-3-OH kinase-dependent regulation of glycogen synthase kinase 3 and protein kinase B/Akt by integrin-linked kinase. Proc. Natl. Acad. Sci. USA **95**:11211-11216.

Figure Legends

Figure 1. Phosphorylation and inhibition of GSK-3 β by forskolin and cpt-cAMP. **(A)** Cerebellar granule neurons were cultured for 7 days, washed twice with BME, and then placed in serum-free medium containing 5 mM KCl. Two hours later, the cells were either left untreated or treated with 10 μM forskolin for the indicated times. Somes neurons were incubated with IGF-I(50 ng/ml) for 30 min as a positive control. Cell lysates were analyzed by immunoblotting with a phospho-specific GSK-3 β (Ser 9) antibody. **(B)** Neurons were pretreated for 30 min in the absence or presence of 25 μM cell-permeable PKI inhibitor, 10 μM of the PKA inhibitor H-89, or 30 μM of the

MEK inhibitor PD98059 prior to incubation with 10 μM forskolin for 30 min. Cell lysates were immunoblotted with anti GSK-3 β (Ser 9) antibody. **(C)** Neurons were pretreated for 30 min in the absence or presence of 25 μM cell-permeable PKI inhibitor, 10 μM of the PKA inhibitor H-89, or 30 μM of the MEK inhibitor PD98059 prior to incubation with 30 μM of the cell-permeable cAMP analog (cpt-cAMP) for 30 min. Results shown are representative of at least three experiments. **(D)** After serum/ 25 mM KCl starvation in 5 mM KCl media, neurons were incubated for 30 min with 10 μM forskolin in the presence or absence of 10 μM H-89 or 25 μM PKI, or 50 ng/ml IGF-I. After incubation, the neurons were lysed, GSK-3β was immunoprecipitated, and its activity was determined as described in Materials and Methods. Control neurons were washed similarly and then placed in serum-containing conditioned media. The results are expressed as fold activity of control neurons and are mean values ± standard errors of results from three experiments. Statistical significance*, according to Student's t test, indicates $p < 0.05$ versus the value for 5 mM KCl.

Figure 2. Phosphorylation of GSK-3 by cAMP/PKA does not require activation of the ERK pathway. Neurons were treated as described in Figure 1A. and then pretreated for 30 min in the absence or presence of 10 μM of the PKA inhibitor H-89 or 30 μM of the MEK inhibitor PD98059 prior to incubation with 10 μM forskolin for 30 min. Cell lysates were immunoblotted with phospho-specific antibodies against ERK (Thr202/Tyr204) (**Top**) , p90 RSK (Ser 381) (**Middle**), and GSK-3α/β (Ser21/9) (**Bottom**). Results shown are representative of at least three experiments.

Figure 3. Phosphorylation of GSK-3 by cAMP/PKA does not require activation of Akt. (A). Cerebellar granule neurons were cultured for 7 days, washed twice, and placed in serum-free medium containing 5 mM KCl. Two hours later, the cells were either left untreated or treated with 10 μM forskolin for the indicated times. Some neurons were incubated with IGF-I(50 ng/ml) in the absence or presence of wortmannin (100nM) for 30 min as positive controls. Cell lysates were immunoblotted with antibodies to phospho-S473 Akt and phospho-T308 Akt. The membrane was then stripped and reprobed with antibodies to phosphorylation independent Akt. **(B)** Neurons were treated as described in part A. Akt was immunoprecipitated from cell lysates with an immobilized Akt antibody and kinase activity was determined by an in vitro kinase assay using 1 μg of recombinant GSK-3α fusion protein as the substrate. Phosphorylation of GSK-3α was detected by immunoblotting with phospho-specific GSK-3α/β (Ser21/9) antibody (bottom panel). The

membranes were stripped and reprobed with the antibody to phosphorylation-independent Akt (top panel). **(C)** Neurons were transfected with the indicated expression vectors (along with pCMV-β-Gal), and 24 hours later they were placed in medium containing 25 mM KCl plus serum or in deprivation media (5 mM KCl, no serum) in the presence or absence of 10 μM forskolin, 500 μM cpt-cAMP or 50 ng/ml IGF-I. After 20 hours, the neurons were fixed and costained with an antibody to β-gal and Hoechst 33258. Apoptosis was quantified by scoring the percentage of transfected neurons in the adherent cell population with condensed or fragmented nuclei. Data are from three experiments and represent the mean ± S.E.M.

Figure 4. In vitro phosphorylation of GSK-3 by purified PKA. The phosphorylation reaction consisted of 4 units of purified PKA catalytic subunit, 1 μg GSK-3β fusion protein, and 100 μM ATP. Reactions were carried out in the absence and presence of the PKA inhibitors H-89 (5 μM) and PKI (2.5 μM). The phosphorylation reaction was allowed to proceed for 30 min at 30 °C and stopped by adding 3 × SDS sample buffer. The phosphorylation of GSK-3β (top) was measured by Western blotting with phospho-GSK-3β (Ser9) antibody. The membrane was stripped and reprobed with a monoclonal phosphorylation-independent antibody to GSK-3 β (bottom).

Figure 5. The effect various agents and inhibitors on apoptosis of rat cerebellar granule neurons. Cerebellar granule neurons were cultured for 7 days, washed twice with BME, and placed in serum-free medium containing 5 mM KCl in the absence or presence of forskolin (10 μM), cpt-cAMP (500 μM), forskolin and H-89 (10 μM), cpt-cAMP and H-89 (10 μM), cpt-cAMP and PD98059 (30 μM), forskolin and PD98059 (30 μM), lithium (15 mM), or valproate (15 mM). After 24 hr neurons were stained with Hoechst 33258 (5 μg/ml) for 5 min and apoptosis was quantified by scoring the percentage of neurons in the adherent cell population with condensed or fragmented nuclei. To obtain unbiased counting, cells were scored blind without knowledge of their prior treatment. Data are presented as mean ± S.E.M., n=4. *, $p<.001$ vs. apoptotic (serum-free 5mM KCl) medium; ϕ, $p<.001$ vs. apoptotic medium + forskolin; **, $p<.001$ vs. apoptotic medium + cpt-cAMP (Student's t test).

Figure 6. Transfection of cerebellar granule neurons with WT-GSK-3β, kinase-inactiveGSK-3β mutant, and ser9-ala-9GSK-3β mutant. Neurons were co-transfected with the control vector, GSK-3β wt, GSK-3β (KI) or GSK-3β (S9A) along with CMV-β-Gal. One day after transfection, the neurons were placed in complete medium (serum/25 mM KCl) or switched to serum-free medium containing 5 mM KCl, with or without cAMP(500 μM) or forskolin (10 μM). After 24 hr the transfected neurons were fixed and immunostained with an antibody to β-Gal (Cy3-coupled secondary antibody) and 12CA5 antibody to HA (FITC-coupled secondary antibody). To reveal nuclear morphology, neurons were also stained with DAPI. **(A)** Demonstration of the triple-staining method in neurons grown in serum and 25 mM KCl. **(B)** The effects of GSK-3β constructs on neuronal survival. The β-galactosidase-positive neurons were scored as healthy or apoptotic as described in Figure 3C. Data presented as mean ± S.E.M., n=4. #, $p<.001$ vs. pcDNA3 in apoptotic (serum-free 5mM KCl) medium; *, $p<.001$ vs. pcDNA3 in apoptotic medium + cpt-cAMP; ϕ, $p<.001$ vs. apoptotic medium + forskolin (Student's *t* test).

Fig.1

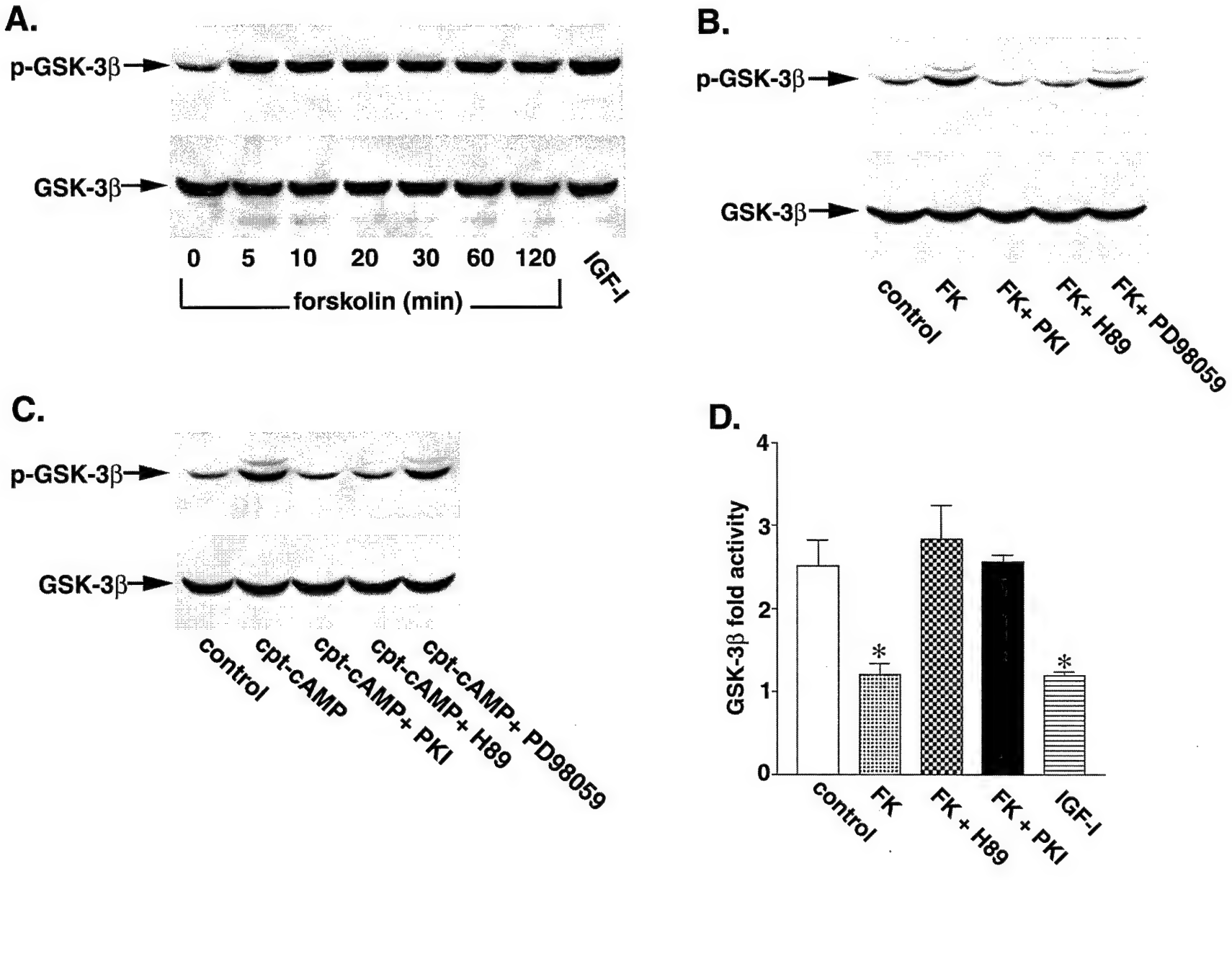
A.
p-GSK-3β
GSK-3β
0 5 10 20 30 60 120 IGF-I
forskolin (min)
B.
p-GSK-3β
GSK-3β
control
FK
FK+ PKI
FK+ H89
FK+ PD98059
C.
p-GSK-3β
GSK-3β
control
cpt-cAMP
cpt-cAMP+ PKI
cpt-cAMP+ H89
cpt-cAMP+ PD98059
D.
GSK-3β fold activity
0
1
2
3
4
*
*
control
FK
FK + H89
FK + PKI
IGF-I

Fig.2

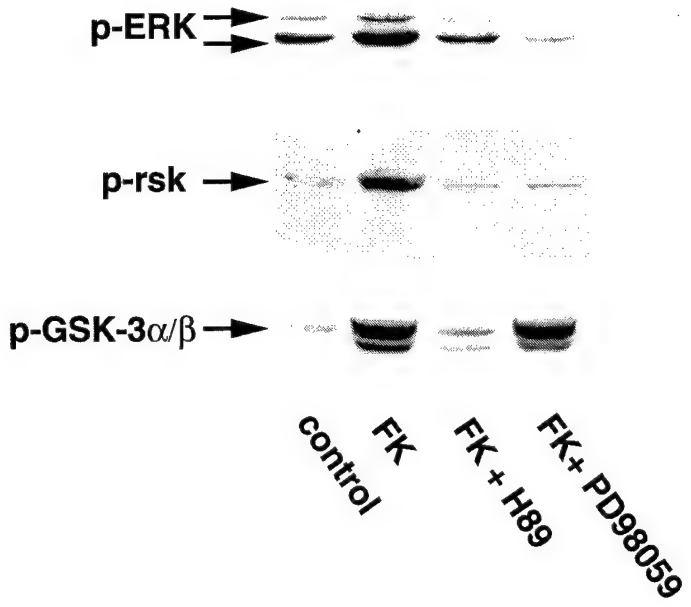

Fig.3

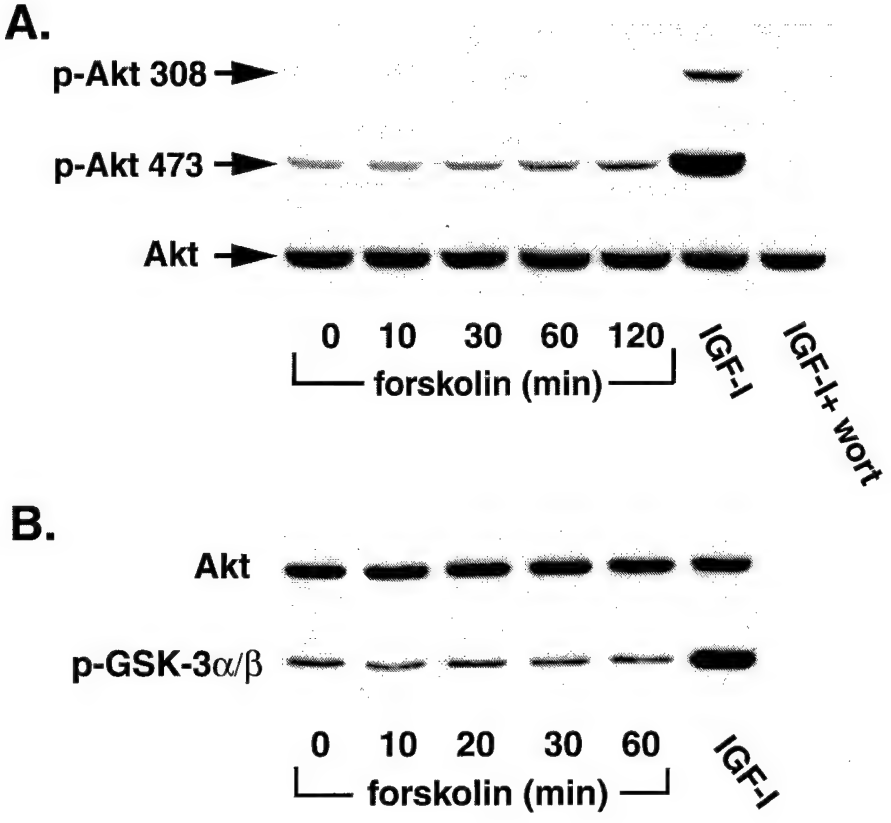
A.
p-Akt 308
p-Akt 473
Akt
0 10 30 60 120
forskolin (min)
IGF-I
IGF-I+ wort
B.
Akt
p-GSK-3α/β
0 10 20 30 60
forskolin (min)
IGF-I
C.
pCMV5
pAkt(K179M)
% apoptosis
60
50
40
30
20
10
0
-serum/5mM K+
+serum/25mM K+
--
FK
cpt-cAMP
IGF-I

Fig.4

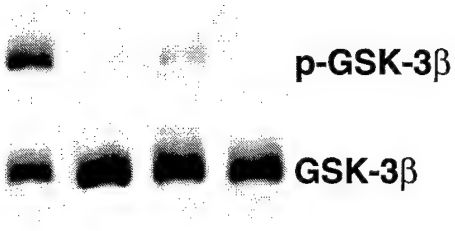

purified PKA	+	-	+	+
GSK-3β	+	+	+	+
ATP	+	+	+	+
H89	-	-	+	-
PKI	-	-	-	+

Fig. 5

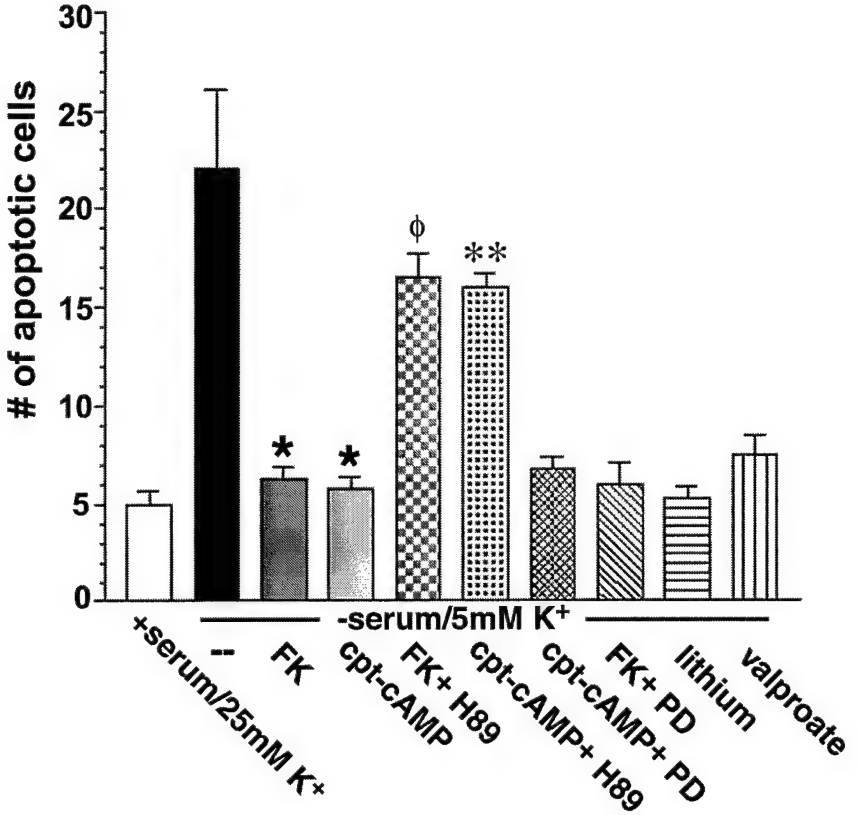
# of apoptotic cells
30
25
20
15
10
5
0
*
*
ϕ
**
-serum/5mM K+
+serum/25mM K+
--
FK
cpt-cAMP
FK+ H89
cpt-cAMP+ H89
cpt-cAMP+ PD
FK+ PD
lithium
valproate

Fig.6

A.

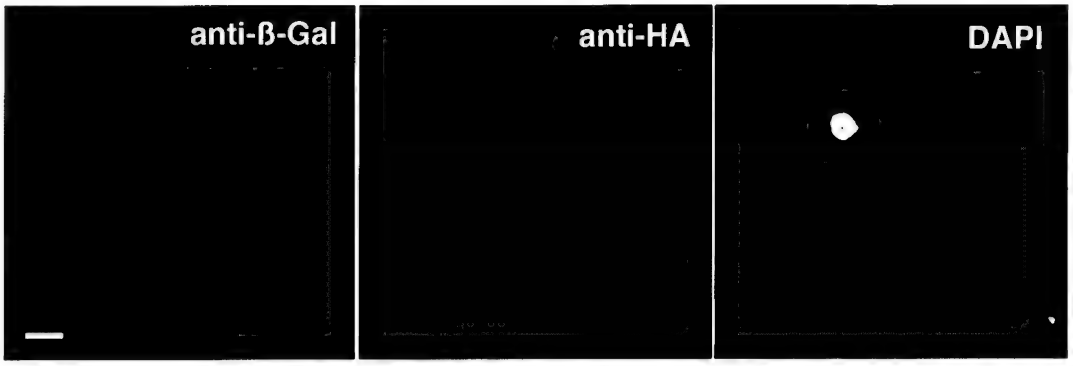
anti-ß-Gal
anti-HA
DAPI

B.

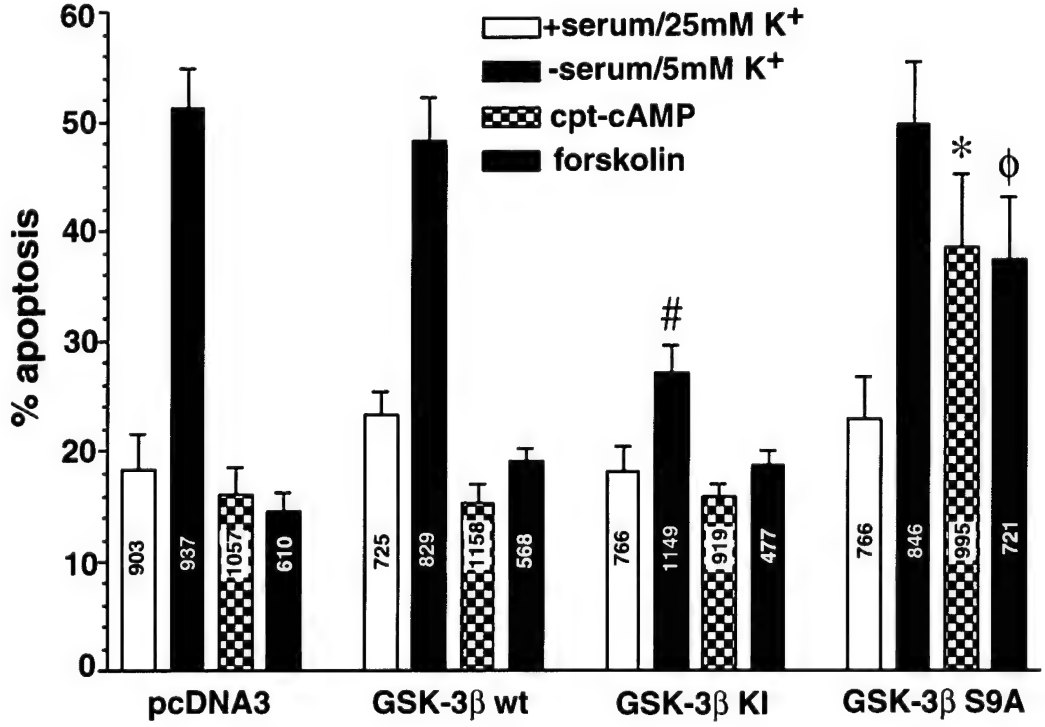
+serum/25mM K+
-serum/5mM K+
cpt-cAMP
forskolin
% apoptosis
60
50
40
30
20
10
0
903
937
1057
610
725
829
1158
568
766
1149
919
477
766
846
995
721
#
*
ϕ
pcDNA3
GSK-3β wt
GSK-3β KI
GSK-3β S9A

Appendix 2

THE JOURNAL OF BIOLOGICAL CHEMISTRY Vol. 274, No. 5, Issue of January 29, pp. 2829–2837, 1999
Printed in U.S.A.

Insulin-like Growth Factor I-mediated Activation of the Transcription Factor cAMP Response Element-binding Protein in PC12 Cells

INVOLVEMENT OF p38 MITOGEN-ACTIVATED PROTEIN KINASE-MEDIATED PATHWAY*

(Received for publication, February 20, 1998, and in revised form, October 8, 1998)

Subbiah Pugazhenthi‡, Tracy Boras‡, Daniel O'Connor§, Mary Kay Meintzer¶, Kim A. Heidenreich¶, and Jane E.-B. Reusch‡

From the Section of Endocrinology, Veterans Affairs Medical Center, Denver, Colorado 80220, the Departments of ‡Endocrinology and §Pharmacology, University of Colorado Health Sciences Center, Denver, Colorado 80262, the §Department of Medicine and Center for Molecular Genetics, University of California, La Jolla, California 92093, and the §Department of Veterans Affairs Medical Center, San Diego, California 92161

IGF-I is known to support growth and to prevent apoptosis in neuronal cells. Activation of the nuclear transcription factor cAMP response element-binding protein (CREB) has emerged as a central determinant in neuronal functions. In the present investigation, we examined the IGF-I-mediated phosphorylation and transcriptional activation of CREB in rat pheochromocytoma (PC12) cells, a cellular model for neuronal differentiation, and defined three distinct postreceptor signaling pathways important for this effect including the p38 mitogen-activated protein kinase (MAPK) pathway. CREB phosphorylation at serine 133 and its transcriptional activation as measured by a CREB-specific Gal4-CREB reporter and the neuroendocrine-specific gene chromogranin A was induced 2–3.3-fold by insulin-like growth factor (IGF)-I. This activation was significantly blocked ($p < 0.001$) by the dominant negative K-CREB or by mutation of the CRE site. IGF-I stimulated chromogranin A gene expression by Northern blot analysis 3.7-fold. Inhibition of MAPK kinase with PD98059, PI 3-kinase with wortmannin, and p38 MAPK with SB203580 blocked IGF-I-mediated phosphorylation and transcriptional activation of CREB by 30–50% ($p < 0.001$). Constitutively active and dominant negative regulators of the Ras and PI 3-kinase pathways confirmed the contribution of these pathways for CREB regulation by IGF-I. Cotransfection of PC12 cells with p38β and constitutively active MAPK kinase 6 resulted in enhanced basal as well as IGF-I-stimulated chromogranin A promoter. IGF-I activated p38 MAPK, which was blocked by the inhibitor SB203580. This is the first description of a p38 MAPK-mediated nuclear signaling pathway for IGF-I leading to CREB-dependent neuronal specific gene expression.

Insulin-like growth factor-I (IGF-I)[1] is a growth-promoting polypeptide with diverse cellular functions. IGF-I is involved in the growth and differentiation of various cell types such as muscle and adipocytes (1–3). Although liver is the primary source of circulating IGF-I, significant expression of this growth factor is seen in various tissues including brain, where it is known to exert autocrine and paracrine functions (4, 5). IGF-I has been shown to stimulate neurite outgrowth and promote survival of neurons in culture (4, 5).

IGF-I exerts its cellular effects through its type I IGF receptor which resembles the insulin receptor in structural as well as functional aspects (reviewed in Refs. 6 and 7). This heterotetrameric transmembrane glycoprotein consists of two α- and two β-subunits. The β-subunit has intrinsic tyrosine kinase activity that is stimulated when IGF-I binds to the α-subunits. The receptor tyrosine kinase in turn phosphorylates intracellular substrates such as insulin receptor substrates 1 and 2 and Shc (7, 8). The tyrosine phosphorylation sites on these docking proteins recruit Src homology 2-containing proteins such as Grb2, Nck, Crk, SHP2, and the p85 subunit of PI 3-kinase. From this intermediary complex of signaling proteins, two significant pathways emerge. One pathway activates extracellular signal-regulated kinase 1/2 (ERK1/2) through Ras/Raf/MEK, and another pathway proceeds through PI 3-kinase. IGF-I has been studied extensively in the PC12 cell line, a model of neuronal tissue. In these cells, IGF-I promotes growth and proliferation, primarily via activation of the ERK pathway (9). For the prevention of apoptosis, IGF-I requires the PI 3-kinase pathway (10).

One of the common nuclear targets of tyrosine kinase signaling cascades is CREB, the Ca^{2+}/cyclic AMP response element-binding protein. CREB is a 43-kDa nuclear transcription factor belonging to the CREB/ATF family (11). Activation of CREB by forskolin, a potent stimulator of cAMP, stimulates PC12 cell differentiation to a sympathetic neuron-like phenotype with neurite extension (12, 13). NGF and IGF-I regulation of CREB is essential for neuronal plasticity, full axonal development, memory consolidation, and neuroprotection (14–20). IGF-I is known to regulate a number of CREB response element (CRE)-containing genes including *bcl-2* and *c-fos* (21, 22). CREB is constitutively expressed, and it binds to the specific sequence, 5′-TGACGTCA-3′ known as CRE. Phosphorylation on the serine 133 residue of CREB increases its transcriptional activity.

* This work was supported by a Veterans Affairs Merit Review and Research Associate Career Development Award and NIDDK, National Institutes of Health, Grant KO8 DK02351 (to J.E.-B.R.). The costs of publication of this article were defrayed in part by the payment of page charges. This article must therefore be hereby marked "*advertisement*" in accordance with 18 U.S.C. Section 1734 solely to indicate this fact.

‡ To whom correspondence should be addressed: Section of Endocrinology (111H), Veterans Affairs Medical Center, 1055 Clermont St., Denver, CO 80220. Tel.: 303-399-8020 (ext. 2775); Fax: 303-393-5271; E-mail: jreusch@sembilan.uchsc.edu.

[1] The abbreviations used are: IGF, insulin-like growth factor; CRE, cAMP response element; CREB, cAMP response element-binding protein; ERK, extracellular regulated kinase; MAPK, mitogen-activated protein kinase; MEK, MAPK kinase; PBS, phosphate-buffered saline; PI 3-kinase, phosphatidylinositol 3-kinase; NGF, nerve growth factor; TK, thymidine kinase; CgA, chromogranin A.

This phosphorylation does not alter the binding of CREB to CRE, but it increases its association with adapter proteins such as CREB-binding protein, leading to the activation of transcriptional machinery. CREB was initially identified as a substrate for PKA and a mediator of cAMP-regulated gene expression (23). Later studies showed that CREB can be phosphorylated and activated by multiple signaling pathways including ERK, protein kinase C, calcium/calmodulin-dependent protein kinases, and p38 MAPK (12, 24–26). Thus, diverse signaling pathways, many of which are activated by IGF-I, are capable of regulating this transcription factor, which plays a role in neuronal growth and survival.

Chromogranin A is an acidic glycoprotein present in secretory granules of the neuroendocrine system (27). The promoter region of this gene has a conserved CRE site, which is essential for transactivation in PC12 cells (28). Chromogranin A, being a physiologically relevant CRE-dependent gene, can serve as a read-out for IGF-I-mediated gene regulation in PC12 cells. We recently demonstrated an ERK-dependent CREB activation by insulin in Hep-G2 and 3T3-L1 cell lines (29). Since CREB is capable of regulating many important functions in neuronal tissues, we investigated whether CREB was important for IGF-I-mediated gene regulation in PC12 cells. The objectives of this investigation were to (*a*) examine whether IGF-I stimulates the phosphorylation and transcriptional activation of the nuclear transcription factor CREB in PC12 cells, (*b*) gain insight into the mechanism by which IGF-I-mediated signal transduction pathways lead to the activation of CREB, and (*c*) assess the impact of IGF-I on the neuronal specific CRE-dependent gene chromogranin A.

We demonstrate that IGF-I increases CREB serine 133 phosphorylation and transcriptional activation of CREB reporter systems and the neuronal specific gene chromogranin A through at least three pathways: PI 3-kinase, MEK/ERK, and p38 MAPK. The novel finding of this study is the contribution of the p38 MAPK-mediated signaling pathway to the regulation of CREB-dependent gene expression by IGF-I.

EXPERIMENTAL PROCEDURES

Materials—PD98059, wortmannin, and rapamycin were purchased from Biomol (Plymouth Meeting, PA). SB203580 and SB202190 were obtained from Calbiochem. Cell culture media and supplies were from Life Technologies, Inc. and Gemini Bio Products, Inc. (Calabasa, CA). The plasmid for the expression of the chimeric protein (Gal4-CREB) consisting of the DNA binding domain of Gal4 and the transactivation domain of CREB and the expression vector for Gal4-CREB protein with serine to alanine substitution at position 133 were a generous gift from Dr. William J. Roesler (University of Saskatchewan, Saskatoon, Canada). An expression vector for the luciferase reporter gene driven by the enhancerless thymidine kinase (TK) promoter linked to four copies of Gal4 regulatory sequence ($pGal_4$-TK-Luc) was provided by Dr. James Hoeffler (Invitrogen, San Diego, CA). Three constructs of mouse chromogranin A promoter linked to luciferase in the promoterless luciferase reporter vector pXP1 were provided by Dr. Daniel O'Connor (San Diego, CA). The full-length promoter pXP1133 contained 1133 bp in the 5′-flanking region. The CRE-containing truncated promoter, which maintains the minimal neuroendocrine specificity, is in pXP77; the CRE-mutated version of pXP77 is pXPM41. Constitutively active and dominant negative Ras and Raf-1 were obtained from Arthur Gutierrez-Hartmann (University of Colorado Health Sciences Center, Denver, CO) and Ulf Rapp (Strathlenkunde, Germany). For the PI 3-kinase, SRα-wild type p85, and SRα-Δp85 were provided by Dr. Masato Kasuga (Kobe, Japan). The constitutively active form of MAPK kinase 6 was obtained from Joel Raingeaud (Institut Curie, Orsay, France), and the pcDNA3-p38β was provided by Jiahuai Han (San Diego, CA). The luciferase assay kit was purchased from Analytical Luminescence Laboratory (San Diego, CA). Antibodies specific for CREB, P-CREB (Ser^{133}), and phospho-ATF-2 and the ATF-2 fusion protein were obtained from New England Biolabs (Beverly, MA). Antibody to p38 MAPK (C-20) was obtained from Santa Cruz Biotechnology, Inc. (Santa Cruz, CA), and the dual phosphorylation site-specific antibody to p38 MAPK was a gift from Dr. Eric Schaefer (Promega). Plasmids for transfection experiments were purified using Qiagen's (Valencia, CA) Maxi kit. All other fine chemicals were purchased from Sigma.

Cell Culture—Rat pheochromocytoma (PC12) cells (provided by Dr. Gary Johnson (Denver, CO) and Drs. Derek LeRoith and Marcelina Parrizas (NIDDK, National Institutes of Health, Bethesda, MD) were maintained in Dulbecco's modified Eagle's medium containing 10% fetal bovine serum, 5% heat-inactivated horse serum, 100 μg/ml streptomycin, and 100 microunits/ml penicillin at 37 °C. The cells were cultured in 60-mm dishes for immunoblotting experiments and in 6 × 35-mm wells for transfection studies. Medium was changed every second day. Confluent cell cultures were split 1:4 and used for the experiments 4 days later. The cells were fasted for 5 h by maintaining them in the medium containing 0.1% fetal bovine serum and 0.05% heat-inactivated horse serum before treatment with growth factors and other agents in the experiments for measuring CREB phosphorylation. The stock solutions of pharmacological inhibitors such as PD98059, wortmannin, and SB203580 were prepared in Me_2SO at a concentration of 1000-fold, so that when they were added to the culture medium, the concentration of Me_2SO was below 0.1%.

Immunoblotting—Immunoblotting for CREB, phospho-CREB, p38 MAPK, and dual phospho-p38 MAPK were carried out as described previously (29, 30). PC12 cells cultured in 60-mm dishes were fasted for 5 h before each experiment. After preincubation with inhibitors for 30 min and incubation with growth factors for appropriate duration, the cells were washed twice with ice-cold PBS, and total cell lysates were prepared by scraping the cells with 200 μl of 1× Laemmli sample buffer containing 100 mM dithiothreitol. The proteins were resolved on 12% SDS-polyacrylamide gels and transferred to polyvinylidene difluoride membranes. The blots were blocked with TBST (20 mM Tris-HCl, pH 7.9, 8.5% NaCl, and 0.1% Tween 20) containing 5% nonfat dry milk (blotting grade) at room temperature for 1 h. The blots were then treated with the primary antibody for P-CREB in TBST containing 5% bovine serum albumin at 4 °C overnight. After three washes with blocking buffer, the blots were incubated with anti-rabbit IgG conjugated to alkaline phosphatase for 1 h at room temperature. This was followed by three washes with blocking buffer, two washes with 10 mM Tris-HCl (pH 9.5), 10 mM NaCl, 1 mM $MgCl_2$, and a 5-min incubation with diluted CDP-Star reagent (New England Biolabs, Beverly, MA) and then exposed to x-ray film. The membranes were then stripped in the buffer containing 62.5 mM Tris-HCl, pH 6.7, 2% SDS, and 100 mM β-mercaptoethanol and reprobed with antibody for CREB by a similar procedure. The intensity of the bands was quantitated by scanning. The extent of CREB phosphorylation was measured by calculating the ratio of P-CREB and CREB bands.

For phospho-p38 and p38, the blots were incubated with the primary antibody against dually phosphorylated p38 (Promega anti-active p38; 140 ng/ml) in TBST for 1 h at room temperature. After three washes with TBST, the blots were incubated with anti-rabbit IgG conjugated to horseradish peroxidase for 1 h at room temperature. This was followed by three washes in TBST and incubation with diluted ECL chemiluminescent reagent for 1 min. The membranes were then stripped and reprobed with antibody against p38 (C-20, Santa Cruz Biotechnology; 50 ng/ml).

p38 MAPK Assay—The cells were treated with IGF-I and inhibitor as described in the figure legends. After washing the cells with PBS, 200 μl of ice-cold cell lysis buffer (20 mM Tris (pH 7.5), 150 mM NaCl, 1 mM EDTA, 1 mM EGTA, 1% Triton X-100, 2.5 mM sodium pyrophosphate, 1 mM β-glycerophosphate, 1 mM sodium orthovanadate, 10 μg/ml leupeptin, 500 nM okadaic acid, and 1 mM phenylmethylsulfonyl fluoride) was added. The cells were scraped, lysed by sonication, and centrifuged for 20 min to collect the supernatant. The lysate (300 μg) was mixed with 4 μl of p38 MAPK antibody overnight at 4 °C. Protein A-Sepharose (20 μl) was added and gently rocked for 3 h at 4 °C. After centrifugation, the pellet was washed twice with cell lysis buffer and twice with kinase assay buffer (25 mM Tris (pH 7.5), 5 mM β-glycerophosphate, 2 mM dithiothreitol, 0.1 mM sodium orthovanadate, 10 mM $MgCl_2$). The pellet was suspended in 30 μl of kinase buffer with 200 μM ATP and 2 μg of ATF-2 fusion protein and incubated for 30 min at 30 °C. The reaction was terminated by the addition of 10 μl of 4× Laemmli sample buffer. These samples were electrophoresed and immunoblotted with antibody to phospho-ATF-2. The intensities of the bands were measured by scanning.

Isolation of Total RNA and Northern Blot Analysis—PC12 cells (90% confluence) were cultured in fasting medium in the absence and presence of 100 ng/ml IGF-I for 24 h. Total RNA was isolated from these cells using the Qiagen RNeasy kit. RNA samples were fractionated on denaturing 1.2% agarose-formaldehyde gels and transferred to Hybond N+ membrane. The 1.6-kilobase pair *Xho*I/*Eco*RI insert of rat chro-

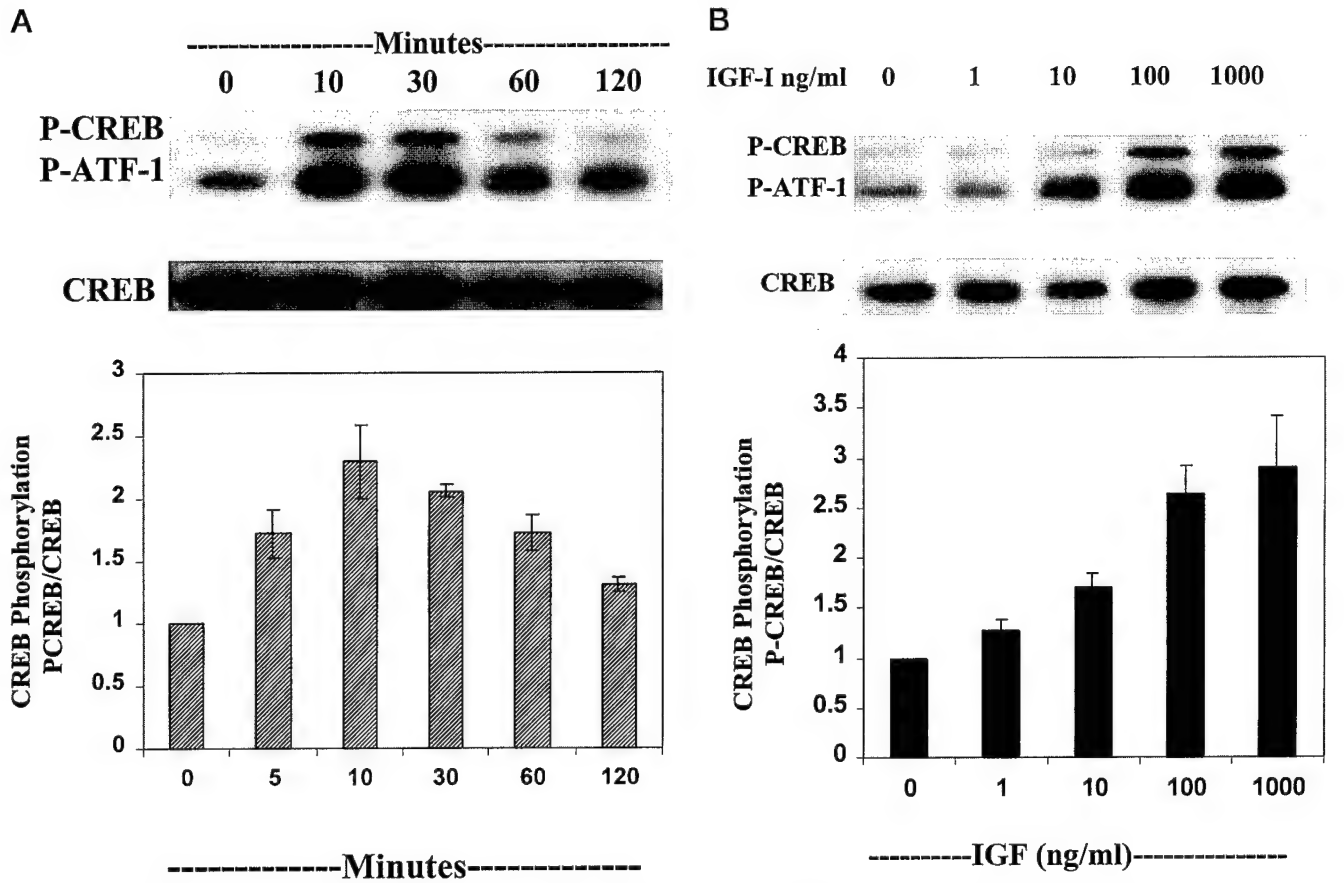

FIG. 1. **Dose- and time-dependent CREB phosphorylation mediated by IGF-I.** PC12 cells were cultured in 60-mm dishes to near confluence and then maintained in serum-free medium for 5 h. They were treated with 100 ng/ml IGF-I for varying periods of time, from 10 to 120 min (*A*). In another set of experiments, the fasted cells were exposed to increasing concentrations of IGF-I for 10 min (*B*). The cells in both experiments were washed in ice-cold PBS at the end of incubation period, and the cell lysates were prepared by the addition of 200 μl of warm 1× Laemmli sample buffer followed by sonication. The samples containing equal amounts of proteins were electrophoresed and immunoblotted with the antibody specific for CREB phosphorylated at Ser^{133}. The membranes were stripped and reprobed with CREB antibody. Quantitation of specific bands was done by scanning densitometry. The ratio of phosphorylated CREB over the nonphosphorylated form was calculated, and this value for the untreated cells was taken as 1. The results are the mean ± S.E. of four independent experiments.

mogranin A cDNA probe was labeled with thermostable alkaline phosphatase using the AlkPhos-Direct kit from Amersham Pharmacia Biotech. Hybridization, washing, and detection by CDP-Star were performed according to manufacturer's protocol. The blots were stripped and reprobed with labeled β-actin by a similar protocol. The expression of chromogranin A was normalized to β-actin expression.

Transfection Procedure—The PC12 cells were cultured to 60–80% confluence for transfection experiments in 6 × 35-mm plates. For each well, 2 μg of plasmids and 20 μg of LipofectAMINE reagents (Life Technologies, Inc.) were used as per the manufacturer's instructions. The plasmid containing the β-galactosidase gene driven by the SV_{40} promoter was included to normalize the transfection efficiency. DNA and the LipofectAMINE reagent were diluted separately in 100 μl of serum-free medium without antibiotics, mixed together, and incubated at room temperature for 30 min. The culture plates were washed with PBS and 800 μl of serum, and antibiotic-free medium was added. The 200 μl of the plasmid LipofectAMINE mixture was then added to each well, and the plates were incubated at 37 °C for 4 h. Then 1.0 ml of high serum medium (20% fetal bovine serum and 10% heat-inactivated horse serum) was added and incubated for approximately 40 h before induction with growth factors for luciferase. After 4 h of induction, the cells were washed in PBS and lysed with 100 μl of reporter lysis buffer. In the case of chromogranin A promoter constructs, the induction was 24 h after transfection for a period of 30 h. The cells were lysed by freezing and thawing, and lysate was centrifuged at 14,000 rpm for 30 min. The supernatant was used for the assay of luciferase and β-galactosidase. Luciferase assays were carried out using the enhanced luciferase assay kit (Analytical Luminescence Laboratory, San Diego, CA) on a Monolight 2010 luminometer. The β-galactosidase assay was performed according to the method of Wadzinski *et al.* (31).

Statistical analysis was carried out by Student's *t* test.

RESULTS

Dose- and Time-dependent Phosphorylation of CREB at Ser^{133} by IGF-I—The nuclear transcription factor CREB was phosphorylated in a time-dependent manner in response to IGF-I. There was a 2.3-fold ($p < 0.001$) increase in CREB phosphorylation at serine 133 (Fig. 1*A*) at 10 min when PC12 cells were stimulated with IGF-I (100 ng/ml). The phosphorylation returned to near basal level by 120 min. The protein level of CREB did not change during this 2-h period in the presence of IGF-I. The time course of CREB phosphorylation mediated by IGF-I was comparable with that of insulin in 3T3-L1 fibroblasts as reported earlier (29). The dose-response curve shows a significant increase in CREB phosphorylation at 10 ng/ml ($p < 0.05$) with dose-dependent increases at higher concentrations (Fig. 1*B*). We observed an additional band with the antibody specific for the phosphorylation sequence around serine 133 of CREB. Serine 63 phosphorylation of ATF-1 is known to be detected by the same antibody as serine 133-phosphorylated CREB, since they are 100% homologous for this consensus phosphorylation sequence (32). The phosphorylation pattern of ATF-1 was parallel to that of CREB in terms of both intensity and time course.

Multiple Signaling Pathways Are Involved in IGF-I-mediated Phosphorylation of CREB—To explore the role of different signaling pathways in CREB phosphorylation, we examined the effect of PD98059 (an inhibitor of MEK) and wortmannin

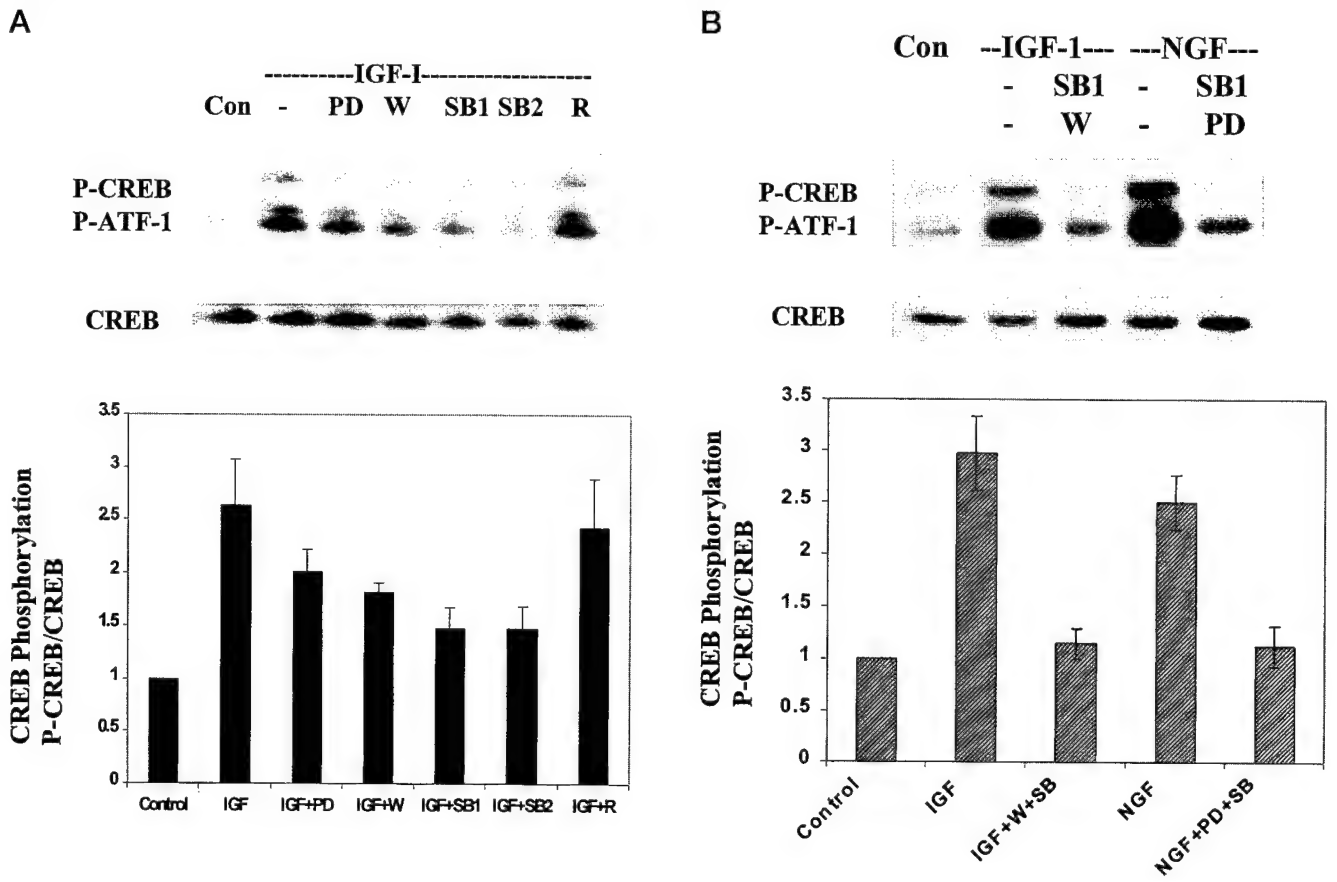

FIG. 2. **Effect of pharmacological inhibitors on growth factor-mediated CREB phosphorylation.** PC12 cells (90% confluent) were fasted for 5 h and preincubated with 30 μM PD98059 (*PD*), 100 nM wortmannin (*W*), 10 μM SB203580 (*SB1*), 10 μM SB202190 (*SB2*), and 10 ng/ml rapamycin (R) for 30 min followed by incubation with 100 ng/ml IGF-I (*A*). In some experiments, the cells were preincubated with combinations of inhibitors before treating them with 100 ng/ml IGF-I or 50 ng/ml NGF (*B*). The cells were washed with ice-cold PBS, solubilized, and immunoblotted for P-CREB. The membranes were stripped and reprobed with the antibody to CREB. The inhibitors did not have any significant effect on CREB phosphorylation and its protein level in control cells (results not shown). The results are the mean ± S.E. of three independent experiments.

(an inhibitor of PI 3-kinase) on IGF-I-induced CREB phosphorylation. In addition, we examined the effects of SB203580 and SB202190, two specific inhibitors of p38 MAPK (33, 34). This protein kinase has been shown to mediate the effects of fibroblast growth factor and NGF on CREB phosphorylation. As shown in Fig. 2*A*, preincubation of PC12 cells with PD98059 (30 μM) or wortmannin (100 nM) resulted in a 25–30% decrease in IGF-I-mediated CREB phosphorylation at serine 133. The addition of 30 μM PD98059 decreased the induction of ERK1/2 MAPK activity as detected by dual phospho-ERK antibody (Promega, Madison, WI) (data not shown). The findings with wortmannin clearly indicate that the PI 3-kinase mediates IGF-I-induced nuclear signaling in addition to the regulation of cytosolic proteins such as glycogen synthase. The inhibitors of p38 MAPK, SB203580 (10 μM), and SB202190 (10 μM) were able to decrease the CREB phosphorylation stimulated by IGF-I significantly ($p < 0.001$), suggesting a novel pathway for nuclear signaling of this growth factor. Rapamycin, an inhibitor of p70 S6 kinase, which is one of the downstream components of the PI 3-kinase signaling system, had no significant impact on IGF-I-induced CREB phosphorylation.

The neurotrophic actions of IGF-I are similar to those of NGF in PC12 cells. Therefore, we compared the effects of IGF-I and NGF on CREB phosphorylation. The partial reduction in NGF-mediated CREB phosphorylation in the presence of individual inhibitors was similar to that of IGF-I (data not shown) with the minor difference that PD98059 was more effective than wortmannin in decreasing NGF-induced CREB phosphorylation. In some experiments, combinations of inhibitors were shown to block the effects of growth factors completely (Fig. 2*B*). For example, in the presence of wortmannin (100 nM) and SB203580 (10 μM), IGF-I did not increase CREB phosphorylation above basal level. The inhibitors PD98059 (30 μM) and SB203580 (10 μM) used together blocked NGF action. For the remainder of the studies, parallel experiments were conducted with NGF as a control. The NGF data will only be presented for selected experiments.

IGF-I Activates p38 MAPK in PC12 Cells—The experiments with pharmacological inhibitors demonstrated that multiple signaling pathways mediate IGF-I-induced phosphorylation of CREB, including ERK, PI 3-kinase, and p38 MAPK. Growth factors have been shown to activate p38 in neuronal cell lines (26, 35, 36). Because the pharmacological inhibition of p38 with the SB compounds suggested a role for p38, we examined p38 activity in response to IGF-I in these cells. To examine whether IGF-I activates p38 MAPK in PC12 cells, experiments were carried out to measure the formation of phospho-p38 MAPK, the active form of this enzyme. As shown in Fig. 3*A*, IGF-I increased the phosphorylation of p38 significantly ($p < 0.001$) over the untreated cells in 5 min and slowly decreased over the remaining 2-h incubation period. Sodium arsenite is a known stimulator of p38 MAPK activity, and it serves as a control for the immunoprecipitation kinase assay. When p38 MAPK was assayed in PC12 cells treated with IGF-I (100 ng/ml) and sodium arsenite (300 μM) by immunoprecipitation followed by phosphorylation of ATF-2 phosphoprotein, 78 and 145% in-

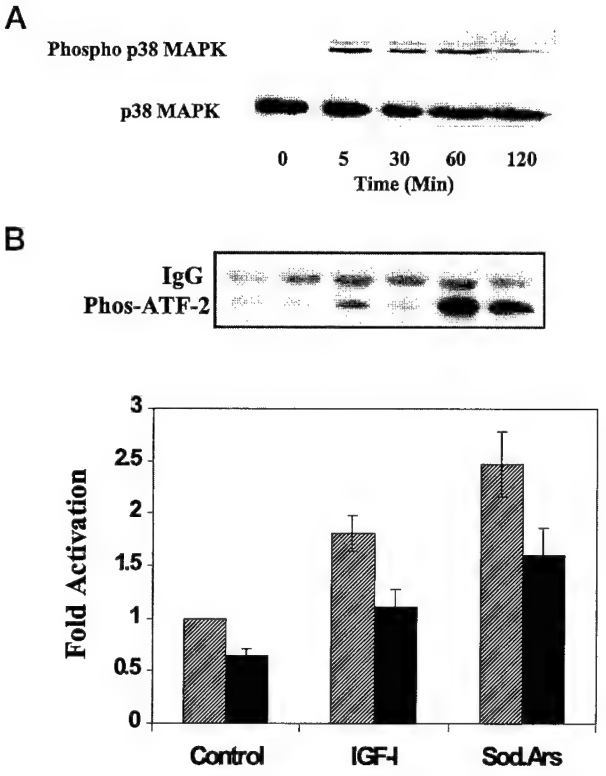

FIG. 3. **Activation of p38 MAPK by IGF-I.** PC12 cells (90% confluent) were fasted for 5 h and exposed to IGF (100 ng/ml) for varying time periods (*A*). The cells were washed and harvested for immunoblotting with the antibody to phospho-p38 MAPK. The membranes were then stripped and reprobed with the antibody to p38 MAPK. In some experiments, the fasted cells were preincubated in the absence (▨) and presence (■) of 10 μM SB203580 for 30 min followed by incubation with IGF (100 ng/ml) for 10 min or sodium arsenite for 300 μM for 1 h (*B*). The activity of p38 MAPK was measured by immunoprecipitating the cell lysates with p38 MAPK antibody and phosphorylating ATF-2 fusion protein followed by immunoblotting phospho-ATF-2. Quantitation of the bands was done by scanning densitometry. The values are the means of three observations.

creases in the enzyme activity were observed, respectively. Pretreatment of cells with the inhibitor SB203580 (10 μM) decreased the stimulated enzyme activity significantly ($p < 0.01$).

IGF-I-mediated CREB Phosphorylation Does Not Involve cAMP-dependent Protein Kinase (Protein Kinase A)—CREB was initially described as a substrate for protein kinase A (23). Therefore, we assessed the role of protein kinase A in IGF-I induced CREB phosphorylation using H89, a pharmacologic inhibitor that specifically inhibits this kinase (data not shown). This inhibitor decreased the formation of P-CREB mediated by dibutyryl cAMP (500 μM) and forskolin (10 μM) significantly ($p < 0.001$). H89 did not block IGF-I and NGF-mediated increases in P-CREB formation.

IGF-I Mediated CREB Phosphorylation Leads to Its Transcriptional Activation—CREB phosphorylation at serine 133 is essential for transcriptional activation, but under some conditions this phosphorylation is inadequate to drive transcription (37). Thus, it was essential to determine whether IGF-I-mediated CREB phosphorylation enhanced its transcriptional activation. For initial experiments, we used a Gal4-TK-Luc reporter system specific for the transactivation of CREB. Since endogenous transcription factors do not bind to the promoter pGal4-TK-Luc, the increase in luciferase activity in the presence of IGF-I is a measure of the stimulation of the transactivational potency of the Gal-CREB chimeric protein through phosphorylation. PC12 cells were transiently transfected with an expression vector for a chimeric protein consisting of the Gal4 DNA binding domain linked to the transactivation domain of CREB and a plasmid containing the luciferase reporter gene linked to an enhancerless thymidine kinase promoter and four copies of Gal4-responsive sequences. By this approach, one could eliminate other CRE-binding endogenous transcription factors binding to the reporter gene. This permits evaluation of the pathways leading specifically to CREB activation. IGF-I increased transcription in a dose-dependent manner to a maximum of 3-fold in this system (Fig. 4*A*). No transcriptional activation was noted in the control experiments without the Gal4-CREB chimeric protein (results not shown). To optimize cell viability after transient transfection, the cells were maintained in serum during the induction with growth factors, because PC12 cells undergo programmed cell death with serum withdrawal. This contributes to the high basal CREB transcriptional activity and also represents the normal physiological context. Consistent increases over the physiological background were noted in response to IGF-I.

To determine the functional significance of phosphorylation of serine 133 by IGF-I for activation of this transcriptional reporter, cotransfection experiments were carried out using the expression vector for Gal4-CREB in which serine was replaced with alanine at position 133. When cotransfected with pGal4-TK-Luc, this mutated fusion protein did not induce luciferase expression significantly when compared with the wild type Gal4-CREB (Fig. 4*B*). Treatment with growth factors did not further enhance the luciferase expression.

IGF-I-mediated Transcriptional Activation of CREB Parallels the Regulation of CREB Phosphorylation—A parallel set of experiments to those described for CREB phosphorylation in Fig. 2 was undertaken to determine the contribution of MEK, p38 MAPK, PI 3-kinase, and p70 S6 kinase in the transcriptional activation of CREB. PC12 cells transfected with pGal4-TK-Luc and pGal-CREB were preincubated with PD98059 (30 μM), wortmannin (100 nM), SB203580 (10 μM), and SB202190 (10 μM). These additions decreased IGF-I-mediated CREB-TA by 27, 44, 31, and 34%, respectively (Fig. 5*A*). Rapamycin did not have any effect on the transcriptional activation by IGF-I. In the case of NGF, significant decreases (25–35%) in transcriptional activation were exerted by the inhibitors PD98059 (30 μM), wortmannin (100 nM), SB203580 (10 μM), and SB202190 (10 μM) (data not shown). As with IGF-I, rapamycin had no effect on NGF action. The inhibition of transcriptional activation by these inhibitors was partial when used alone. Parallel to our observation of the impact of combined inhibitors in Fig. 2, IGF-I-induced luciferase production was decreased to the basal level when the cells were preincubated with wortmannin and SB203580 together (Fig. 5*B*). These findings clearly demonstrate that IGF-I uses novel signaling pathways to increase the transcriptional activation of CREB in PC12 cells.

IGF-I Activates Transcription of CRE-containing Chromogranin A Promoter Constructs—Once the transcriptional activating potential of IGF-I on CREB had been determined using the Gal4-TK-Luc reporter system, we did a series of experiments to assess the physiological relevance of CREB activation by IGF-I. For these experiments, we employed the neuronal specific CRE-containing chromogranin A promoters. The promoter with 1133 bp of 5′-flanking region was stimulated 3.3-fold by IGF-I, whereas the truncated promoter with the CRE (pXP77) was activated 2.5-fold. To determine whether this activity was dependent upon CREB, we did a series of experiments cotransfecting a dominant negative CREB, K-CREB, as well as the truncated chromogranin A promoter with the CRE site mutated (Fig. 6*A*). The dominant negative K-CREB decreased basal and total IGF-I stimulation compared

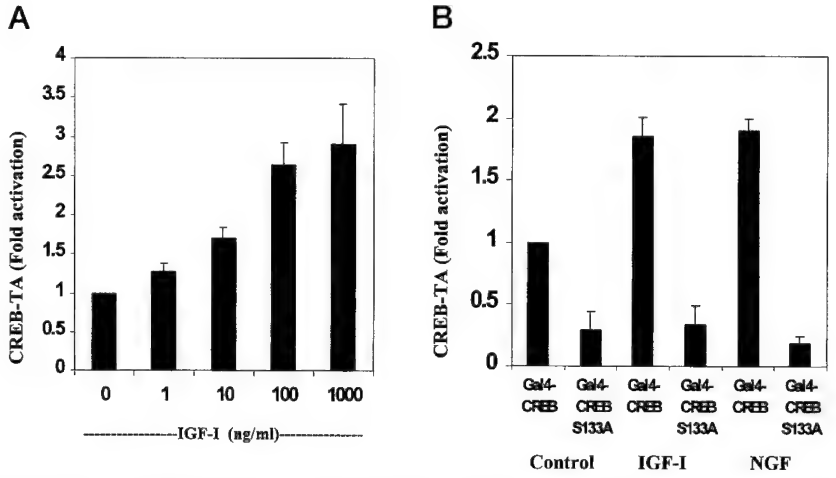

FIG. 4. **Transcriptional activation of CREB by IGF-I in PC12 cells.** PC12 cells were cultured in 6 × 35-mm wells to around 70% confluence. The cells were cotransfected with pGal4-TK-Luc, pRSV-Gal4-CREB-341, and pRSV β-galactosidase in the medium containing no serum and antibiotics by the LipofectAMINE transfection method for 4 h. For each well, 2 μg of plasmids and 20 μg of LipofectAMINE reagent were used. Induction for luciferase with different agents for 4 h was carried out 48 h after the initiation of transfection. *A*, the transfected cells were incubated with varying doses of IGF-I as indicated. *B*, in the transfection protocol for this experiment either pRSV-Gal4-CREB or pRSV-Gal4-CREB S133A was used, and later the transfected cells were induced with 100 ng/ml IGF or 50 ng/ml NGF. Cell lysates were prepared, and the transcription was measured by assaying the luciferase activity by the procedure described under "Experimental Procedures." In these lysates, β-galactosidase activity was also assayed to correct for the efficiency of transfection. The transcription mediated by IGF-I and other agents was expressed as -fold induction over the basal transcription in transfected but untreated cells. Results are means ± S.E. of three independent experiments.

with controls, as did the CRE mutant. Some increase in activity was seen in response to IGF-I, indicating both CREB-dependent and CREB-independent regulation of chromogranin A by IGF-I. We also noted a 3.7-fold increase in chromogranin A mRNA when PC12 cells were exposed to 100 ng/ml of IGF-I for 24 h (Fig. 6*B*), demonstrating that the endogenous gene and the reporter constructs respond similarly.

Impact of Constituitively Active or Dominant Negative Ras and Raf-1 on IGF-I-mediated Stimulation of Chromogranin A—Pharmacological inhibition of MEK using PD98059 (Figs. 2 and 5) indicated a role for the ERK1/2 MAPK cascade in IGF-I regulation of CREB activity. To confirm these data using another strategy, we cotransfected PC12 cells with a truncated CREB-responsive chromogranin A reporter construct and plasmids for constitutively active Ras and Raf-1 (pSVRas and pRSV BxBraf, respectively) or dominant negative Ras (pZCRN17Ras). Activation of the Ras → Raf → MEK → ERK pathway using the constitutively active iosforms of either Ras or Raf-1 (Fig. 7*A*) led to a significant increase in basal chromogranin A activity, demonstrating responsiveness to this pathway. IGF-I treatment gave an additional stimulation of 1.5-fold over the high basal level, suggesting that there are other pathways in addition to ERK1/2 that contribute to the IGF-I response. Dominant negative Ras decreased basal activity with a restoration toward basal upon exposure to IGF-I. Taken together, these data support a role for ERK1/2 activation of chromogranin A by IGF-I. They also suggest that additional pathways are involved.

Role of PI 3-Kinase in the IGF-I-mediated Activation of Chromogranin A—The PI 3-kinase inhibitor data suggested that one of the additional pathways involved PI 3-kinase. As demonstrated in Figs. 2*A* and 5*A*, wortmannin, an inhibitor of PI 3-kinase, interferes with both CREB phosphorylation and its transcriptional activation by IGF-I. Hence, we examined the effect of transient transfection of wild-type and dominant negative p85 subunits (courtesy of Dr. Masato Kasuga, Kobe, Japan) in PC12 cells. The wild type p85 subunit exerted a small increase in basal and IGF-I-mediated transcriptional activation, whereas Δp85, the kinase-dead PI 3-kinase isoform, inhibited IGF-I activation of chromogranin A ($p < 0.001$). These results demonstrate a PI 3-kinase-dependent activation of chromogranin A in PC12 cells.

MAPK Kinase 6 and p38β Enhance the Activation of Chromogranin A Promoter by IGF-I—Previous studies have indicated that, among p38 MAPK isozymes, the β isoform is involved in the hypertrophic action. Hence, we cotransfected the PC12 cells with p38β and the constitutively active form of its upstream kinase, MAPK kinase 6, and examined the promoter activity of chromogranin A (pXp77). The stimulation of p38β resulted in the increase of basal and IGF-I-induced chromogranin A promoter activity by 80–90%. This increase was significantly ($p < 0.001$) blocked when the cells were preincubated with the p38 MAPK inhibitor SB203580 (10 μM). The results of this experiment further support the role of the p38 MAPK pathway in IGF-I-mediated activation of the nuclear transcription factor CREB.

DISCUSSION

In this investigation, we demonstrate that IGF-I stimulates phosphorylation of the nuclear transcription factor, CREB, the Ca^{2+}/cAMP response element-binding protein, at serine 133 in PC12 cells. This post-translational modification leads to an increase in CREB's transcriptional activity as demonstrated by the Gal4-TK-Luc reporter system. IGF-I is also capable of regulating chromogranin A, a neuroendocrine-specific gene, by a CREB-dependent mechanism. Using specific inhibitors such as PD98059, SB203580, or wortmannin or by cotransfecting constitutively active and dominant negative components of the Ras and PI 3-kinase pathways, we demonstrate that IGF-I-mediated CREB activation proceeds through three distinct pathways involving ERK, PI 3-kinase, and p38 MAPK. IGF-I is known to exert its actions on cellular proliferation, survival, and differentiation through the ERK and PI 3-kinase pathways. In this study, we show for the first time that some of the CREB-dependent gene regulatory actions of IGF-I proceed through the p38 MAPK pathway.

In neuronal cells, the nuclear transcription factor CREB plays a central role in several critical functions. It is important for protein synthesis-dependent long term memory formation, since targeted mutation of CREB leads to a decrease in long term memory in mice (14, 15). Hormonal regulation of dentritic spine formation in cultured hippocampal neurons requires the phosphorylation of CREB (19). In PC12 cells, a cell culture

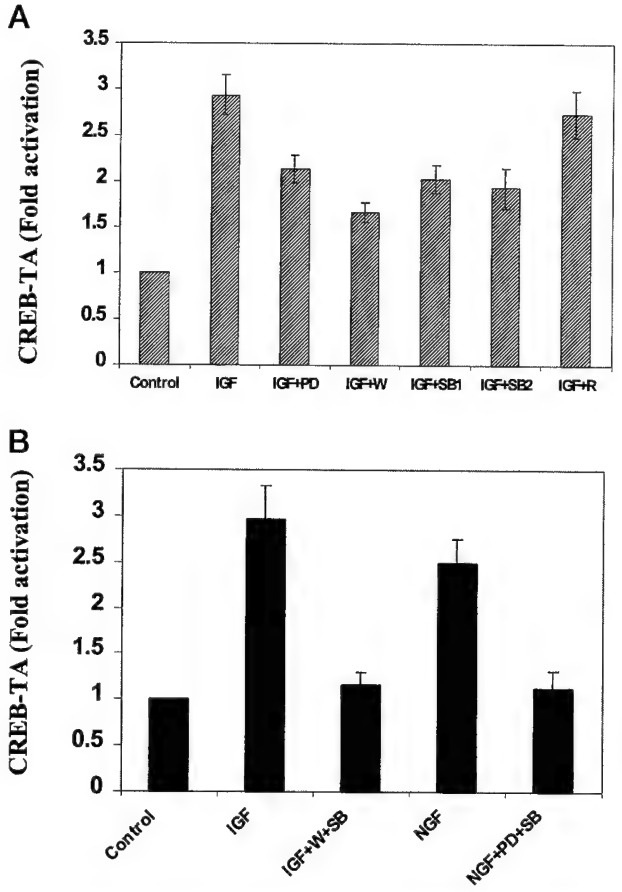

FIG. 5. **Growth factor-mediated CREB activation involves multiple signaling pathways in PC12 cells.** PC12 cells cultured in 6 × 35-mm wells were transfected with pGal4-TK-Luc, pRSV-Gal4-CREB-341, and pRSV β-galactosidase for 4 h by the LipofectAMINE transfection method using 2 μg of total plasmids and 20 μg of LipofectAMINE reagent. After 48 h, the cells were first exposed to the 30 μM PD98059 (*PD*), 100 nM wortmannin (*W*) 10 μM SB203580 (*SB1*), 10 μM SB202190 (*SB2*), and 10 ng/ml rapamycin (*R*) for 30 min and then incubated with 100 ng/ml IGF-I (*A*) for 4 h. In some experiments, the cells were preincubated with combinations of inhibitors before exposure to 100 ng/ml IGF-I or 50 ng/ml NGF (*B*). The activities of luciferase and β-galactosidase were measured in the cell lysates. The -fold increases in CREB activation by IGF-I and NGF were calculated after correcting for transfection efficiency. The values represent means ± S.E. of three observations.

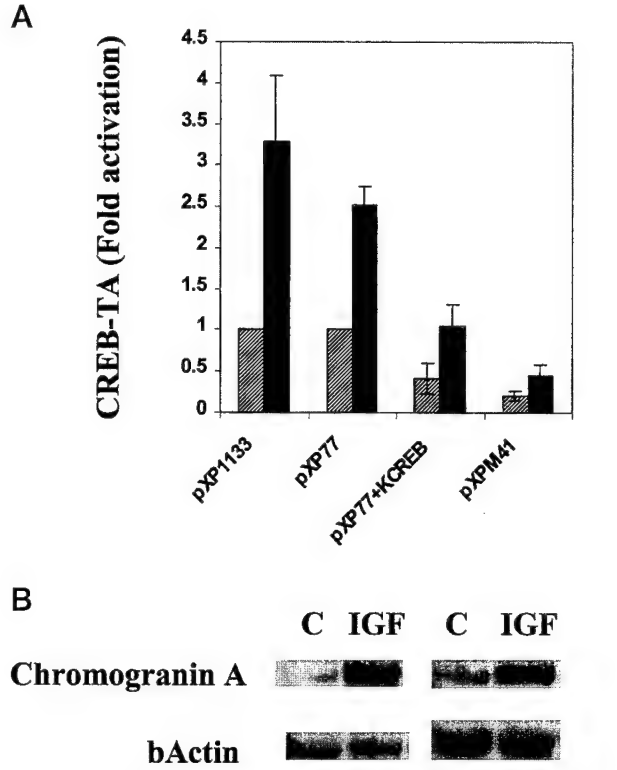

FIG. 6. **IGF-I-mediated induction of the chromogranin A gene in PC12 cells.** *A*, PC12 cells were cultured in 6 × 35-mm wells to around 70% confluence. The cells were cotransfected with pxP1133, pxP77, pxPM41, and pxP77 with dominant negative K-CREB and pRSV β-galactosidase for 4 h by the LipofectAMINE transfection method using 2 μg of total plasmids and 20 μg of LipofectAMINE reagent. After 24 h, the cells were cultured in the absence (▨) and presence (■) of 100 ng/ml of IGF for 30 h. The cell lysates were prepared, and luciferase and β galactosidase were assayed. Results are means ± S.E. of three independent experiments. *B*, PC12 cells (90% confluent) were cultured in fasting medium in the absence and presence of 100 ng/ml IGF for 24 h. Total RNA was isolated from these cells using Qiagen's RNeasy kit. RNA 10-μg samples were resolved on formaldehyde-agarose gels and transferred to Hybond N+ membranes and probed with the chromogranin A cDNA probe labeled with alkaline phosphatase and detected with the CDP-Star system. The blots were then stripped and reprobed with labeled β-actin by a similar procedure. Two representative blots from the set of five are shown here.

model of neurons, the CREB/ATF-1 family of transcription factors are needed for the neurite outgrowth (38). Dominant negative ATF-1 blocks cAMP-induced neurite formation by inhibiting cAMP-mediated CREB activation in these cells (38). Interference of CREB and other ATF family members with E1A viral antigen also blocks PC12 cell differentiation (13). Additionally, CREB is critical for the induction of immediate early gene c-*fos* by NGF (12). The promoter regions of several neuronal specific genes such as chromogranin A (CgA) and *vgf* contain CREB response elements. Because of the diverse neuronal responses that require CREB, it is important to understand the specific mechanisms whereby IGF-I, an important neurotrophin, regulates CREB dependent transcription.

CREB is regulated by multiple factors in PC12 cells including forskolin, NGF, epidermal growth factor, and 12-*O*-tetradecanoylphorbol-13-acetate (12, 28). These diverse stimuli can result in divergent cell fates including proliferation and differentiation. With respect to the diversity of factors that can impact CREB- and CRE-regulated transcription, we present important new information on CREB regulation by IGF-I in PC12 cells. We present convincing data that IGF-I treatment at a physiologically relevant concentration leads to transcriptionally important phosphorylation of CREB at serine 133. Additionally, CREB activation plays a major role in the IGF-I-mediated regulation of the neuronal specific chromogranin A gene. We see an impact of IGF-I on both the chromogranin A promoter and induction of chromogranin A mRNA. The experiments described define many parallels between NGF and IGF-I for CREB regulation in this cell line. Both agents employ multiple signaling pathways for CREB regulation. From inhibitor studies, it appears that the dominant pathways for IGF-1 are p38 MAPK and PI 3-kinase, whereas MEK is the dominant pathway for NGF with a contribution from p38 MAPK. This role of p38 MAPK activation by growth factors is a new and rapidly evolving area of research. The current data do not permit a detailed comparison between the IGF-I and NGF, but the differences noted between the two neurotrophins could provide insight into their divergent impacts on cell fate, survival, and proliferation.

IGF-I has been shown to have significant neurotrophic actions such as survival and regeneration of neurons (4, 5). In diabetes, IGF-I activity is decreased in neuronal tissues, and this could contribute to the development of diabetic neuropathy (39). IGF-I is being considered as a potential therapeutic agent

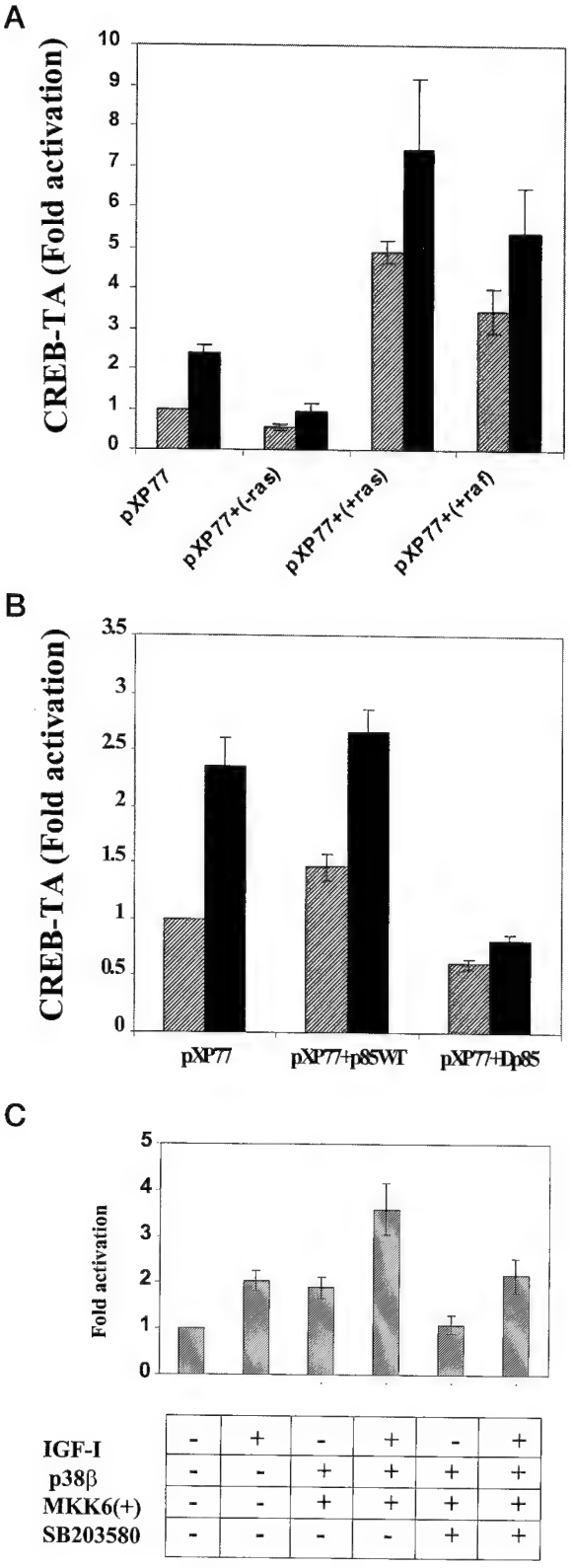

FIG. 7. **Activation of chromogranin A promoter by IGF through multiple signaling pathways.** PC12 cells (70% confluence) cultured in 6 × 35-mm wells were transfected with pxP77 and pRSV β-galactosidase along with indicated plasmids for 4 h by the LipofectAMINE transfection method using 2 μg of total plasmids and 20 μg of LipofectAMINE reagent. In these transfection experiments, plasmids for the modulation of signaling pathways involving Ras (*A*), PI 3-kinase (*B*), and p38β (*C*) were also included. After 1 day of transfection, the cells were cultured in the absence (▨) and presence (■) of 100 ng/ml IGF-I (*A* and *B*) or as indicated (*C*) for 30 h. The activities of luciferase and β-galactosidase were measured in the cell lysates. The -fold increases in CREB activation by IGF-I and NGF were calculated after correcting for transfection efficiency. The values represent means ± S.E. of three observations.

in the treatment of neurodegenerative diseases (40). For these reasons, it is essential to understand the mechanism by which this growth factor regulates gene expression in neuronal cells. Our present findings show that IGF-I mediated the activation of the nuclear transcription factor CREB through multiple signaling pathways and that this leads to enhanced expression of a neuroendocrine-specific gene, CgA. We chose to examine CgA because it is known to be regulated in a CREB-dependent manner in PC12 cells (27, 28). This tool establishes a neuronal context for the experiments designed to define the important signaling pathways. CREB is known to bind the promoters of mouse and human CgA (27, 41). In the present investigation, we observed an enhanced expression of CgA in IGF-I-treated PC12 cells, as measured by the Northern blot analysis of mRNA. Further, IGF-I-mediated activation of CREB through multiple signaling pathways leads to the stimulation of full-length as well as the CRE-containing truncated promoter of CgA. Studies with dominant negative K-CREB and the promoter containing mutated CRE clearly demonstrate that CREB plays a significant role in mediating IGF-I action. These findings indicate that IGF-I-stimulated CREB activation is involved in the physiologically relevant gene expression in neuronal cells.

Our observation that IGF-1 stimulates the phosphorylation of nuclear transcription factor CREB through a p38 MAPK is new, and the physiological relevance remains to be determined. To briefly review the current understanding of the p38 MAPK family, they are a family of serine/threonine kinases, activated by dual phosphorylation on threonine and tyrosine residues. In mammalian cells, three distinct MAPKs have been identified: ERK1/2, stress-activated protein kinase/c-Jun N-terminal kinase, and RK cytokine suppressive anti-inflammatory drug binding protein p38 MAPK. The pathways mediated by c-Jun N-terminal kinase and p38 MAPK have been shown to play a significant role in stress-mediated signal transduction. The p38 MAPK is associated with apoptosis, and it opposes the actions of ERK in PC12 cells (30, 42). However, p38 and ERK MAPKs cooperate in the transcriptional activation of c-*fos* in response to UV irradiation (43). Further, p38 MAPK participates in the protein phosphorylation cascade resulting from activation of growth factor/hormone receptors. For example, fibroblast growth factor activates p38 MAPK in SK-N-MC cells, and insulin stimulates this kinase in L6 muscle cells (26, 44). NGF has been shown to activate CREB through the ERK as well as p38 MAPK pathway (35). IGF-I stimulates p38 MAPK activity in SH-SY5Y neurobastoma cells (36). In a recent study, Scrimgeour *et al.* (45) used a mutant of the IGF-I receptor in which tyrosines at positions 1250 and 1251 in the carboxyl-terminal region had been replaced to demonstrate that some of the actions of IGF-I could involve a third pathway other than ERK and PI 3-kinase pathways. We support this possibility by showing in this study that IGF-I does activate CREB by a third pathway involving p38 MAPK. IGF-I-mediated phosphorylation and activation of CREB decreased significantly in the presence of SB203580. This pyridinyl imidazole derivative has been shown to be specific for p38 MAPK, and it did not have any inhibitory action toward 12 other protein kinases tested *in vitro* (34). Several isoenzymes of p38 MAPK have been identified that are likely to have differential actions (46, 47). Wang *et al.* demonstrated in cardiomyocytes that p38β mediates hypertrophic response, whereas p38α induces apoptosis (48). In a recent study, this β isoform has been also shown to provide

protective effect against apoptotic signals (49). We have also observed in the present study an increase of IGF-I-induced chromogranin A promoter activity when the PC12 cells were cotransfected with p38β and the constitutively active form of MAPK kinase 6.

IGF-I has been shown to activate the ERK and PI 3-kinase pathways in several cell types including PC12 cells (1, 6, 50, 51). In the present study, the MEK inhibitor (PD98059) partially decreases the phosphorylation and activation of CREB mediated by IGF-I. Figs. 2 and 5 demonstrate only a partial, albeit significant, inhibition of IGF-I-mediated CREB phosphorylation and activation using PD98059. Cotransfection experiments with constitutively active Ras and Raf-1 demonstrate a role for this pathway in the activation of CgA. However, IGF-I was able to drive transcription of CgA even in the face of constitutively active Ras and Raf-1. These data suggest that the Ras $\rightarrow$ Raf-1 $\rightarrow$ MEK pathway is important but is not the dominant pathway for IGF-1-mediated CREB activation. In a recent study, however, we observed that the ERK pathway plays a major role in the insulin-mediated CREB activation in HepG2 and 3T3-L1 cell line, suggesting cell-specific variations in signaling pathways. The PI 3-kinase pathway, which is critical for IGF-I-mediated neuronal survival under stress conditions, strongly contributes to IGF-I-mediated CREB activation. The importance of PI 3-kinase for IGF-I activation of CREB is clearly demonstrated by the wortmannin inhibitor studies. It is further supported by cotransfection of Δp85 PI 3-kinase, the kinase-dead mutant, which ablates IGF-I-mediated stimulation of CgA. Akt, the downstream component of the PI 3-kinase pathway, is known to regulate the covalent modification of cytosolic proteins such as glycogen synthase and the proapoptotic protein BAD in PC12 cells (51, 52). In the present study, we demonstrate the involvement of this pathway in the nuclear actions of IGF-I. It has been previously shown that the expression of Bcl-xL and the *bcl-2* are increased by IGF-I (21, 53). These proteins belong to the Bcl-2 family, which is known to protect the cells from programmed cell death (21). It is possible that IGF-I-mediated CREB activation is involved in the regulation of the expression of *bcl-2*, since it is a CREB-dependent gene (54).

To summarize, the data presented in this paper demonstrate IGF-1 activation of CREB, an important transcription factor for neurotrophin activity. This activation employs signaling pathways mediated by PI 3-kinase and p38 MAPK. Future studies will explore the implications of each of these signaling pathways for CREB-responsive genes important for cell cycle regulation, survival, and differentiation.

Acknowledgments—We thank Dr. William. J. Roesler, Dr. Arthur Gutierrez-Hartmann, Dr. Ulf Rapp, Dr. Masato Kasuga, and Dr. James Hoeffler for providing valuable reagents. We acknowledge the excellent secretarial support of Gloria Smith and the technical assistance provided by Ari Ballonoff and Kimberly Felder. We thank Dr. Boris Draznin for critically reading the manuscript.

REFERENCES

1. Coolican, S. A., Samuel, D. S., Ewton, D. Z., McWade, F. J., and Florini, J. R. (1997) *J. Biol. Chem.* **272,** 6653–6662
2. Valverde, A. M., Lorenzo, M., Navarro, P., and Benito, M. (1997) *Mol. Endocrinol.* **11,** 595–607
3. Engert, J. C., Berglund, E. B., and Rosenthal, N. (1996) *J. Cell Biol.* **135,** 431–440
4. Ishii, D. N., Glazner, G. W., and Pu, S.-F. (1994) *Pharmacol. Ther.* **62,** 125–144
5. D'Ercole, A. J., Ye, P., Calikoglu, A. S., and Gutierrez-Ospina, G. (1996) *Mol. Neurobiol.* **13,** 227–255
6. LeRoith, D., Werner, H., Beitner-Johnson, D., and Roberts, C. T., Jr. (1995) *Endocr. Rev.* **16,** 143–161
7. Saltiel, A. R. (1996) *Am. J. Physiol.* **270,** E375–E385
8. He, W., Craparo, A., Zhu, Y., O'Neill, T. J., Wang, L.-M., Pierce, J. H., and Gustafson, T. A. (1996) *J. Biol. Chem.* **271,** 11641–11645
9. Foncea, R., Andersson, M., Ketterman, A., Blakesley, V., Sapag-Hagar, M., Sugden, P. H., LeRoith, D., and Lavandero, S. (1997) *J. Biol. Chem.* **272,** 19115–19124
10. Kulik, G., Klippel, A., and Weber, M. J. (1997) *Mol. Cell. Biol.* (1997) **17,** 1595–1606
11. Meyer, T. E., and Habener, J. F. (1993) *Endocr. Rev.* **14,** 269–290
12. Ginty, D. D., Bonni, A., and Greenberg, M. E. (1994) *Cell* **77,** 713–725
13. Heasley, L. E., Benedict, S., Gleavy J., and Johnson, G. L. (1991) *Cell Regul.* **2,** 479–489
14. Guzowski, J. F., and McGaugh J. L. (1997) *Proc. Natl. Acad. Sci. U. S. A.* **94,** 2693–2698
15. Yin, J. C., and Tully, T., (1996) *Curr. Opin. Neurobiol.* **6,** 264–268
16. Bevilaqua, L., Ardenghi, P., Schroder, N., Bromberg, E., Quevedo, J., Schmitz, P. K., Bianchin, M., Walz, R., Schaeffer, E., Medina, M. J., and Izquierdo, I. (1997) *Braz. J. Med. Biol. Res.* **30,** 967–970
17. Martin, K. C., and Kandel, E. R. (1996) *Neuron* **17,** 567–570
18. Das, S., Grunert, M., Williams, L., and Vincent, S. R. (1997) *Synapse* **25,** 227–233
19. Murphy, D. D., Segal, M. (1997) *Proc. Natl. Acad. Sci. U. S. A.* **94,** 1482–1487
20. Finkbeiner, S., Tavazoie, S. F., Maloratsky, A., Jacobs, K. M., Harris, K. M., Greenberg, M. E. (1997) *Neuron* **19,** 1031–1047
21. Parrizas, M., and LeRoith, D. (1997) *Endocrinology* **138,** 1355–1358
22. Monnier, D., Boutillier, A. L., Giraud, P., Chiu, R., Aunis, D., Feltz, P., Zwiller, J., and Loeffler, J. P. (1994) *Mol. Cell. Endocrinol.* **104,** 139–145
23. Gonzalez, G. A., and Montminy, M. R. (1989) *Cell* **59,** 675–680
24. Xie, H., and Rothstein, T. L. (1995) *J. Immunol.* **154,** 1717–1723
25. Sheng, M., Thompson, M. A., and Greenberg, M. E. (1991) *Science* **252,** 1427–1430
26. Tan, Y., Rouse, J., Zhang, A., Cariati, S., Cohen, P., and Comb, M. J. (1996) *EMBO J.* **15,** 4629–4642
27. Wu, H., Mahata, S. K., Mahata, M., Webster, N. J. G., Parmer, R. J., and O'Connor, D. T. (1995) *J. Clin. Invest.* **96,** 568–578
28. Tang, K., Wu, H., Mahata, S. K., Taupenot, L., Rozansky, D. J., Parmer, R. J., and O'Connor, D. T. (1996) *J. Biol. Chem.* **271,** 28382–28390
29. Klemm, D. J., Roesler, W. J., Boras, T., Colton, L. A., Felder, K., and Reusch, J. E-B. (1998) *J. Biol. Chem.* **273,** 917–923
30. Kummer, J. L., Rao, P. K., and Heidenreich, K. A. (1997) *J. Biol. Chem.* **272,** 20490–20494
31. Wadzinski, B. E., Wheat, W. H., Jaspers, S., Peruski, L. F., Lickteig, R. L., Johnson, G. L., and Klemm, D. J. (1993) *Mol. Cell. Biol.* **13,** 2822–2834
32. Iordanov, M., Bender, K., Ade, T., Schmid, W., Sachsenmaier, C., Engel, K., Gaestel, M., Rahmsdorf, H. J., and Herrlich, P. (1997) *EMBO J.* **16,** 1009–1022
33. Lee, J. C., Laydon, J. T., McDonnell, P. C., Gallagher, T. F., Kumar, S., Green, D., McNulty, D., Blumenthal, M. J., Heys, J. R., Landvatter, S. W., Strickler, J. E., McLaughlin, M. M., Siemens, I. R., Fisher, S. M., Livi, G. P., White, J. R., Adams, J. L., and Young, P. R. (1994) *Nature* **372,** 739–746
34. Cuenda, A., Rouse, J., Doza, Y. N., Meier, R., Cohen, P., Gallagher, T. F., Young, P. R., and Lee, J. C. (1995) *FEBS Lett.* **364,** 229–233
35. Xing, J., Kornhauser, J. M., Xia, Z., Thiele, E. A., and Greenberg, M. E. (1998) *Mol. Cell. Biol.* **18,** 1946–1955
36. Cheng, H-L., and Feldman, E. L. (1998) *J. Biol. Chem.* **273,** 14560–14565
37. Lee, C. Q., Yun, Y., Hoeffler, J. P., and Habener, J. F. (1990) *EMBO J.* **9,** 4455–4465
38. Shimomura, A., Okamoto, Y., Hirata, Y., Kobayashi, M., Kawakami, K., Kiuchi, K., Wakabayashi, T., and Hagiwara, M. (1998) *J. Neurochem.* **70,** 1029–1034
39. Ishii, D. N. (1995) *Brain Res. Rev.* **20,** 47–67
40. Vinik, A. I., Newlon, P. G., Lauterio, T. J., Liuzzi, F. J., Depto, A. S., Pittenger, G. L., and Richardson, D. W. (1995) *Diabetes Rev.* **3,** 139–157
41. Canaff, L., Bevan, S., Wheeler, D. G., Mouland, A. J., Rehfuss, R. P., White, J. H., and Hendy, G. N. (1998) *Endocrinology* **139,** 1184–1196
42. Xia, Z., Dickens, M., Raingeaud, J., Davis, R. J., and Greenberg, M. E. (1995) *Science* **270,** 1326–1331
43. Price, M. A., Cruzalegui, F. H., and Treisman, R. (1996) *EMBO J.* **15,** 6552–6563
44. Tsakiridis, T., Taha, C., Grinstein, S., and Klip, A. (1996) *J. Biol. Chem.* **271,** 19664–19667
45. Scrimgeour, A. G., Blakesley, V. A., Stannard, B. S., and LeRoith, D. (1997) *Endocrinology* **138,** 2552–2558
46. Jiang, Y., Chen, C., Li, Z., Guo, W., Gegner, J. A., Lin, S., and Han, J (1996) *J. Biol. Chem.* **271,** 17920–17926
47. Li, Z., Jiang, Y., Ulevitch, R. J., and Han, J (1996) *Biochem. Biophys. Res. Commun.* **228,** 334–340
48. Wang Y., Huang, S., Sah, V. P., Ross, J., Jr., Brown, J. H., Han, J., and Chien, K. R. (1998) *J. Biol. Chem.* **273,** 2161–2168
49. Nemoto S., Xiang J., Huang, S., and Lin, A. (1998) *J. Biol. Chem.* **273,** 16415–16420
50. Parrizas, M., Saltiel, A. R., and LeRoith, D. (1997) *J. Biol. Chem.* **272,** 154–161
51. Yamamoto-Honda, R., Tobe, K., Kaburagi, Y., Ueki, K., Asai, S., Yachi, M., Shirouzu, M., Yodoi, J., Akanuma, Y., Yokoyama, S., Yazaki, Y., and Kadowaki, T. (1995) *J. Biol. Chem.* **270,** 2729–2734
52. Datta, S. R., Dudek, H., Tao, X., Masters, S., Fu, H., Gotoh, Y., and Greenberg, M. E. (1997) *Cell* **91,** 231–241
53. Singleton, J. R., Dixit, V. M., and Feldman, E. L. (1996) *J. Biol. Chem.* **271,** 31791–31794
54. Wilson, B. E., Mochon, E., and Boxer, L. M. (1996) *Mol. Cell. Biol.* **16,** 5546–5556

THE JOURNAL OF BIOLOGICAL CHEMISTRY Appendix 3 Vol. 275, No. 15, Issue of April 14, pp. 10761–10766, 2000
Printed in U.S.A.

Akt/Protein Kinase B Up-regulates Bcl-2 Expression through cAMP-response Element-binding Protein*

(Received for publication, November 3, 1999, and in revised form, January 3, 2000)

Subbiah Pugazhenthi‡§, Albina Nesterova‡§, Carol Sable§¶, Kim A. Heidenreich§¶, Linda M. Boxer‖, Lynn E. Heasley, and Jane E.-B. Reusch‡§‡‡**

*From the Departments of ‡Endocrinology, ¶Pharmacology, and **Medicine, University of Colorado Health Sciences Center, Denver, Colorado 80262, the §Section of Endocrinology, Veterans Affairs Medical Center, Denver, Colorado 80220, and ‖Department of Medicine, Stanford University School of Medicine, Stanford, California 94305*

In our previous study we showed that insulin-like growth factor-I induces a cAMP-response element (CRE) site-containing Bcl-2 promoter through a novel signaling pathway involving mitogen-activated protein kinase kinase 6/p38β mitogen-activated protein kinase/MAP kinase-activated protein kinase-3/cAMP-response element-binding protein (CREB) (Pugazhenthi, S., Miller, E., Sable, C., Young, P., Heidenreich, K. A., Boxer, L. M., and Reusch, J. E.-B. (1999) *J. Biol. Chem.* 274, 27529–27535). In the present investigation, we define a second pathway contributing to CREB-dependent up-regulation of Bcl-2 expression as a novel anti-apoptotic function of Akt signaling. To examine the role of Akt on Bcl-2 expression, a series of transient transfections using a luciferase reporter gene driven by the promoter region of Bcl-2 containing a CRE were carried out. Pharmacological inhibition of phosphatidylinositol (PI) 3-kinase, the upstream kinase of Akt, with LY294002 led to a 45% decrease in Bcl-2 promoter activity. The reporter activity was enhanced 2.3-fold by overexpression of active p110 subunit of PI 3-kinase and inhibited 44% by the dominant negative p85 subunit of PI 3-kinase. Cotransfection with 3-phosphoinositide-dependent kinase (PDK1), which is required for the full activation of Akt, resulted in enhanced luciferase activity. Insulin-like growth factor-I-mediated induction of Bcl-2 promoter activity was decreased significantly ($p < 0.01$) by the dominant negative forms of p85 subunit of PI 3-kinase, PDK1, and Akt. These data indicate that regulation of Bcl-2 expression by IGF-I involves a signaling cascade mediated by PI 3-kinase/PDK1/Akt/CREB. Furthermore, we measured the Bcl-2 mRNA in PC12 cells overexpressing Akt by real-time quantitative reverse transcription-polymerase chain reaction using the TaqMan™ fluorogenic probe system. We observed a 2.1-fold increase in Bcl-2 mRNA levels in the Akt cell line compared with control PC12 cells, supporting the observation that enhanced CREB activity by Akt signaling leads to increased Bcl-2 promoter activity and cell survival.

The serine threonine kinase Akt/protein kinase B is an important mediator of metabolic as well as survival responses to insulin and growth factors (1). Akt is activated by translocation to plasma membrane when the PI 3-kinase-generated 3-phosphoinositides bind to its pleckstrin homology domain (2). For its full activation it needs to be further phosphorylated by 3-phosphoinositide-dependent kinase1 (PDK1)[1] at Thr-308 and by PDK2 at Ser-473. The metabolic actions of insulin mediated by Akt include stimulation of GLUT4 translocation and activation of glycogen synthase and the glycolytic enzyme 6-phosphofructose-2-kinase (1).

In addition to its metabolic actions, Akt/protein kinase B has been shown to promote cell survival by growth factors against several apoptotic stimuli (3, 4). The Bcl-2 family of proteins consisting of pro-apoptotic Bad, Bik, Bid. Etc. and anti-apoptotic Bcl-2 and Bcl-xL are important regulators of mammalian apoptosis (5). Bcl-2/Bcl-xL prevents the activation of caspase-9 by Apaf-1 and cytochrome *c* (6). Bcl-2 and Bad heterodimerize and neutralize each other's function. The fate of cells exposed to apoptotic signal is determined by the balance between pro- and anti-apoptotic proteins. One mechanism by which Akt prevents apoptosis is considered to proceed through phosphorylation of the pro-apoptotic protein Bad on Ser-136 (7). Phosphorylated Bad is sequestered by 14-3-3 protein, leading to its down-regulation. It has been also suggested that additional mechanisms might exist for the cell survival-promoting action of Akt (8, 9).

Up-regulation of Bcl-2 expression has been identified as a critical mechanism by which growth factors promote cell survival (10–13). The promoter region of Bcl-2 contains a cAMP-response element (CRE) site, and the transcription factor CREB has been identified as a positive regulator of Bcl-2 expression (13, 14). Akt, a target of IGF-I signaling, has been shown to activate CREB (15). Thus, it seemed possible that Akt activation through PI 3-kinase could mediate regulation of Bcl-2 expression by IGF-I.

In our previous studies in PC12 cells, we identified that three post-receptor pathways activated by IGF-I through extracellular-regulated kinase, p38β MAPK, and PI 3-kinase are capable of mediating Ser-133 phosphorylation of CREB (13, 16). However, in the context of CREB-driven Bcl-2 promoter, activation of the extracellular-regulated kinase pathway has been shown to have a negative regulatory effect through Ets domain transcription factors (14). We identified a novel IGF-I-mediated signaling cascade involving MAP kinase kinase 6/p38β MAPK/

* The work was supported by a Veterans Affairs Merit review grant and an American Diabetes Association research award and National Institute of Health Grant KO8 DK02351 (NIDDK) (to J. E.-B. R.) and a Veterans Affairs Research Enhancement Award Program grant (to J. E.-B. R. and K. A. H.). The costs of publication of this article were defrayed in part by the payment of page charges. This article must therefore be hereby marked "*advertisement*" in accordance with 18 U.S.C. Section 1734 solely to indicate this fact.

‡‡ To whom correspondence should be addressed: Section of Endocrinology (111H), Veterans Affairs Medical Center, 1055 Clermont St., Denver, CO 80220. Tel.: 303-399-8020 (ext. 2775); Fax: 303-393-5271; E-mail: ReuschJ@den-res.org.

[1] The abbreviations used are: PDK1, 3-phosphoinositide-dependent kinase 1; IGF, insulin-like growth factor; CRE, cAMP response element; CREB, CRE-binding protein; MAPK, mitogen-activated protein (MAP) kinase; PBS, phosphate-buffered saline; PI 3-kinase, phosphatidylinositol 3-kinase; RT-PCR, reverse transcription-polymerase chain reaction.

MAP kinase-activated protein kinase-3/CREB, leading to the induction of Bcl-2 promoter (13). However, SB203580, the p38 MAPK inhibitor blocked IGF-I-induced Bcl-2 promoter activity only partially. Earlier work in our laboratory demonstrated that IGF-I-mediated CREB phosphorylation and activation of CRE site-containing chromogranin A promoter requires PI 3-kinase (16). In that study, a dominant negative form of the regulatory subunit of PI 3-kinase was able to block IGF-I-mediated induction of a CRE site-containing promoter of chromogranin A, a neuro endocrine-specific gene. Du and Montminy (15) demonstrated recently that Akt stimulates the phosphorylation and the transcriptional activity of the CREB in HEK 293 cells. These reports clearly raise the possibility that Akt could mediate part of the IGF-I-induced increase in the expression of Bcl-2 at the transcriptional level. The objective of the present study was to examine whether IGF-I mediated signaling through PI 3-kinase and Akt leads to a CREB-dependent increase in Bcl-2 promoter activity.

EXPERIMENTAL PROCEDURES

Materials—The pharmacological inhibitors LY294002 and rapamycin were from Biomol (Plymouth Meeting, PA). Cell culture media and supplies were purchased from Gemini Bio Products, Inc (Calabasas, CA) and Life Technologies, Inc. The CRE site-containing promoter region of *bcl-2* gene was linked to a luciferase reporter as described previously (14). A luciferase reporter gene driven by TATA box joined to tandem repeats of CRE (4×) was purchased from Stratagene (La Jolla, CA). Plasmids for transfection experiments were purified using Qiagen's (Valencia, CA) maxi kit. Antibodies specific for Phospho (Ser-133) CREB and CREB were from New England Biolabs (Beverly, MA). The luciferase assay kit was purchased from Pharmingen (San Diego, CA).

Cell Culture—Rat pheochromocytoma (PC12) cells (provided by Dr. Derek LeRoith (NIDDK, National Institutes of Health, Bethesda, MD) were maintained in Dulbecco's modified Eagle's medium containing 10% fetal bovine serum, 5% heat-inactivated horse serum, 100 μg/ml streptomycin, and 100 microunits/ml penicillin at 37 °C in a humidified atmosphere at 8% CO_2. A cDNA encoding Akt with the Src myristoylation sequence at the N terminus (17) in the retroviral vector pLNCX (18) was packaged into replication-defective retrovirus using 293T cells along with the plasmids SV-ψ-A-MLV and SV-ψ-env$^-$-MLV by the procedure described previously (19, 20). Secreted retrovirus was supplemented with polybrene (8 μg/ml), filtered (0.45 μm), and incubated with PC12 cells for 24 h. Cells expressing Akt were selected by culturing them in medium containing G418. Apoptosis was induced in control PC12 (Neo-21) and the Akt clone by exposing them to serum-free medium for 72 h, and the viable cells were counted. Alternatively, the cells in regular medium were UV-irradiated (32 J/M^2), and 24 h later, the viable cells were counted. Cells were cultured in 6 × 35-mm wells coated with poly-L-lysine for transfection studies.

Isolation of Total RNA and Real-time Quantitative RT-PCR—Control and Akt-overexpressing PC12 cells were cultured in regular medium. Total RNA was isolated from these cells using TRIzol reagent (Life Technologies, Inc.) as per the manufacturer's protocol. RNA samples were further purified by DNase digestion and extraction with phenol and chloroform. The mRNA for Bcl-2 was measured by real-time quantitative RT-PCR using PE Applied Biosystems prism model 7700 sequence detection instrument. The sequences of forward and reverse primers as designed by Primer Express (PE ABI) were 5′-TGGGATGCCTTTGTGGAACT-3′ and 5′-GAGACAGCCAGGAGAAATCAAAC-3′, respectively. The TaqMan™ fluorogenic probe used was 5′-6FAM-TGGCCCCAGCATGCGACCTC-TAMRA-3′. During PCR amplification, 5′ nucleolytic activity of *Taq* polymerase cleaves the probe separating the 5′ reporter fluorescent dye from the 3′ quencher dye (21, 22). Threshold cycle, C_t, which correlates inversely with the target mRNA levels, was measured as the cycle number at which the reporter fluorescent emission increases above a threshold level. The Bcl-2 mRNA levels were corrected for 18 S ribosomal RNA, which was measured using a kit (PEABI, P/N 4308310) from Perkin-Elmer as per the manufacturer's protocol.

Immunoblotting—PC12 cells cultured in poly-L-lysine-coated 60-mm dishes under appropriate conditions were washed twice with ice-cold PBS, and the cell lysates were prepared. Protein content of lysates was measured (23), and appropriately diluted samples (containing equal amounts of protein) were mixed with 2× Laemmli sample buffer containing 100 mM dithiothreitol. The proteins resolved on a 12% SDS-polyacrylamide gels were transferred to polyvinylidene difluoride membranes. After blocking with Tris-buffered saline with Tween (20 mM Tris-HCl (pH 7.9), 8.5% NaCl, and 0.1% Tween 20) containing 5% non-fat dry milk at room temperature for 1 h, the blots were treated with the primary antibody in blocking buffer at 4 °C overnight. The blots were washed with blocking buffer and incubated with anti-rabbit IgG conjugated to alkaline phosphatase for 1 h at room temperature. After further washes with blocking buffer and with 10 mM Tris-HCl (pH 9.5), 10 mM NaCl, 1 mM $MgCl_2$, the blots were developed with CDP-Star reagent (New England Biolabs) and exposed to x-ray film.

Transfection Procedure—Transient transfections were carried out by the procedure described earlier using LipofectAMINE Plus reagent (Life Technologies, Inc.) (13). The cells were cultured to around 70% confluence in 6 × 35-mm plates. One μg of plasmid, 3 μl of Plus reagent, and 10 μg of LipofectAMINE reagent were used for each well. To normalize the transfection efficiency, the plasmid containing β-galactosidase gene driven by SV_{40} promoter was included. DNA and the LipofectAMINE reagent diluted in 100 μl of serum and antibiotic-free medium were mixed together and incubated at room temperature for 30 min. After washing the cells with PBS, 800 μl of serum and antibiotic-free medium was added. The plasmid and LipofectAMINE mixture was added to each well and incubated for 5 h. Then the cells were cultured in regular medium for 24 h before appropriate treatment. The cells were washed with cold PBS and lysed with 100 μl of reporter lysis buffer. After freezing and thawing, the lysate was centrifuged at 14,000 rpm for 30 min to collect the supernatant. Luciferase was assayed using the enhanced luciferase assay kit (Pharmingen) on a Monolight 2010 luminometer. The β-galactosidase assay was carried out as described earlier (13). Statistical analysis was performed by Student's *t* test.

RESULTS

Modulation of PI 3-Kinase Impacts Basal and IGF-I-stimulated Bcl-2 Promoter Activity—To investigate the role of PI 3-kinase in the regulation of Bcl-2 expression, PC12 cells transfected with a Bcl-2 promoter construct containing a CRE site were treated with the PI 3-kinase inhibitor LY294002. There was a 45% decrease ($p < 0.01$) in the reporter activity in the presence of the inhibitor (Fig. 1*A*), suggesting a positive role for PI 3-kinase. To confirm these observations, a series of transient transfections with constitutively active p110 subunit and the dominant negative p85 subunit of PI 3-kinase were carried out. Fig. 1*B* demonstrates the ability of PI 3 kinase activation to augment basal and IGF-I-stimulated Bcl-2 promoter activity. The basal activity increased by 2.3-fold in the presence of p110, whereas it was decreased to 56% of control by Δ p85. IGF-I-mediated regulation of Bcl-2 promoter activity was similarly affected. These observations indicate that IGF-I-induced Bcl-2 expression proceeds in part through activation of PI 3-kinase. Rapamycin did not inhibit the Bcl-2 promoter activity (Fig. 1*A*), suggesting a role for Akt rather than p70 s6 kinase in mediating PI 3-kinase action.

Full activation of Akt is known to require phosphorylation on Thr-308 by PDK-1, a kinase downstream of PI 3-kinase (1). We therefore examined the impact of PDK1 and dominant negative PDK1 on Bcl-2 promoter activity. Cotransfection of PC12 cells with PDK1 resulted in a 2.0-fold increase in reporter activity (Fig. 1*C*). The increase in reporter activity by PDK1 was further enhanced 66% by IGF-I, probably due to its induction through p38β MAPK mediated pathway (13). In contrast, kinase dead PDK1 decreased basal and IGF-I-mediated reporter activity by 37 and 62%, respectively. These data demonstrate important roles for PI 3-kinase and PDK1 in the transcriptional regulation of Bcl-2 expression.

Akt Regulation of Bcl-2 Expression Requires CREB—Akt is one of the downstream targets of PI 3-kinase signaling. Du and Montminy (15) recently reported the positive regulation of CREB activity by Akt. To explore whether Akt regulation of Bcl-2 required CREB, we examined the impact of dominant negative form of CREB, KCREB, on the Akt-stimulated Bcl-2 promoter activity. As shown in Fig. 2*A*, Akt-stimulated Bcl-2 reporter activity is decreased by KCREB. However, KCREB did

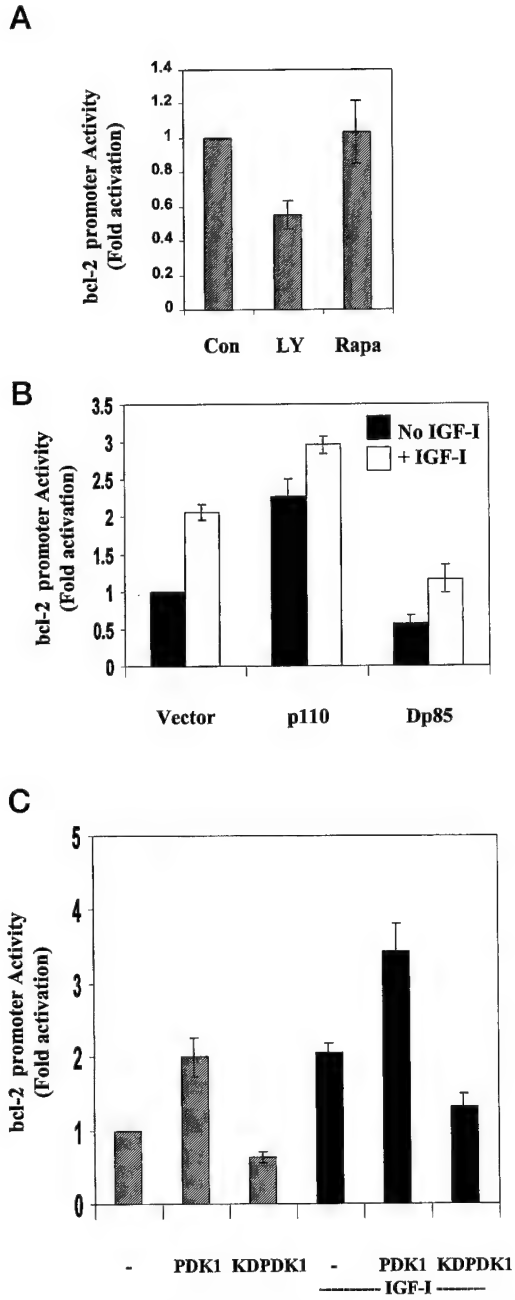

FIG. 1. **Activation of Bcl-2 promoter by PI 3-kinase signaling pathway.** PC12 cells cultured to 70% confluence in 6 × 35-mm wells were transfected with Bcl-2 reporter construct, pRSV β-galactosidase, and indicated plasmids (1 μg of total plasmids, 3 μl of plus reagent, and 10 μg of LipofectAMINE reagent/well). The reporter was cotransfected (*B* and *C*) with constitutively active catalytic subunit (*p110*) and dominant negative regulatory subunit (*Dp85*) of PI 3-kinase, wild type PDK1, and kinase dead PDK1 (*KDPDK1*). 24 h after transfection, the cells were treated with LY294002 (*LY*; 40 μM) and rapamycin (*Rapa*; 10 ng/ml) (*A*) and IGF-I (100 ng/ml; *B* and *C*) as indicated for another 24 h. The inhibitors were added to the culture medium the second time after 12 h. Cell lysates were prepared and assayed for luciferase and β-galactosidase. The values represent mean ± S.E. of observations from four independent experiments, each carried out in duplicate.

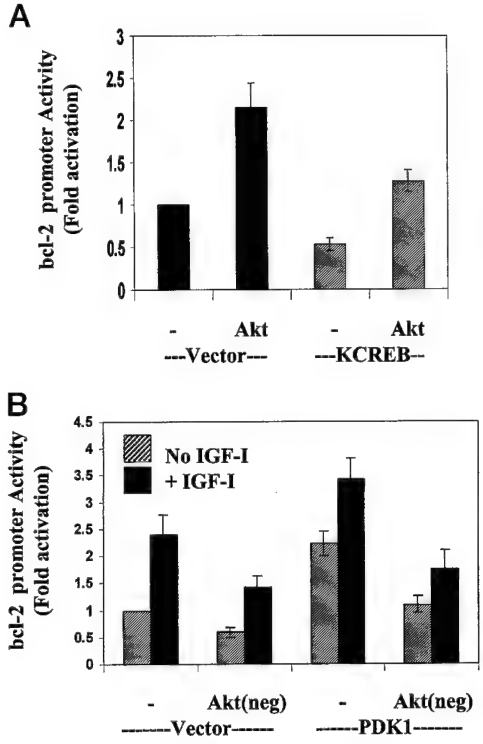

FIG. 2. **Modulation of Bcl-2 expression by Akt through CREB.** PC12 cells cultured to around 70% confluence were transfected with a CRE site-containing Bcl-2 reporter construct along with wild type Akt, dominant negative Akt (*Akt(neg)*; T308A; S473A), wild type PDK1, and KCREB as indicated for 5 h in serum and antibiotic-free medium followed by culturing in regular medium. One day later, the transfected cells were exposed to IGF-I (100 ng/ml) for another 24 h. Luciferase and β-galactosidase were assayed in the cell lysates. Values are means ± S.E. of four independent experiments.

not completely block Akt-mediated activation of the reporter. This could be due to the CREB-independent component in the activation of Bcl-2 promoter (14). In our previous study, we observed that the promoter retained modest activity after deletion or mutation of the CRE site (13). Furthermore cotransfection of the reporter with the dominant negative Akt (T308A; S473A) decreased basal and IGF-I-stimulated luciferase activity by 40% ($p < 0.01$) (Fig. 2*B*). These data support a role for the PI 3-kinase/PDK1/Akt/CREB pathway as a second signaling pathway important for IGF-I regulation of *bcl-2* gene expression. However PDK1 is known to have potential targets such as p90rsk and protein kinase C isoforms in addition to Akt that are capable of activating CREB. Hence we examined the effect of dominant negative Akt on PDK1-mediated induction. We did observe that PDK1 mediated stimulation of Bcl-2 promoter activity in the absence and presence of IGF-I to be decreased by 51 and 48%, respectively, when the dominant negative Akt was included in the cotransfection experiments. The possibility of PDK1 modestly activating Bcl-2 promoter through other pathways involving p90rsk and protein kinase C isoforms cannot be ruled out. Further studies are needed to explore these pathways in detail.

Increased CREB Activity and Bcl-2 Expression in PC12 Cell Line-expressing Akt—The results of previous experiments clearly demonstrated that Akt-mediated signaling activates Bcl-2 promoter through CREB, and this transcription factor needs to be phosphorylated for its activation. We therefore examined whether CREB phosphorylation on Ser-133 activation site is increased in PC12 cells expressing myristoylated Akt. We noted a significant (90%; $p < 0.01$) increase in CREB phosphorylation in these cells in the absence of IGF-I (Fig. 3, *A* and *B*). When these cells were treated with IGF-I (100 ng/ml) for 10 min, CREB phosphorylation increased from 2.2-fold in control cells to 2.9-fold in Akt-expressing cells. This enhanced PCREB formation could be due to growth factor action through p38β MAPK-mediated pathway as shown in our previous study (13). The CREB protein levels did not change significantly

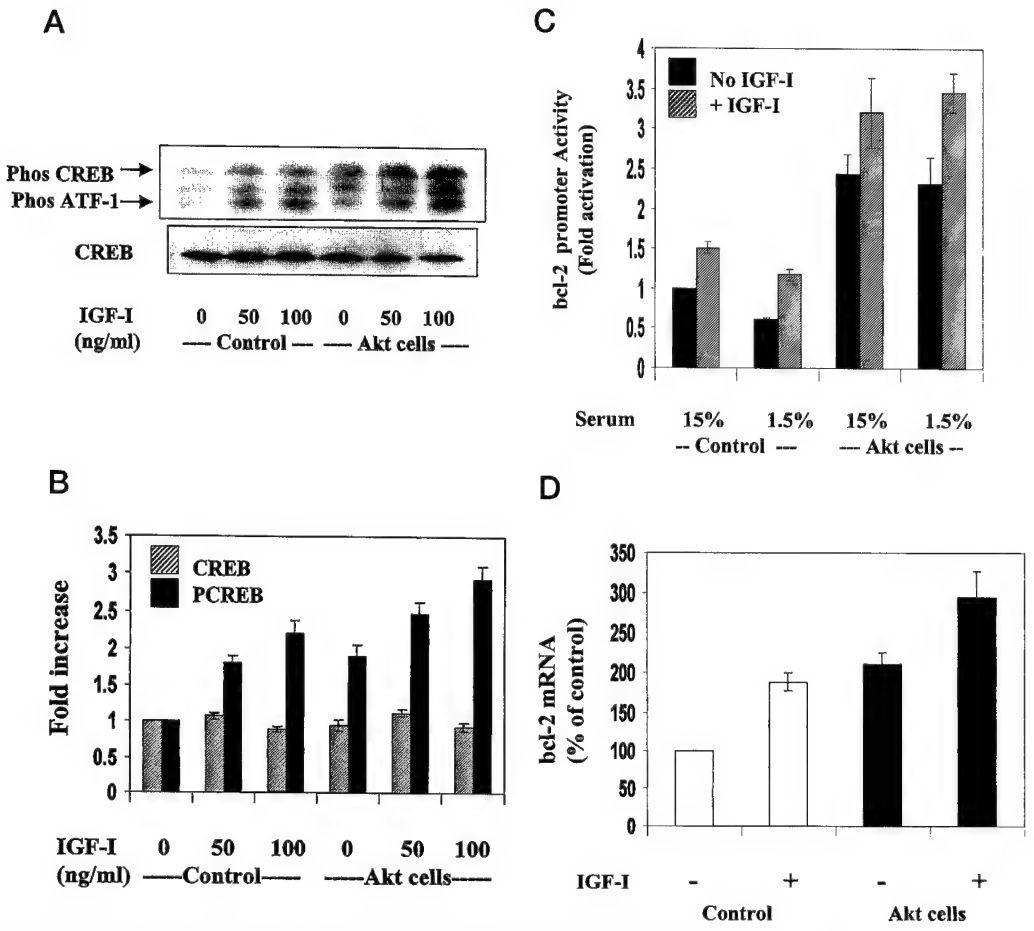

FIG. 3. **Increased CREB activity and Bcl-2 expression in PC12 cells expressing Akt.** *A* and *B*, control and Akt-expressing PC12 cells were cultured to 80% confluence in 60-mm dishes and then maintained in serum-free medium for 5 h. They were treated with the indicated concentrations of IGF-I for 10 min. The cells were washed with ice-cold PBS, and the cell lysates were prepared. Diluted cell lysates with equal protein content were mixed with 2× Laemmli sample buffer followed by sonication. The protein samples were electrophoresed and immunoblotted for phospho CREB (*PCREB*) and CREB. The blots were scanned, and the intensities of bands were quantitated using the Bio-Rad software Quantity One (*B*). *C*, control and Akt-expressing PC12 cells were transfected with a Bcl-2 reporter construct along with pRSV β-galactosidase for 5 h in serum and antibiotic-free medium. After 24 h of transfection, the transfected cells were exposed to media containing the indicated concentrations of serum in the absence and presence of IGF-I for another 24 h. A luciferase assay was carried out in the cell lysates and corrected for transfection efficiency by measuring the activity of β-galactosidase. The values are means ± S.E. of observations from four independent experiments. *D*, control and Akt-expressing PC12 cells cultured to 80% confluence were transferred to a low serum medium (0.1% fetal bovine serum and 0.05% heat-inactivated serum) in the absence and presence of IGF-I (100 ng/ml). After washing the cells with ice-cold PBS, TRIzol reagent was added to the cells, and total RNA was isolated. The Bcl-2 mRNA level was measured in these cells by real-time quantitative RT-PCR using the TaqMan™ fluorogenic probe system by PE Applied Biosystem.

under different experimental conditions (Fig. 3*B*). Hence Akt seems to activate CREB at the post-translational level. We next examined the CREB activity in the cells expressing Akt using a luciferase reporter driven by a CRE site-containing Bcl-2 promoter. The promoter activity was elevated in Akt cells both in the absence and presence of IGF-I (Fig. 3*C*), correlating with the increased CREB phosphorylation observed in the previous experiment (Fig. 3*A*). Interestingly, culturing transfected control cells in low serum medium resulted in a 40% decrease in promoter activity, whereas cells expressing Akt maintained its activation in the presence of low serum (Fig. 3*C*). Similar results were obtained with a luciferase reporter driven by four tandem repeats of CRE sites (results not shown). Furthermore, PC12 cells expressing Akt were found to have increased survival after serum withdrawal and exposure to UV (Table I). After 72 h of culture in serum-free medium, the survival rate was as high as 86% in the Akt clone as compared with 26% control cells. In addition, Akt increased survival in UV-exposed PC12 cells to 76% from 38% seen in control cells.

Data from the studies described above demonstrate the impact of PI 3-kinase/PDK1/Akt on the luciferase reporter construct driven by Bcl-2 promoter. To confirm the role of Akt in the up-regulation of endogenous Bcl-2 expression, we used the PC12 cell line overexpressing constitutively active myristoy-

TABLE I
Serum withdrawal-mediated and UV-induced apoptosis in PC12 cells expressing Akt

PC12 cells expressing the vector LNCX (Neo-21) or LNCX-Myr-Akt were cultured in Dulbecco's modified Eagle's medium without serum for 72 h, after which the viable cells were counted. The cell survival rate was expressed as percentage of viable cells that has been cultured in Dulbecco's modified Eagle's medium containing 1% horse serum. Furthermore, the above mentioned clones were UV-irradiated (32 J/m^2), and after 24 h, the viable cells were counted. The data are presented as percentage of viable cells in a control culture without radiation. The results are the mean ± S.E. of three independent experiments.

	Cell survival	
	Serum-free	UV
	% of control	
Neo-21	26.0 ± 9.9	37.9 ± 11.4
Akt	86.2 ± 14.5[a]	75.6 ± 14.2[a]

[a] < 0.01 *vs.* Neo-21.

lated Akt. We measured Bcl-2 mRNA levels in these cells by a sensitive real-time quantitative RT-PCR using the TaqMan™ fluorogenic probe system. Applied Biosystems prism model 7700 sequence detection instrument was used to measure the reporter fluorescence emission. As shown in Fig. 3*D*, there is a 2.1-fold increase in Bcl-2 mRNA level in Akt clone as compared with the control vector-only clone. Treatment of these cells with 100 ng/ml IGF-I increased the Bcl-2 mRNA level further to 3.0-fold, which could be due to IGF-I action through p38β MAPK (13). This experiment clearly provides a physiological relevance to the significance of Akt-mediated CREB activation.

DISCUSSION

Great insight has been gained over the recent few years regarding the mechanism of neuronal programmed cell death and the ability of growth factors to serve as anti-apoptotic agents. The majority of the data has suggested post-translational modification of the apoptotic machinery (7). The importance of PI 3-kinase and Akt for these effects has been reported by a number of groups (3, 4). The present study defines an additional critical regulatory function for Akt involving transcriptional regulation of the anti-apoptotic protein Bcl-2. We recently reported the induction of Bcl-2 by IGF-I through a novel signaling pathway mediated by MAP kinase kinase 6/p38β MAP kinase/MAP kinase-activated protein kinase-3 (13). Now we identify an additional pathway involving Akt for IGF-I-mediated activation of Bcl-2 promoter.

Regulation of neuronal survival by growth factors is known to proceed through the PI 3-kinase-mediated signaling (3). Low potassium-induced apoptosis in cerebellar granule neurons has been shown to be prevented by synthetic lipid products of PI 3-kinase when added to the culture medium (24). Downstream of this kinase, two signaling pathways involving Akt and p70 s6k have been identified. Dudek *et al.* (3) show that dominant negative Akt is able to induce apoptosis in rat cerebellar granular neurons, and rapamycin, an inhibitor of p70 s6 kinase, does not block insulin-mediated promotion of cell survival (3). Expression of a myristoylated Akt, the active form in immortalized rat hippocampal neuronal cells, leads to increased survival against apoptotic signal (25).

Akt-mediated phosphorylation of cytosolic proteins such as glycogen synthase kinase-3 and Bad is known to play a critical role in the regulation of metabolic pathways as well as prevention of cell death by insulin and growth factors (7). Recent studies indicate that Akt can regulate gene expression at the transcriptional level, suggesting a nuclear site of action. Akt increases the expression of GLUT1 in hepatoma cells (26) and leptin in adipocytes (27). Interleukin-2-mediated Akt activation in BAF/3 cells results in increased expression of Bcl-2. Furthermore, forkhead transcription factor has been identified as a nuclear target for Akt (28–32). It is known to induce insulin-like growth factor-binding protein-1 by stimulating its promoter activity. Akt has been shown to phosphorylate forkhead transcription factor at Thr-24, Ser-256, and Ser-319, the consensus phosphorylation sites both *in vitro* and *in vivo* (29). This covalent modification leads to the nuclear exclusion of forkhead transcription factor, leading to negative regulation of forkhead transcription factor -responsive genes by Akt (28).

Studies have indeed shown that this protein kinase can translocate to nucleus (33–35). Akt/protein kinase B is first translocated to the plasma membrane, where it is activated following phosphorylation on Thr-308 and Ser-473. Subsequently, Akt can be translocated to the nucleus. Meier *et al.* have demonstrated by confocal microscopy the nuclear translocation of Akt 20–30 min after mitogenic stimulation (34). Significant to our present study, it has been demonstrated that myristoylated Akt, which is membrane-directed, can also undergo partial nuclear localization (35), whereas Akt construct having both myristoylation and palmitoylation signals does not (34). The probable explanation for the difference seems to be that they anchor to the plasma membrane with different levels of affinity. We were able to observe increased CREB activity in PC12 cells expressing Akt with a myristoylation signal (Fig. 3*C*).

The transcription factor CREB has also been identified as a target for several signaling pathways mediated by growth factors. Nerve growth factor is known to increase CREB phosphorylation through Ras/MAP kinase kinase/extracellular-regulated kinase/Rsk2 (36). Fibroblast growth factor and IGF-I induce CRE site- containing promoters by activating p38 MAPK and MAPKAP-K2/3 (13, 37). IGF-I-stimulated CREB phosphorylation in PC12 cells is decreased by wortmannin, an inhibitor of PI 3-kinase, but not by rapamycin, an inhibitor of p70 s6k, suggesting that Akt is likely to be involved in CREB activation (16). In a recent study, Du and Montminy (15) demonstrated that Akt/protein kinase B stimulates the phosphorylation of CREB on serine 133 and promotes the recruitment of the coactivator CREB-binding protein (15). They also showed that Akt-mediated induction of CRE-driven gene expression is blocked by a serine to alanine mutation at position 133 using the Gal4 CREB system. In the present investigation, we further demonstrate the physiological importance of this signaling pathway in the activation of an endogenous CRE site-containing Bcl-2 promoter. When the luciferase reporter construct driven by Bcl-2 promoter was cotransfected with p110, PDK1, and Akt, there was significant stimulation of basal and IGF-I-induced luciferase activity. The dominant negative forms of the regulatory subunit of PI 3-kinase, Δp85, and Akt were able to decrease the promoter activity, suggesting that growth factor-mediated signaling through PI 3-kinase/PDK1/Akt could be involved in the induction of Bcl-2 expression. Hence Akt seems to promote cell survival through inactivation of Bad by phosphorylation and up-regulation of Bcl-2 by transcriptional activation.

Acknowledgments—We thank Dr. Nicholas Webster, Dr. Emmanuel Van Obberghen, and Dr. Richard Goodman for providing valuable reagents. We acknowledge the excellent secretarial support of Gloria Smith. We thank Dr. Boris Draznin for critically reading the manuscript. Quantitative RT-PCR was performed at the University of Colorado Cancer Center core facility.

REFERENCES

1. Coffer, P. J., Jin, J., and Woodgett, J. R. (1998) *Biochem. J.* **335,** 1–13
2. Downward, J. (1998) *Curr. Opin. Cell Biol.* **10,** 262–267
3. Dudek, H., Datta, S. R., Franke, T. F., Birnbaum, M. J., Yao, R., Cooper, G. M., Segal, R. A., Kaplan, D. R., and Greenberg, M. E. (1997) *Science* **275,** 661–664
4. Kulik, G., Klippel, A., and Weber, M. J. (1997) *Mol. Cell. Biol.* **17,** 1595–1606
5. Merry, D. E., and Korsmeyer, S. J. (1997) *Annu. Rev. Neurosci.* **20,** 245–267
6. Adams, J. M., and Cory, S. (1998) *Science* **281,** 1322–1326
7. Datta, S. R., Dudek, H., Tao, X., Masters, S., Fu, H., Gotoh, Y., and Greenberg, M. E. (1997) *Cell* **91,** 231–241
8. Hinton, H. J., and Welham, M. J. (1999) *J. Immunol.* **162,** 7002–7009
9. Scheid, M. P., and Duronio, V. (1998) *Proc. Natl. Acad. Sci. U. S. A.* **95,** 7439–7444
10. Singleton, J. R., Dixit, V. M., and Feldman, E. L. (1996) *J. Biol. Chem.* **271,** 31791–31794
11. Tamatani, M., Ogawa, S., and Tohyama, M. (1998) *Mol. Brain Res.* **58,** 27–39
12. Minshall, C., Arkins, S., Straza, J., Conners, J., Dantzer, R., Freund, G. G., and Kelley, K. W. (1997) *J. Immunol.* **159,** 1225–1232
13. Pugazhenthi, S., Miller, E., Sable, C., Young, P., Heidenreich, K. A., Boxer, L. M., and Reusch, J. E.-B. (1999) *J. Biol. Chem.* **274,** 27529–27535
14. Wilson, B. E., Mochon, E., and Boxer, L. M. (1996) *Mol. Cell. Biol.* **16,** 5546–5556
15. Du, K., and Montminy, M. (1998) *J. Biol. Chem.* **273,** 32377–32379
16. Pugazhenthi, S., Boras, T., O'Connor, D., Meintzer, M. K., Heidenreich, K. A., and Reusch, J. E.-B. (1999) *J. Biol. Chem.* **274,** 2829–2837
17. Ahmed, N. N., Grimes, H. L., Bellacosa, A., Chan, T. O., and Tsichlis, P. N. (1997) *Proc. Natl. Acad. Sci. U. S. A.* **94,** 3627–3632
18. Miller, A. D., and Rosman, G. J. (1989) *Biotechniques* **7,** 980–990
19. Landau, N. R., and Littman, D. R. (1992) *J. Virol.* **66,** 5110–5113
20. Pear, W. S., Nolan, G. P., Scott, M. L., and Baltimore, D. (1993) *Proc. Natl. Acad. Sci. U. S. A.* **90,** 8392–8396

21. Heid, C. A., Stevens, J., Livak, K. J., and Williams, P. M. (1996) *Genome Res.* **6,** 986–994
22. Gibson, U. E. M., Heid, C. A., and Williams, P. M. (1996) *Genome Res.* **6,** 995–1001
23. Bradford, M. M. (1976) *Anal. Biochem.* **72,** 248–254
24. Shimoke, K., Yamada, M., Ikeuchi, T., and Hatanaka, H. (1998) *FEBS Lett.* **437,** 221–224
25. Eves, E. M., Xiong, W., Bellacosa, A., Kennedy, S. G., Tsichlis, P. N., Rosner, M. R., and Hay, N. (1998) *Mol. Cell. Biol.* **18,** 2143–2152
26. Barthel, A., Okino, S. T., Liao, J., Nakatani, K., Li, J., Whitlock, J. P., Jr., and Roth, R. A. (1999) *J. Biol. Chem.* **274,** 20281–20286
27. Barthel, A., Kohn, A. D., Luo, Y., and Roth, R. A. (1997) *Endocrinology* **138,** 3559–3562
28. Tang, E. D., Nunez, G., Barr, F. G., and Guan, K.-L. (1999) *J. Biol. Chem.* **274,** 16741–16746
29. Rena, G., Guo, S., Cichy, S. C., Unterman, T. G., and Cohen, P. (1999) *J. Biol. Chem.* **274,** 17179–17183
30. Guo, S., Rena, G., Cichy, S., He, X., Cohen, P., and Unterman, T. (1999) *J. Biol. Chem.* **274,** 17184–17192
31. Biggs, W. H., Meisenhelder, J., Hunter, T., Cavenee, W. K., and Arden, K. C. (1999) *Proc. Natl. Acad. Sci. U. S. A.* **96,** 7421–7426
32. Brunet, A., Bonni, A., Zigmond, M. J., Lin, M. Z., Juo, P., Hu, L. S., Anderson, M. J., Arden, K. C., Blenis, J., and Greenberg, M. E. (1999) *Cell* **96,** 857–868
33. Andjelkovic, M., Alessi, D. R., Meier, R., Fernandez, A., Lamb, N. J. C., Frech, M., Cron, P., Cohen, P., Lucocq, J. M., and Hemmings, B. A. (1997) *J. Biol. Chem.* **272,** 31515–31524
34. Meier, R., Alessi, D. R., Cron, P., Andjelkovic, M., and Hemmings, B. A. (1997) *J. Biol. Chem.* **272,** 30491–30497
35. Ahmed, N. N., Franke, T. F., Bellacosa, A., Datta, K., Gonzalez-Portal, M.-E., Taguchi, T., Testa, J. R., and Tsichlis, P. N. (1993) *Oncogene* **8,** 1957–1963
36. Xing, J., Ginty, D. D., and Greenberg, M. E. (1996) *Science* **273,** 959–963
37. Tan, Y., Rouse, J., Zhang, A., Cariati, S., Cohen, P., and Comb, M. J. (1996) *EMBO J.* **15,** 4629–4642

Growth Arrest-Specific Gene 6 (Gas6)/Adhesion Related Kinase (Ark) Signaling Promotes Gonadotropin-Releasing Hormone Neuronal Survival via Extracellular Signal-Regulated Kinase (ERK) and Akt

Melissa P. Allen, Chan Zeng, Kristina Schneider, Xiaoyan Xiong, Mary Kay Meintzer, Paola Bellosta, Claudio Basilico, Brian Varnum, Kim A. Heidenreich, and Margaret E. Wierman

Research Service (M.P.A., C.Z., K.S., X.X., M.K.M., K.A.H., M.E.W.)
Veterans Affairs Medical Center and
Departments of Medicine and Pharmacology
University of Colorado School of Medicine
Denver, Colorado 80220

Department of Microbiology and the Kaplan Cancer Center (P.B., C.P.)
New York University School of Medicine
New York, New York 10016

Amgen (B.V.)
Thousand Oaks, California 91320

We identified Ark, the mouse homolog of the receptor tyrosine kinase Axl (Ufo, Tyro7), in a screen for novel factors involved in GnRH neuronal migration by using differential-display PCR on cell lines derived at two windows during GnRH neuronal development. Ark is expressed in Gn10 GnRH cells, developed from a tumor in the olfactory area when GnRH neurons are migrating, but not in GT1–7 cells, derived from a tumor in the forebrain when GnRH neurons are postmigratory. Since Ark (Axl) signaling protects from programmed cell death in fibroblasts, we hypothesized that it may play an antiapoptotic role in GnRH neurons. Gn10 (Ark positive) GnRH cells were more resistant to serum withdrawal-induced apoptosis than GT1–7 (Ark negative) cells, and this effect was augmented with the addition of Gas6, the Ark (Axl) ligand. Gas6/Ark stimulated the extracellular signal-regulated kinase, ERK, and the serine-threonine kinase, Akt, a downstream component of the phosphoinositide 3-kinase (PI3-K) pathway. To determine whether ERK or Akt activation is required for the antiapoptotic effects of Gas6/Ark in GnRH neurons, cells were serum starved in the absence or presence of Gas6, with or without inhibitors of ERK and PI3-K signaling cascades. Gas6 rescued Gn10 cells from apoptosis, and this effect was blocked by coincubation of the cells with the mitogen-activated protein/ERK kinase (MEK) inhibitor, PD98059, or wortmannin (but not rapamycin). These data support an important role for Gas6/Ark signaling via the ERK and PI3-K (via Akt) pathways in the protection of GnRH neurons from programmed cell death across neuronal migration. (Molecular Endocrinology 13: 191–201, 1999)

0888-8809/99/$3.00/0
Molecular Endocrinology

INTRODUCTION

GnRH Neurons: A Model of Tightly Controlled Neuronal Migration across Embryogenesis

GnRH is the hypothalamic releasing hormone that controls pituitary gonadotropin subunit biosynthesis and, ultimately, reproductive function (1). The GnRH neuronal population is unique, in that 800-1000 neurons migrate from the olfactory placode to the forebrain across embryogenesis in the rodent (2–5). The neurons migrate adjacent to olfactory neurons, but then diverge to reach their final destination in the hypothalamus. GnRH neurons innervate the anterior

pituitary and deliver an episodic pattern of hormone signaling to the gonadotropes that ultimately leads to normal reproductive function (1). Failure of this targeted GnRH neuronal migration results in failure of sexual maturation and GnRH deficiency syndromes (6–7). In the human, the X-linked form of GnRH deficiency has been found to result from a defect in the KAL gene, which encodes a neural cell adhesion molecule expressed in cells adjacent to GnRH neurons (8–10). The molecular defects for other forms of GnRH deficiency are unknown due, in part, to the lack of information concerning the factors that control GnRH neuronal migration.

GnRH Neuronal Cell Lines: Models to Study GnRH Expression

Our ability to directly study GnRH gene expression was advanced by the development of GnRH-producing cell lines. Mellon and colleagues (11) used the rat GnRH promoter fused to the SV_{40} T antigen in transgenic animals to target immortalization of the GnRH neuronal population. One animal developed a tumor in the forebrain, a time when GnRH neurons are postmigratory. The GT cell lines were derived from that tumor and produce large amounts of GnRH mRNA and protein (12). Similarly, Radovick and co-workers (13) used the human GnRH promoter fused to the SV_{40} T antigen in transgenic mice. An animal developed a GnRH neuronal tumor in the olfactory area, a locus for migrating GnRH neurons. The resultant Gn10, Gn11, and NLT cell lines express low levels of GnRH mRNA and protein (Ref. 13, and M. E. Wierman, unpublished observations). Based on the divergent phenotypes of the two neuronal cell lines, we hypothesized that by using the technique of differential display PCR, we could identify novel factors involved in GnRH neuronal migration and/or gene expression (14). We reasoned that GT1–7 cells would express factors resulting in high level GnRH expression and a postmigratory status. Conversely, Gn10 cells would express factors involved in GnRH neuronal migration and factors that repress GnRH expression (or lack activators of gene expression). Gn8–01 is a cDNA clone characterized in this screen from Gn10 cells and was identified as Ark, a membrane receptor tyrosine kinase that may play a role in GnRH neuronal migration, gene expression, and protection from apoptosis.

Ark (Axl): Role in Protection from Apoptosis

Ark is a mouse protein identified during a screen for homologs of the BEK fibroblast growth factor receptor (15). Ark and its human homolog, Axl, Ufo, or Tyro7 (16–18), are members of a new family of receptor tyrosine kinases that includes Tyro3 (with many alternative names) (17, 19) and Mer (20). This family is unique in that the N-terminal, extracellular portion of the molecule contains two Ig-like repeats and two fibronectin type III repeats (15–20). This combination of structural elements has been classically observed in cell adhesion molecules or receptor tyrosine phosphatases, but not in receptor tyrosine kinases. Although initially isolated as candidate growth factor receptors, members of the Ark (Axl) family are not mitogenic unless they are overexpressed at high levels in tumor cell lines (21–22). Some have suggested the importance of the extracellular domain of Ark in cell-cell adhesion due to its ability to induce homophilic binding independent of ligand in fibroblasts (21), although others have not shown an effect independent of ligand using Axl expressing 32D cells (23). The nuclear transcription factors and gene targets downstream in the Ark-signaling pathway have not been identified.

Gas6/Ark Signaling in Other Systems Protects from Programmed Cell Death

Recently, the ligand for Ark (Axl) and Tyro3 was identified as Gas6, a gene induced after growth arrest of fibroblast cells in culture (24–26). Gas6 is a soluble, vitamin K-dependent protein with homology to protein S (24–26). Studies have suggested the importance of Gas6/Axl-induced chemotaxis of 32D and vascular smooth muscle cells (23, 27). Additional studies show that Gas6/Ark or Axl signaling reduces the rate of programmed cell death in fibroblasts (28–29). We were intrigued by the identification of Ark in Gn10 GnRH neuronal cells, which were derived from migrating GnRH neurons, and hypothesized that Ark (Axl) may play a role in protection of the GnRH neuronal population from apoptosis during their migration into the forebrain. Thus, we designed experiments in the two divergent GnRH-producing cell lines to address the role of Gas6/Ark (Axl) signaling during neuronal cell death and the pathways that are activated in this process.

Pathways Involved in Neuronal Apoptosis

The downstream signaling cascades involved in apoptosis are a focus of active investigation. Many of the pathways are similar among cell types, but some cell-specific pathways have been identified. Studies have shown the importance of the extracellular signal-regulated kinase (ERK) pathway in rescue from cell death (30–35). It is unclear however, whether the activation of ERK is to trigger mitogenesis and thereby indirectly regulate apoptosis or to act directly in this process (28). Studies have also shown the importance of Akt [also called protein kinase B (PKB) and related to A and C protein kinase (RAC-PK)], a downstream component of the phosphoinositide 3-kinase (PI3-K) pathway, in the protection of cells from apoptosis (36–41). Recently, investigators have demonstrated that Akt phosphorylates the BCL-2 member, BAD, deactivating its proapoptotic actions (42). In addition to antiapoptotic signaling cascades, stress-activated proapoptotic pathways converge in activation of p38 mitogen-activated protein (MAP) kinase in neuronal cells (43).

Inhibitors of p38 have been shown to protect from various triggers of programmed cell death (43). With this background, we examined which of these pathways may be involved in Gas6/Ark signaling in GnRH neuronal cells.

RESULTS

The Ark Tyrosine Kinase Receptor mRNA and Protein Are Expressed in Gn10 and Not GT1–7 Neuronal Cells

To confirm that Ark mRNA and functional Ark protein were expressed in GnRH neuronal cells from which the clone Gn8–01 was isolated, Northern and Western blots from each neuronal cell line were performed. The full-length mouse Ark cDNA was used to probe the Northern (15). An Ark-specific antisera, no. 318, which recognizes the Ark extracellular domain (21), was used to detect the Ark protein. Figure 1 shows the presence of the Ark 3.4-kb mRNA and the 120–140 kDa protein doublet in the Gn10, but not in the GT1–7 neuronal cells. [Additional studies showed that neither neuronal cell line contains detectable levels of Gas6 mRNA or protein (data not shown).]

Ark-Positive Gn10 Neurons Are More Resistant to Growth Factor Withdrawal- Induced Apoptosis than Ark-Negative GT1–7 Cells

Prior experiments in fibroblast cell lines demonstrated that Gas6/Ark (Axl) signaling is important in protecting or rescuing cells from programmed cell death induced by serum withdrawal (28, 29). This finding prompted us to determine whether a similar function is important in GnRH neuronal cells. If Ark expression and activation protect neurons from apoptosis, then the Gn10 (Ark positive) cells might be more resistant than GT1–7 (Ark negative) neurons to growth factor withdrawal, a standard paradigm to trigger apoptosis. To test this hypothesis, the GT1–7 and Gn10 cells were grown under normal conditions and then changed to serum-free media. Various times after serum withdrawal (2–72 h), cells were stained for condensed, hyperchromatic nuclei using the Hoescht stain (33258). Gn10 GnRH neurons were less sensitive to serum withdrawal than GT1–7 cells. At baseline, they exhibited a low rate of apoptosis (2.2%) that did not increase over the first 24 h and then gradually increased to 7.3% and 12.4% at 48 and 72 h, respectively. In contrast, GT1–7 GnRH neurons were more sensitive to growth factor removal. They showed a basal level of apoptosis of 2.9%. This increased to 13.8%, 42.3%, and 41.2% at 24 h, 36 h, and 48 h, respectively. When serum was removed, both neuronal cells lost their ability to remain attached to the tissue culture dishes, which was partially prevented by culturing on polylysine-coated slides.

To further map the time course of sensitivity to serum withdrawal, both neuronal cells were placed in serum-free conditions, and cells were stained at various time intervals with acridine orange/ethidium bromide to detect apoptotic nuclei as orange-red condensed fragments (Fig. 2). In this assay, cells are lifted, thereby capturing both attached and detached cells. In GT1–7 cells, the basal level of apoptosis in serum was 2.1% and was similar at 3% at 8 h after serum withdrawal, but then increased to 28%, 35%, and 38% at 24 h, 48 h, and 72 h. In contrast in Gn10 neuronal cells, the basal rate of apoptosis was 2% and was stable over the first 24 h of serum withdrawal (2.1% and 2.5%). The levels of apoptosis then increased gradually over the next 2 days to 10.6% and 13% at 48 and 72 h (Fig. 2). Thus, there was a clear dichotomy between Ark-positive Gn10 and Ark-negative GT1–7 cells in apoptotic rates after serum deprivation. We hypothesize that

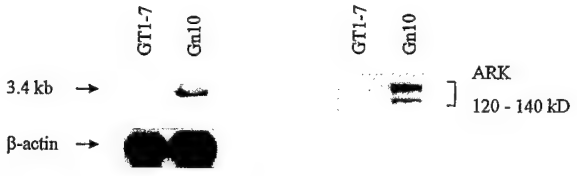

Fig. 1. Ark Is Expressed in Gn10 and Not GT1–7 Neuronal Cells

Twenty micrograms of total RNA from each neuronal cell line were separated by electrophoresis on a 1.4% agarose gel, transferred to nitrocellulose, and hybridized with a radiolabeled Ark cDNA. The 3.4-kb mRNA is Ark. Total cell lysates of the two neuronal cells were separated by electrophoresis on a 10% SDS-PAGE gel, transferred to PVDF, and probed with the No. 318 Ark antisera. The *arrow* indicates the 120- to 140-kDa Ark protein.

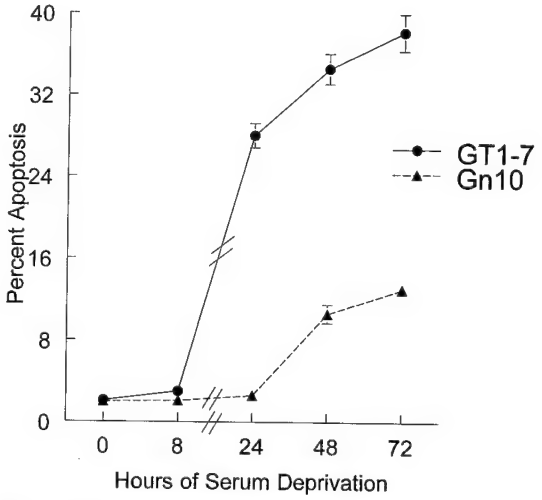

Fig. 2. Gn10 Cells Are More Resistant to Serum Deprivation-Induced Programmed Cell Death Than GT1–7 GnRH Neuronal Cells

Numbers of apoptotic cells were determined by ethidium bromide/acridine orange staining at various times after cells were placed in serum-free media.

Ark is one of many factors contributing to the differences between the two GnRH neuronal cell lines that may play a role in the regulation of programmed cell death in GnRH neurons.

Gas6/Ark Activation Triggers Multiple Signaling Cascades in GnRH Neuronal Cells

To explore the intracellular pathways by which Gas6/Ark might modulate the sensitivity to apoptosis in GnRH neurons, we asked whether rhGas6 triggered changes in the activation of ERK and Akt. ERK1 and ERK2 are components of the MAP kinase pathway known to be critical in mitogenic as well as antiapoptotic signaling in certain cell systems (30–31, 44). Akt is a downstream component of the PI3-K pathway, known to be activated by growth factors and to protect cells from apoptotic stimuli (30, 36, 38–41, 45). Phosphorylation of these proteins, as detected by phospho antisera, is correlated with their activation. GT1–7 and Gn10 cells were grown in the presence or absence of serum (48 h), and Gn10 cells were stimulated with rhGas6, 400 ng/ml, for various periods of time. Whole-cell lysates were analyzed by Western blot and probed with antisera specific for phospho-ERK and ERK (Fig. 3A) or phospho-Akt and Akt (Fig. 3B). Of interest, GT1–7, Ark-negative, cells grown in serum had lower levels of activated ERK and Akt than Gn10, Ark-containing neurons, and levels did not change with serum withdrawal (lanes 1 and 2 *vs.* lanes 3 and 4, panels A and B). However, in the presence of serum, Gn10 neuronal cells have relatively high levels of active ERK and Akt (lanes 3 and 5, panels A and B).

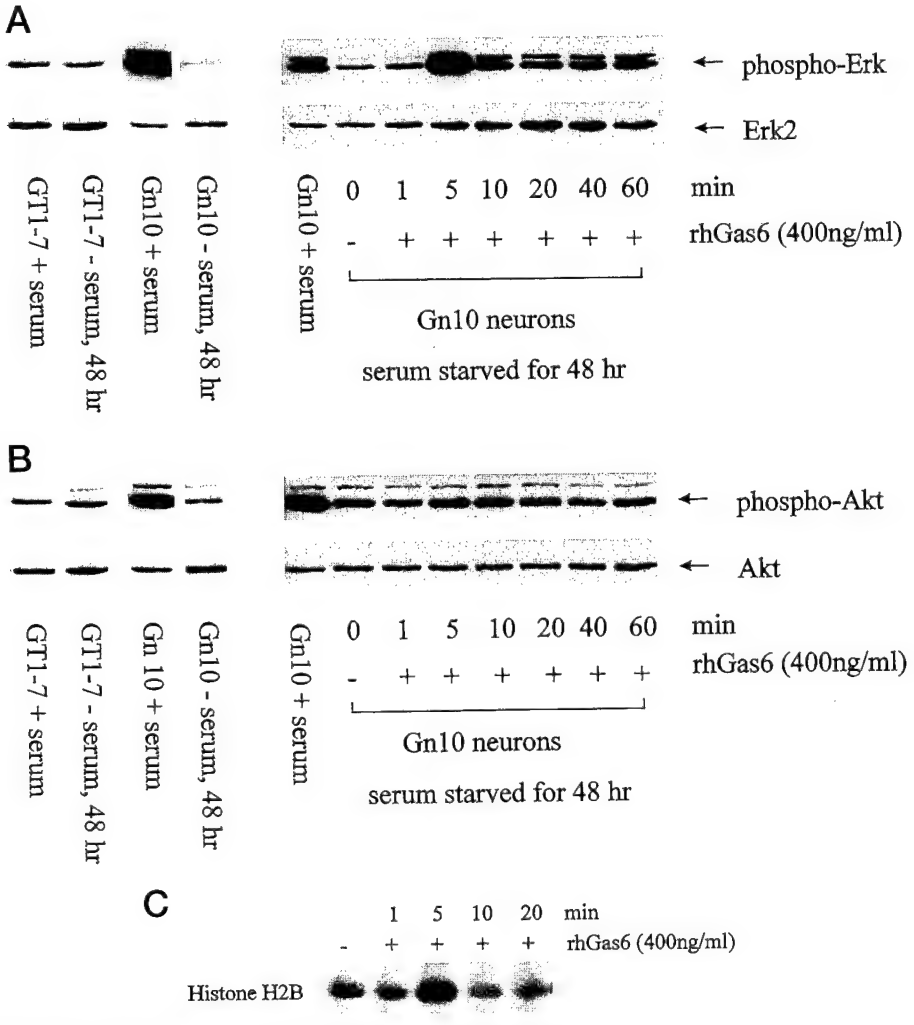

Fig. 3. Gas6/Ark Activation Is Associated with Activation of ERK and Akt

GT1–7 and Gn10 cells were grown in serum or serum starved for 48 h (*left*), and Gn10 cells were then treated with vehicle or rhGas6 (400 ng/ml) for 1–60 min (*right*). Cell lysates were separated by electrophoresis, transferred to PVDF, and incubated with antisera specific for phospho-ERK, ERK (panel A), or phospho-Akt and Akt (panel B). Results are shown from a representative experiment from three to five performed. Panel C shows phosphorylation of histone H2B by Akt in response to rhGas6 (400 ng/ml) for 1–20 min.

Serum withdrawal decreased levels of phospho-ERK and Akt in the Gn10 cells with more dramatic effects on ERK. In Gn10 cells, addition of rhGas6 under serum-free conditions stimulated ERK (13-fold) and Akt (1.5-fold) ($P < 0.05$) activity with no significant effect on ERK or Akt levels. The activation of ERK was rapid and returned to a baseline higher than control by 60 min. The activation of Akt was rapid but transient, reaching a maximum at 5 min and returning to basal by 20 min.

To confirm the increases in levels of phospho-Akt by Gas6, an alternative assessment of Akt activity was made by testing its ability to phosphorylate the substrate histone H2B in an immunocomplex kinase assay (40). Gn-10 cell lysates were harvested after exposure to serum or after serum withdrawal in the absence or presence of rhGas6. Figure 3C shows a rapid 2.3-fold increase in the phosphorylation of histone H2B by Akt at 5 min after addition of rhGas6 with a rapid return to basal levels. These data confirm that Gas6/Ark (Axl) signals through Akt in Gn10 cells.

The activity of p38 MAP kinase was also assessed in the neuronal cells, as it has recently been shown to trigger neuronal apoptosis (43) and was expected to be inhibited by Gas6 (Fig. 4). The activity of p38 MAP kinase was undetectable in Gn10 neurons after 48 h of serum deprivation in the absence or presence of rhGas6. This lack of activity was observed despite fairly high basal concentrations of the enzyme (Fig. 4). Together, these data suggest the potential importance of the ERK and PI3-K pathways and not p38 MAP kinase to transmit the Ark (Axl) signal in GnRH neuronal cells.

The Mitogen-Activated Protein/ERK Kinase (MEK) Inhibitor, PD98059, Blocks ERK Activation by Gas6

To test the hypothesis that activation of the ERK pathway is involved in Gas6/Ark rescue from neuronal programmed cell death, Gn10 cells were grown in serum or in serum-free media for 48 h. Cells were treated with vehicle, rhGas6 (400 ng/ml, 5 min), or IGF-I (100 ng/ml, 15 min). Some cells were preincubated with the MEK inhibitor, PD98059, which blocks upstream of ERK (31, 43), for 1 h before the addition of rhGas6. Cell lysates were analyzed by Western blot with ERK and phospho-ERK antibodies. Serum deprivation decreased the levels of activated ERK in the neuronal cells (Fig. 5, lanes 1 and 2), while rhGas6 triggered a 10- to 20-fold increase in levels of phospho-ERK at 5 min (lane 3). The stimulation of ERK by rhGas6 was greater than that achieved by addition of IGF-I in these neuronal cells (IGF-I, 2-fold stimulation, lane 4). The activation of ERK by rhGas6 or IGF-I was blocked in the presence of the MEK inhibitor, PD98059, to below that in unstimulated cells (lanes 6 and 7). There were no changes observed in total ERK levels after rhGas6 addition.

Inhibitors of the ERK Pathway Block Gas6/Ark Protection from Neuronal Apoptosis

To investigate the importance of the ERK-signaling pathway in Gas6/Ark protection of GnRH neuronal cells during serum withdrawal-induced cell death, Gn10 cells were grown in serum-free media in the presence or absence of rhGas6 (400 ng/ml) with or without the MEK inhibitor, PD98059 (Fig. 6). Serum withdrawal for 48 h resulted in an increase in apoptosis as measured by Hoescht staining from 2.3% to 12.3% (lanes 1 and 2). rhGas6 protected Gn10 cells from programmed cell death, decreasing levels to 4.8% (lane 3). Incubation of cells with the MEK inhibitor alone had no effect on serum withdrawal induced apoptosis (lane 4); however, Gas6 protection was lost in

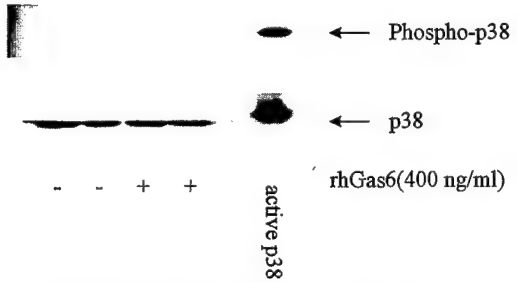

Fig. 4. Serum Deprivation and Gas6 Do Not Activate p38 MAP Kinase in Gn10 Neuronal Cells

Gn10 cells were grown in serum-free media for 48 h and then treated with vehicle or rhGas6 (400 ng/ml) for 10 min. Cell lysates were separated by electrophoresis, transferred to PVDF, and incubated with antisera specific for phospho-p38 MAP kinase and p38 MAP kinase. Lane 5 contains active p38 as a control.

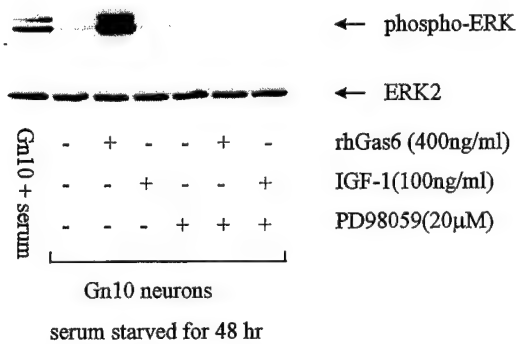

Fig. 5. The MEK Inhibitor, PD98059, Blocks ERK Activation by Gas6

Gn10 cells were serum starved for 48 h and then treated with rhGas6 (400 ng/ml) for 5 min or IGF-I (100 ng/ml) for 15 min. In some cases, the cells were pretreated with PD98059 (20 μM) for 1 h. Cell lysates were separated by electrophoresis, transferred to PVDF, and incubated with antisera specific for phospho-ERK and ERK. Lane 1, Gn10 cells grown in serum; lane 2, serum starved; lane 3, with rhGas6; lane 4, with IGF-I; lane 5, with PD98059; lane 6, with rhGas6 and PD98059; lane 7, with IGF-I and PD98059.

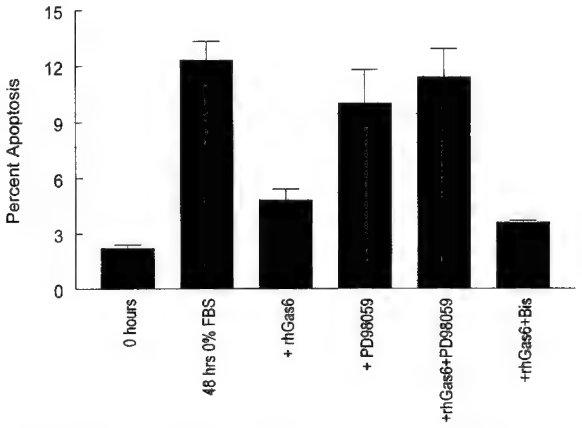

Fig. 6. Inhibition of the ERK Pathway Blocks Gas6 Rescue of Gn10 Neuronal Cells from Apoptosis

Gn10 cells were grown in serum-free media for 48 h in the absence or presence of rhGas6 (400 ng/ml) and/or the MEK inhibitor, PD98059 (20 μM), or bisindolymaleimide (100 nM). Apoptotic cells were counted by Hoescht staining. Results are the mean ± SEM of three experiments. Lane 1, Baseline apoptosis; lane 2, 48 h of serum deprivation; lane 3, with rhGas6; lane 4, with PD98059; lane 5, with rhGas6 and PD98059; lane 6, with rhGas6 and bisindolymaleimide.

the presence of the MEK inhibitor (lane 5). As another control, there was no effect of bisindolymaleimide, an inhibitor of the protein kinase C pathway (46), on Gas6 rescue of GnRH neuronal cells from growth factor withdrawal-induced cell death (lane 6). These results show the importance of the ERK pathway in Gas6/Ark (Axl) antiapoptotic signaling in GnRH neuronal cells.

Recent studies suggested that ERK activation by Gas6/Ark involves induction of mitogenesis that may indirectly contribute to protection from apoptosis (28). Therefore, Gn10 neuronal cells were grown in the presence or absence of Gas6, and cell counts were determined. There were no significant mitogenic effects of Gas6 in these neuronal cells as assessed by cell counts (data not shown). Additional studies were performed using BrdU incorporation in the absence or presence of Gas6. Cells were serum starved for 24 h and incubated in the presence or absence of rhGas6 (400 ng/ml) for 24 h. These studies also showed no effect of rhGas6 on Gn10 neuronal cells to augment BrdU incorporation (rhGas6 69.8 ± 0.13% *vs.* serum-starved control cells 100 ± 0.12%). Together, these experiments suggest that activation of the ERK pathway during Gas6/Ark rescue from neuronal apoptosis is not dependent on a mitogenic signal to trigger entry into the cell cycle and support the direct role of the pathway in protection from programmed cell death.

Wortmannin Blocks Akt Activation by Gas6

To test whether Akt is also important in Gas6/Ark protection of GnRH neurons from apoptosis, Gn10 neuronal cells were grown in serum-free media for 48 h and then treated with vehicle, rhGas6, or IGF-I as a control growth factor stimulus. Some cells were preincubated with wortmannin (1 μM) to inhibit the PI3-K pathway upstream of Akt (4). Cell lysates were analyzed by Western blot with phospho-Akt and Akt antisera (Fig. 7). Growth factor withdrawal decreased, but did not abolish, activated Akt levels (*lower band*, lanes 1 and 2). rhGas6 addition, however, consistently increased the levels of phospho-Akt by 5 min (*lower band*, lane 3). The stimulation of Akt by rhGas6 was comparable to the stimulation of Akt by IGF-I (*lower band*, lane 4). Wortmannin completely blocked the stimulation of Akt by both rhGas6 and IGF-I (lanes 6 and 7). In addition, wortmannin lowered phospho-Akt levels to below baseline, again supporting the importance of other factors in Gn10 cells that sustain an activated PI3-K via Akt signal. No changes in the protein levels of Akt were observed in the various experimental manipulations.

Inhibition of the PI3-K Pathway Blocks Gas6/Ark Rescue of Gn10 GnRH Neurons from Serum Withdrawal-Induced Apoptosis

To confirm that the changes observed in Akt activation were directly relevant to Gas6/Ark protection from neuronal apoptosis, Gn10 neurons were grown in serum-free media in the absence or presence of wortmannin (100 nM), rapamycin (20 ng/ml), rhGas6 (400 ng/ml), or combinations of the above (Fig. 8). Gn10 cells exposed to growth factor withdrawal for 48 h had an increased rate of apoptosis as determined by Hoescht staining from 2.2% to 11.7% (lanes 1 and 2). Incubation with rhGas6 partially rescued the Gn10 neurons from programmed cell death (5.4% at 48 h, lane 3). Incubation of neuronal cells with wortmannin resulted in higher levels of apoptosis (20.9%, lane 4)

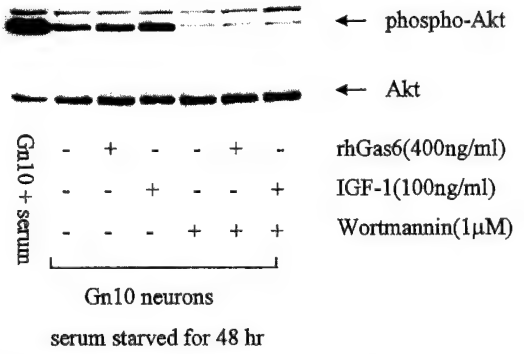

Fig. 7. Wortmannin Blocks Akt Activation by Gas6

Gn10 cells were serum starved for 48 h and treated with vehicle or rhGas6 (400 ng/ml) for 5 min or IGF-I (100 ng/ml) for 15 min in the absence or presence of pretreatment with wortmannin (1 μM) for 20 min. Cell lysates were separated by electrophoresis, transferred to PVDF, and incubated with phospho-Akt and Akt antisera. Lane 1, Gn10 cells grown in serum; lane 2, serum starved; lane 3, with rhGas6; lane 4, with IGF-I; lane 5, with wortmannin; lane 6, with rhGas6 and wortmannin; lane 7, with IGF-I and wortmannin.

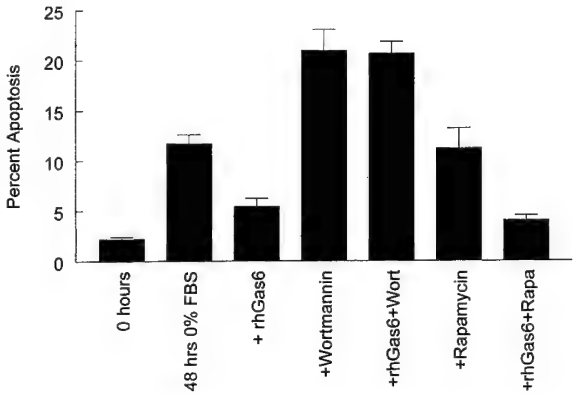

Fig. 8. Inhibition of the PI3-K Pathway Blocks Gas6 Rescue of Gn10 Neurons from Serum Withdrawal-Induced Apoptosis

Gn10 neurons were grown in serum-free media for 48 h in the absence or presence of rhGas6 (400 ng/ml), wortmannin (100 nM), rapamycin (20 ng/ml), or combinations of the above. Cells were harvested and rates of apoptosis determined by staining with Hoescht 33258. Results are the mean ± SEM of three experiments. Lane 1, Baseline apoptotic cells in Gn10 cells; lane 2, 48 h in serum-free media; lane 3, with rhGas6; lane 4, with wortmannin; lane 5, with rhGas6 and wortmannin; lane 6, with rapamycin; lane 7, with rhGas6 and rapamycin.

compared with serum withdrawal (11.7%). These results suggest the PI3-K pathway is used by other membrane receptors to protect GnRH neurons from cell death in addition to those controlling apoptosis due to growth factor deprivation. rhGas6 was unable to protect the neuronal cells in the presence of the wortmannin blockade of the PI3-K pathway (lane 5). There was no effect of rapamycin, a selective inhibitor of S6 kinase that is also downstream of PI3-K (47), on the rates of apoptosis (lane 6). In addition, rapamycin did not influence the ability of rhGas6 to rescue from neuronal apoptosis (lane 7), suggesting that Akt and not S6 kinase is the important downstream target of PI3-K in these cells. Together, these data support the hypothesis that Gas6/Ark protection of GnRH neurons is mediated through mechanisms that involve Akt as well as ERK.

DISCUSSION

Programmed Cell Death in GnRH Neurons

During development, apoptosis plays a critical role in determining the ultimate fate of neuronal populations. Studies have estimated that 20–80% of the neurons expressed during embryogenesis die before maturation of the organism (34). The GnRH neuronal population is unique in that, unlike other neurons that express hypothalamic releasing factors, the neurons must migrate from the olfactory placode into the forebrain. In addition, the population is small, with only 800–1000 neurons in the rodent making the journey (2–5). Because of the ultimate importance of appropriately targeting this subpopulation of neurons into the hypothalamus for reproductive competence, one might expect a complex series of mechanisms to modulate the rate of programmed cell death during their migratory journey. The ability to identify factors involved in this process has been limited by the small size of the neuronal population and difficulty in working with primary cultures. We took advantage of two available GnRH-producing neuronal cell lines to use differential display-PCR to clone candidate cDNAs that might play a role in GnRH neuronal migration or gene expression (14). Ark, expressed in Gn10 GnRH cells derived when GnRH neurons are migrating, is the first candidate to be studied functionally. The potential role of Ark (Axl) in cell-cell contact has been suggested in 32D myeloid cells (23–27) and in vascular smooth muscle cells (27), but it has not been studied in neuronal cells. The role of Ark (Axl) in the modulation of GnRH gene expression is under active investigation in the laboratory (48). The present study strongly supports Ark's role in protection of the GnRH neuronal population from programmed cell death.

Since Ark is not expressed in the GT1–7 cells derived from GnRH neurons in the forebrain, one might expect that additional protective mechanisms against apoptosis of the GnRH population are not needed once the appropriate targeting has taken place. Gas6 is not expressed in these neuronal cells, so one would hypothesize that adjacent glia or neuronal cells synthesize the Ark (Axl) ligand during the migratory process. This is consistent with an increasing literature supporting the role of glial elements in neuronal migration and survival (49).

The Functional Role of Ark to Protect from Programmed Cell Death

Serum deprivation is a classic model system to study programmed cell death. Although most studies of the Ark (Axl) family have been performed in this model system, Bellosta *et al.* (21) recently reported that Gas6/Ark signaling protects fibroblasts from apoptosis induced by tumor necrosis factor-α and c-Myc but not that induced by UV irradiation or staurosporine. Similar studies of Ark function in neuronal cells using these alternative model systems of apoptosis have not yet been performed. To support the physiological importance of Ark (Axl), however, embryonic fibroblasts from Ark (Axl) knockout mice were found to be more susceptible to growth factor withdrawal-induced apoptosis than wild-type cells (21). Together, these data suggest the general role of Ark (Axl) in modulating the rate of programmed cell death.

Gas6/Ark Signaling in Neuronal Cells Is Different Than in Other Systems

Ark was initially derived in studies searching for novel growth factor receptors, and Axl has been found to be

overexpressed in some leukemia cell lines (18, 27). Initial studies focused on the role of the kinase as a mitogenic stimulus, but recent studies have suggested Ark (Axl) is only a weak mitogen unless overexpressed (22, 28). In GnRH neuronal cells, Gas6/Ark (Axl) signaling is not associated with a mitogenic response, which is expected since neuronal cells are not subject to significant proliferative responses.

In the GnRH neuronal cell lines, both the ERK and Akt pathways were activated in the presence of serum. The Gn-10 (Ark positive) cells, however, had higher levels of activated ERK and Akt than the GT1–7 (Ark negative) cells, suggesting that the high endogenous levels were not due solely to SV_{40} TAg immortalization. In addition, growth factor withdrawal decreased activated ERK levels dramatically with less effect on activated Akt levels, supporting the recent observations that many neuronal cells use the PI3-K via Akt pathway as the major control point for multiple endogenous signals that mediate neuronal survival (38, 40, 45).

The ERK intracellular signaling system has been associated with both proapoptotic and antiapoptotic effects (reviewed in Ref. 32). Gardner and Johnson (33) demonstrated that fibroblast growth factor 2 suppression of tumor necrosis factor-α mediated apoptosis required Ras activation of ERK in L929 cells. Párrizas *et al.* (44) showed the activation of both ERK and PI3-K pathways in IGF-I-mediated rescue from apoptosis in differentiated PC12 cells (44). Bellosta and co-workers (21) have shown in NIH-3T3 cells that Ark triggered a modest increase in ERK activity that accompanied the increased survival of cells at concentrations that did not promote DNA synthesis. In our studies, incubation with the MEK inhibitor (PD98059) completely reversed Gas6 protection from programmed cell death in GnRH neuronal cells. These data show the critical role of the ERK pathway in transmitting the Gas6 signal from the membrane to the appropriate intracellular targets to rescue these neuronal cells from growth factor withdrawal-induced apoptosis. In contrast to Gas6/Ark, IGF-I triggered activation of Akt to a greater extent than ERK. These results confirm the cell specificity of intracellular signaling pathways downstream of growth factor receptors.

In prior studies of other downstream signaling pathways activated by Gas6/Ark (Axl), divergent results have been reported (22, 28, 29). Goruppi and coworkers (29) have suggested the importance of PI3-K working through S6K as well as Src activation in both mitogenic and survival activities by Gas6/Axl signaling in NIH-3T3 cells. The data concerning Src activation are complex since the Axl cytoplasmic domain lacks Src consensus binding sequences, and Src could not be coimmunoprecipitated with the receptor (29). Since the NIH-3T3 cells contain Tyro3, another family member that heterodimerizes with Ark (Axl), the complement of protein partners in each cell may influence the importance of different signaling pathways. However, the GnRH neuronal cells do not express Tyro3 (X. Xiong and M. E. Wierman, unpublished observations), suggesting the observed responses are due solely to Ark (Axl) activation.

Goruppi and colleagues (29) also found that rapamycin treatment inhibited the ability of Gas6 to prevent apoptosis-associated Gas2 proteolytic cleavage. In our studies, rapamycin had no effect on Gas6 protection from apoptosis, in contrast to wortmannin. Together with the data showing increased phospho-Akt and phosphorylation of the Akt substrate, histone H2B, by Gas6, these results suggest that in GnRH neurons, the PI3-K pathway triggers Akt as an additional downstream effector to modulate the sensitivity of GnRH neurons to trophic factor withdrawal. The recent demonstration that Akt inhibits apoptosis in cerebellar neurons (40), in rat hippocamal H19–7 neuronal cells (45), and in sympathetic neurons (38) and that Akt also phosphorylates the proapoptotic BCL-2 member, BAD, in neuronal cells to inactivate it (42) are all supportive of the major importance of this pathway in mediating multiple receptor-mediated antiapoptotic signals. Since blockade of either the PI3-K or the ERK pathways reversed the protective effect of Gas6, it is unclear whether these are parallel independent signaling systems or whether there is cross-talk at some level between the components. Future studies will be needed to investigate these possibilities.

MATERIALS AND METHODS

Cell Culture

GT1–7 and Gn10 GnRH neuronal cells were grown in DMEM supplemented with 5% FCS, penicillin (100 U/ml), and streptomycin (100 μg/ml). For serum starvation, cells were plated at 60% confluency, grown overnight, and changed to serum-free media, and the incubation was continued for 6–72 h depending on the experimental design.

Reagents

Wortmannin [a specific inhibitor of PI3-K (50)], rapamycin [a specific inhibitor of p70 S6 kinase (47)], bisindolymaleimide [a specific inhibitor of protein kinase C (46)], and insulin-like growth factor 1 (IGF-I) were purchased from Sigma Chemical Co. (St. Louis, MO). PD98059 (an inhibitor of MEK1 and MEK2, the upstream regulators of ERK) was purchased from New England Biolabs, Inc. (Beverly, MA) Purified IgG Ark#318 was raised against the Ark extracellular domain (21). Antibodies specific to Akt and phospho-Akt were purchased from New England Biolabs, Inc. Antiactive MAP kinase pAb (phospho-ERK) and anti-active p38 antibodies were purchased from Promega, Inc. (Madison, WI). Antisera specific to ERK2 and p38 MAP kinase were purchased from Santa Cruz Biotechnology, Inc. (Santa Cruz, CA). Recombinant human Gas6 (rhGas6) from Amgen (Thousand Oaks, CA) was used in all studies (26).

Quantification of Apoptotic Cells

Neuronal cells were grown in standard conditions with or without FCS for various time intervals. For Hoescht staining, cells were fixed on dishes or polylysine-coated slides in 1% paraformaldehyde for 2 min at room temperature followed by

70% ethanol in glycine buffer (100 mM, pH 3.0) for 20 min at −20 C. After fixation, the cells were washed with PBS three times and then incubated in Hoescht 33258 stain (8 μg/ml in PBS) for 15 min at room temperature. The cells were washed with PBS three times and then stored in the dark immersed in PBS. The stained cells were viewed under a fluorescent microscope (Olympus IMT-2 inverted microscope, Olympus Corp., Lake Success, NY). Apoptotic cells were measured by counting the number of neuronal cells with condensed or fragmented chromatin. These cells typically appeared small and rounded and bright green. One thousand cells were counted from eight randomly chosen fields. The rate of apoptosis was expressed as a percentage of total counted cells.

For ethidium bromide/acridine orange staining, cells (floating and attached) were resuspended in cold PBS. A 1:2 dilution of 100 μg/ml solutions of ethidium bromide and acridine orange was mixed with the resuspended cells. The stained cells were viewed as above. Apoptotic cells were scored as those with orange-red fragmented, condensed nuclei. The rate of apoptosis was expressed as a percentage of total counted cells.

Western Blot Analysis

Three million GT1–7 or Gn10 neuronal cells were grown for 48 h in standard media with or without serum. After the experimental manipulation, cells were washed twice with PBS (4 C), and lysed in 250–500 μl of cell lysis buffer containing 10 mM Tris-Cl, pH 7.5, 150 mM NaCl, 1 mM EDTA, 1 mM EGTA, 0.1% NP-40, 1% glycerol, 1 mM dithiothreitol, one protease inhibitor tablet/50 ml (Boehringer Mannheim, Indianapolis, IN), and freshly added 20 mM Na_3VO_4, 25 mM NaF, and 20 mM sodium pyrophosphate at 4 C. Lysed cells were sonicated (Branson sonifier 250, at power 3, Branson Sonic Power Co., Danbury, CT) for 10 pulses. The lysate was then spun at 14,000 × *g* for 10 min at 4 C. The supernatant was then assayed for protein concentration with the BCA protein assay kit (Pierce, Inc., Rockford, IL). An aliquot of 20–30 μg of total protein was resolved by SDS/PAGE on 10–12% gels using a Bio-Rad mini-gel system (Bio-Rad Laboratories, Richmond, CA). Subsequently, proteins were transferred to Hybond polyvinylidene difluoride (PVDF) (Amersham Lifesciences, Inc., Arlington Heights, IL) at 100 V for 1 h at 4 C. The membranes were blocked in 5% milk, TBS-T buffer (20 mM Tris-Cl, pH 7.6, 137 mM NaCl, 0.1% Tween-20) overnight at room temperature. Protein present on the blot was visualized using enhanced chemiluminescence (ECL) immunodetection reagents (Amersham Life Sciences, Inc.). For each antiserum, the primary antibody was diluted to 1:500–1:2000 and incubated with the membrane at room temperature for 2 h. The secondary antibody was diluted 1:2000–1:3000 and incubated with the membrane for 1 h at room temperature. An additional four washes were performed before immunodetection according to the manufacturer's instruction (Amersham Lifesciences, Inc.).

Immune-Complex Kinase Assay for Akt Activity

Gn10 cells were growth for 48 h in normal growth media or serum-free media. The serum-starved cells were incubated with 400 ng/ml rhGas6 for various times, washed once with PBS (4 C), and lysed in 137 mM NaCl, 10% glycerol, 1% NP-40, 20 mM Tris, pH 8, one protease inhibitor tablet/50 ml, 20 mM Na_3VO_4, 25 mM NaF, and 20 mM sodium pyrophosphate at 4 C. The lysed cells were sonicated and spun as described above. Total protein (2–5 mg) was immunoprecipitated with 10 μg of antihuman Akt-1 pleckstrin homology domain antibody (Upstate Biotechnology, Lake Placid, NY) for 1.5 h at 4 C with constant mixing. Subsequently, 100 μl of protein A/G agarose (Calbiochem, La Jolla, CA) was added and the incubation continued for 1 h. The immune complexes were washed three times in lysis buffer, once in dH_2O, and once in kinase assay buffer minus ATP (20 mM HEPES, pH 7.4, 10 mM $MgCl_2$, 10 mM $MnCl_2$) at 4 C. Akt kinase activity was determined by incubating the immune complexes with 2 μg histone H2B, 10 μCi [γ^{32}P]ATP, 5 μM ATP, and kinase assay buffer for 30 min at room temperature. The supernatants were resolved by 15% SDS-PAGE, and the phosphorylation of histone H2B was detected by autoradiography.

Northern Analyses

Twenty micrograms of total RNA isolated from GT1–7 and Gn10 neuronal cells were separated by electrophoresis in a 1.4% formaldehyde agarose gel transferred to nitrocellulose and baked at −80 C as previously described (14). The blot was hybridized with ^{32}P-radiolabeled Ark cDNA (15), washed, and exposed to film at −70 C for 1–2 days.

BrdU Labeling for Cell Proliferation

Gn10 neuronal cells were grown in serum-free media for 24 h and then incubated with vehicle or rhGas6 (400 ng/ml) for 24 h. Cells were then labeled with BrdU for 2–4 h using the cell proliferation enzyme-linked immunosorbent assay (ELISA) colorometric kit from Boehringer Mannheim. BrdU incorporation was assessed by colorometric assay using a Biotek ELISA reader. Data represent the mean ± SEM of six to eight dishes.

Acknowledgments

We acknowledge the excellent secretarial support of Ms. Gloria Smith.

Received June 19, 1998. Revision received October 6, 1998. Accepted October 16, 1998.

Address requests for reprints to: Dr. Margaret E. Wierman, Endocrinology (111H), Veterans Affairs Medical Center, 1055 Clermont Street, Denver, Colorado 80220. E-mail: margaret.wierman@uchsc.edu.

This work was supported by NIH Grant HD-31191 (to M.E.W.). Dr. Wierman has a Career Development Award from the Veterans Administration.

REFERENCES

1. Seeburg PH, Mason AJ, Stewart TA, Nikolics K 1987 The mammalian GnRH gene and its pivotal role in reproduction. Recent Prog Horm Res 43:69–98
2. Jennes L 1989 Prenatal development of the gonadotropin-releasing hormone-containing systems in rat brain. Brain Res 482:97–108
3. Schwanzel-Fukuda M, Pfaff DW 1989 Origin of luteinizing hormone-releasing hormone neurons. Nature 338: 161–164
4. Silverman A-J, Jhamandas J, Renaud LP 1987 Localization of luteinizing hormone-releasing hormone (LHRH) neurons that project to the median eminence. J Neurosci 7:2312–2319
5. Wray S, Grant P, Garner H 1989 Evidence that cells expressing luteinizing hormone-releasing hormone mRNA in the mouse is derived from progenitor cells in the olfactory placode. Proc Natl Acad Sci USA 86: 8132–8136
6. Kallmann FJ, Schoenfeld WA, Barrera SE 1944 The genetic aspects of primary eunuchoidism. Am J Ment Defic 48:203–236

7. Whitcomb RW, Crowley Jr WF 1990 Clinical review 4: diagnosis and treatment of isolated gonadotropin-releasing hormone deficiency in men. J Clin Endocrinol Metab 70:3–7
8. Legouis R, Hardelin J-P, Levilliers J, Claverie J-M, Compain S, Wunderle V, Millasseau P, Le Paslier D, Cohen D, Caterina D, Bougueleret L, Delemarre-Van de Waal H, Lutfalla G, Weissenbach J, Petit C 1991 The candidate gene for the X-linked Kallmann syndrome encodes a protein related to adhesion molecules. Cell 67:423–435
9. Lutz B, Rugarli EI, Eichele G, Ballabio A 1993 X-linked Kallmann syndrome. A neuronal targeting defect in the olfactory system? FEBS Lett 325:128–134
10. Schwanzel-Fukuda M, Bick D, Pfaff DW 1989 Luteinizing hormone-releasing hormone (LHRH)-expressing cells do not migrate normally in an inherited hypogonadal (Kallmann) syndrome. Brain Res Mol Brain Res 6:311–326
11. Mellon PL, Windle JJ, Goldsmith PC, Padula CA, Roberts JL, Weiner RI 1990 Immortalization of hypothalamic GnRH neurons by genetically targeted tumorigenesis. Neuron 5:1–10
12. Wetsel WC, Valenca MM, Merchenthaler I, Liposits Z, Lopez FJ, Weiner RI, Mellon PL, Negro-Vilar A 1992 Intrinsic pulsatile secretory activity of immortalized luteinizing hormone-releasing hormone-secreting neurons. Proc Natl Acad Sci USA 89:4149–4153
13. Radovick S, Wray S, Lee E, Nicols DK, Nakayama Y, Weintraub BD, Westphal H, Cutler Jr GB, Wondisford FE 1991 Migratory arrest of gonadotropin-releasing hormone neurons in transgenic mice. Proc Natl Acad Sci USA 88:3402–3406
14. Fang Z, Xiong X, James A, Gordon DF, Wierman ME 1998 Identification of novel factors that regulate GnRH gene expression and neuronal migration. Endocrinology 139:3654–3657
15. Rescigno J, Mansukhani A, Basilico C 1991 A putative receptor tyrosine kinase with unique structural topology. Oncogene 6:1909–1913
16. Janssen JWG, Schulz AS, Steenvoorden ACM, Schmidberger M, Strehl S, Ambros PF, Bartram CR 1991 A novel putative tyrosine kinase receptor with oncogenic potential. Oncogene 6:2113–2120
17. Lai C, Lemke G 1991 An extended family of protein-tyrosine kinase genes differentially expressed in the vertebrate nervous system. Neuron 6:691–704
18. O'Bryan JP, Frye RA, Cogswell PC, Neubauer A, Kitch B, Prokop C, Espinosa RIII, Le Beau MM, Earp HS, Liu ET 1991 axl, a transforming gene isolated from primary human myeloid leukemia cells, encodes a novel receptor tyrosine kinase. Mol Cell Biol 11:5016–5031
19. Schulz NT, Paulhiac CI, Lee L, Zhou R 1995 Isolation and expression analysis of tyro3, a murine growth factor receptor tyrosine kinase preferentially expressed in adult brain. Brain Res Mol Brain Res 28:273–280
20. Graham DK, Bowman GW, Dawson TL, Stanford WL, Earp HS, Snodgrass HR 1995 Cloning and developmental expression analysis of the murine c-mer tyrosine kinase. Oncogene 10:2349–2359
21. Bellosta P, Costa M, Lin DA, Basilico C 1995 The receptor tyrosine kinase ARK mediates cell aggregation by homophilic binding. Mol Cell Biol 15:614–625
22. Fridell Y-WC, Jin Y, Quilliam LA, Burchert A, McCloskey P, Spizz G, Varnum B, Der C, Liu ET 1996 Differential activation of the Ras/extracellular-signal-regulated protein kinase pathway is responsible for the biological consequences induced the axl receptor tyrosine kinase. Mol Cell Biol 16:135–145
23. McCloskey P, Fridell Y-W, Attar E, Villa J, Jin Y, Varnum B, Liu ET 1997 GAS6 mediates adhesion of cells expressing the receptor tyrosine kinase Axl. J Biol Chem 272:23285–23291
24. Manfioletti G, Brancolini C, Avanzi G, Schneider C 1993 The protein encoded by a growth arrest-specific gene (Gas6) is a new member of the vitamin K-dependent proteins related to protein S, a negative coregulator in the blood coagulation cascade. Mol Cell Biol 13: 4976–4985
25. Nagata K, Ohashi K, Nakano T, Arita H, Zong C, Hanafusa H, Mizuno K 1996 Identification of the product of growth arrest-specific gene 6 as a common ligand for Axl, Sky, and Mer receptor tyrosine kinases. J Biol Chem 271:30022–30027
26. Varnum BC, Young C, Elliott G, Garcia A, Bartley TD, Fridell Y-W, Hunt RW, Trail G, Clogston C, Toso RJ, Yanagihara D, Bennett L, Sylber M, Merewether LA, Tseng A, Escobar E, Liu ET, Yamane HK 1995 Axl receptor tyrosine kinase stimulated by the vitamin K-dependent protein encoded by growth-arrest-specific gene 6. Nature 373:623–626
27. Fridell Y-WC, Villa Jr J, Attar EC, Liu ET 1998 GAS6 induces Axl-mediated chemotaxis of vascular smooth muscle cells. J Biol Chem 273:7123–7126
28. Bellosta P, Zhang Q, Goff SP, Basilico C 1997 Signaling through the ARK tyrosine kinase receptor protects from apoptosis in the absence of growth stimulation. Oncogene 15:2387–2397
29. Goruppi S, Ruaro E, Varnum B, Schneider C 1997 Requirement of phosphatidylinositol 3-kinase-dependent pathway and Src for Gas6-Axl mitogenic and survival activities in NIH 3T3 fibroblasts. Mol Cell Biol 17:4442–4453
30. Cano E, LC Mahadevan. 1995 Parallel signal processing among mammalian MAPKs. Trends Biochem Sci 20:117–122
31. Cobb MH, Goldsmith EH 1995 How MAP kinases are regulated. J Biol Chem 270:14843–14846
32. Downward J 1998 Ras signalling and apoptosis. Curr Opin Genet Dev 8:49–54
33. Gardner AM, Johnson GL 1996 Fibroblast growth factor-2 suppression of tumor necrosis factor α-mediated apoptosis requires ras and the activation of mitogen-activated protein kinase. J Biol Chem 271:14560–14566
34. Oppenhein RW 1991 Cell death during development of the nervous system. Annu Rev Neurosci 14:453–501
35. Xia Z, Dickens M, Raingeaud J, Davis RJ, Greenberg ME 1995 Opposing effects of ERK and JNK-p38 MAP kinases on apoptosis. Science 270:1326–1331
36. Burgering BMT, Coffer PJ 1995 Protein kinase B (Akt) in phosphatidylinositol-3-OH kinase signal transduction. Nature 376:599–602
37. Carpenter LC, Cantley LC 1996 Phosphoinositide kinases. Curr Biol 8:153–158
38. Crowder RJ, Freeman RS 1998 Phosphatidylinositol 3-kinase and Akt protein kinase are necessary and sufficient for the survival of nerve growth factor-dependent sympathetic neurons. J Neurosci 18:2933–2943
39. Dhand R, Hara K, Hiles I, Bax B, Gout I, Panayotou G, Fry MJ, Yonezawa K, Kasuga M, Waterfield MD 1994 PI3-kinase: structural and functional analysis of intersubunit interactions. EMBO J 13:511–521
40. Dudek H, Datta SR, Franke TF, Birnbaum MJ, Yao R, Cooper GM, Segal RA, Kaplan DR, Greenberg ME 1997 Regulation of neuronal survival by the serine-threonine protein kinase Akt. Science 275:661–668
41. Franke TF, Kaplan DR, Cantley LW 1997 PI3K downstream action blocks apoptosis. Cell 88:435–437
42. Datta SR, Dudek H, Tao X, Masters S, Fu H, Gotoh Y, Greenberg ME 1997 Akt phosphorylation of BAD couples survival signals to the cell-intrinsic death machinery. Cell 91:231–241
43. Kummer JL, Rao PK, Heidenreich KA 1997 Apoptosis induced by withdrawal of trophic factors is mediated by p38 mitogen-activated protein kinase. J Biol Chem 272:20490–20494
44. Párrizas M, Saltiel AR, LeRoith D 1997 Insulin-like growth factor 1 inhibits apoptosis using the phosphatidylinositol

3′-kinase and mitogen-activated protein kinase pathways. J Biol Chem 272:154–161
45. Eves EM, Xiong W, Bellaccosa A, Kennedy SG, Tsichlis PN, Rosner MR, May N 1998 Akt, a target of phosphatidylinositol 3-kinase, inhibits apoptosis in a differentiating neuronal cell line. Mol Cell Biol 18:2143–2152
46. Toullec D, Pianetti P, Coste H, Bellevergue P, Grand-Perret T, Ajakane M, Baudet V, Boissin P, Boursier E, Loriolle F, Duhamel L, Charon D, Kirilovsky J 1991 The bisindolylmaleimide GF 109203X is a potent and selective inhibitor of protein kinase C. J Biol Chem 266:15771–15781
47. Downward J 1996 Regulating S6 kinase. Nature 371:378–379
48. Xiong X, Zeng C, Schneider K, Meintzer MK, Heidenreich KA, Wierman ME, Regulation of neuronal GnRH transcription and apoptosis by growth arrest specific gene 6 (Gas6)/adhesion related kinase (Ark) signaling. Program of the 80th Annual Meeting of The Endocrine Society, New Orleans, LA, 1998 (Abstract)
49. Rakic P 1990 Principles of neural cell migration. Experientia 46:882–891
50. Ui M, Okada T, Hazeki K, Hazeki O 1995 Wortmannin as a unique probe for an intracellular signaling protein, phosphoinositide 3-kinase. Trends Biochem Sci 20: 303–307

1999 Gordon Research Conference on Hormone Action: Preliminary Program

July 25–July 30, 1999, Kimball Union Academy, Meriden, New Hampshire

Holly A. Ingraham, UCSF, Chair

Gary L. Firestone, UCB, Vice-Chair

Sunday, July 25

7:30 pm **Opening lecture:** ***To be Announced***

Monday, July 26

9:00 am **Cell Signaling in Development**
Discussion leader: **Sally Camper**, Univ. Michigan, Ann Arbor
Gail Martin, UCSF, CA, *FGF Signaling*; **Mike German**, UCSF, CA, *Molecular Determinants of Pancreatic Development*; **Gary Ruvkun**, Harvard Medical School, Boston, MA, *Metabolic Signaling in Invertebrates*; **Phil Beachy**, Johns Hopkins, Baltimore, MD, *Hedgehog Signaling in Vertebrate Development.*

4:00 pm **Poster Session Group I**

7:30 pm **Signaling and Cross Talk**
Discussion leader: **Gary Firestone**, UCB, CA
Stephen Foord, Glaxo Wellcome Medicines Research Center, Hertfordshire, UK, *RAMPs and G-Protein Receptor Specificity*; **Michael Karin**, UCSD, CA, *Protein Kinase Cascades and the Pro-inflammatory Response*; **Tom Wilke**, UT Southwestern, TX, *RGS Proteins and Ca^{2+} in Signaling Specificity.*

Tuesday, July 27

9:00 am **Technical Advances in the Discovery of Peptides and Receptors**
Discussion leader: **Wylie Vale**, The Salk Institute, La Jolla, CA
Baldomero Olivera, University of Utah, Salt Lake City, UT, *Conus Peptides: Biomedical Applications and Insights into Neuropharmacological Principles*; **Roger Cone**, Vollum Institute, Portland, OR, *Peptide Signaling in Metabolism*; **Masashi Yanagisawa**, UT, Southwestern Medical School/HHMI, Dallas, TX, *Discovery of New Peptides Regulating Food Intake and Metabolism*; **David Julius**, UCSF, CA, *Discovery of New Receptors in the Sensory System.*

4:00 pm **Poster Session Group II**

7:30 pm **Hormones and Behavior**
Discussion leader: **Kelly Mayo**, Northwestern University, Evanston, IL
Catherine Woolley, Northwestern University, Evanston, IL, *Estrogen and the Hippocampus*; **Allison Doupe**, UCSF, CA, *Hormones and Imprinting in Birdsong Acquisition*; **Richard Axel**, Columbia University/HHMI, New York, NY, *Pheromones in Wiring of the Reproductive Circuitry*

Wednesday, July 28

9:00 am **Structure and Transcription by Nuclear Receptors**
Discussion leader: **Chris Glass**, UCSD, CA
Tom Scanlan, UCSF, CA, *Chemistry and Biology of Thyroid Receptor Action*; **Michael G. Rosenfeld**, UCSD/HHMI, CA, *Integration of Extracellular Signaling and Nuclear Receptor Function*; **Keith Yamamoto**, UCSF, CA, *Signals and Surfaces Affecting Intracellular Receptor Function*; **Robert Roeder**, Rockefeller University, New York, NY, *Transcriptional Regulation by Nuclear Receptors.*

7:30 pm **In Vivo Models for Probing Steroid Actions**
Discussion Leader: **Bill Schrader**, Ligand Pharmaceuticals, San Diego, CA
David Russell, University of Texas, SW Medical Center, Dallas, TX, *In Vivo Mutants of Steroid Synthesis in Reproduction*; **Gunther Schütz**, German Cancer Research Center, Heidelberg, Germany, *Designer Receptors for Probing Function of Glucocorticoids*; **Jeffrey Miner**, Ligand Pharmaceuticals, San Diego, CA, *Novel Non-Steroidal Therapeutic GR Ligands.*

Thursday, July 29

9:00 am **Orphan Nuclear Receptor Function**
Discussion Leader: **Keith Parker**, UTSW Medical Center, Dallas, TX
Yoel Sadovsky, Washington University, St. Louis, MO, *SF-1 in Reproductive and Adrenal Physiology*; **David Moore**, Baylor College of Medicine, Houston, TX, *SHP, A Novel Orphan Nuclear Receptor*; **Larry Jameson**, Massachusetts General Hospital, Boston, MA, *Dax-1 in Adrenal Function and Sex Determination*; **Frances Sladek**, UCR, CA, *HNF-4, Insights into Liver Function and Diabetes.*

7:30 pm **Nuclear Receptor Function**

Ron Evans, Salk Institute/HHMI, San Diego, CA, *Nuclear Receptor Function in Adipose Development*; **Bert O'Malley**, Baylor College of Medicine, Houston, TX, *Nuclear Receptor Cofactors and Transcription.*

Society for Neuroscience 2000

Read all instructions before typing abstract.
See *Call for Abstracts* and reverse of this sheet.
Complete abstract and all boxes at left and below.
(Please type or print in black ink.)

each replacement abstract. Replacement abstracts must be RECEIVED by Wednesday, May 3, 2000.

Appendix 5

First (Presenting) Author

Provide full name (no initials), address, and phone numbers *of first author on abstract. You may present (first author) only one abstract.* (Please type or print in black ink.)

Mingtao Li
Denver VAMC 111-H
1055 Clermont
Denver, CO 80220
Fax: (303) 393-5271
Office: (303) 399-8020 (2627) Home: ( )
E-mail: mingtaoli@uchsc.edu

SMALLEST RECOMMENDED TYPE SIZE: 10 POINT

SAMPLE:
2000 Annual Meeting
New Orleans, La.
November 4–9, 2000

POSTMARK DEADLINE:

MONDAY, APRIL 24, 2000

An asterisk must be placed after the sponsor's (signing member) name on the abstract.

MANDATORY: The present scientific work may involve a real or perceived financial conflict of interest. (See page 4, item 11.)

☐ yes ☐ no If yes:

Presentation Preference

Check one: ☒ poster only ☐ slide/poster

Themes and Topics

See list of themes and topics, pp. 17–18. Indicate below a first and second choice appropriate for programming and publishing your paper.

1st theme title: Development; Regeneration theme letter: A
1st topic title: Neuronal Death topic number: 17

2nd theme title: Cell Biology theme letter: B
2nd topic title: Gene structure and function topic number: 29

Special Requests (for example, projection, video, or computer requirements)

Include nonrefundable **abstract handling fee of $50.** Fill out payment information form below. Purchase orders will not be accepted. Submission of abstract handling fee does not include registration for the Annual Meeting.

MYOCYTE ENHANCER FACTOR-2 (MEF2)-A AND -D REGULATE SURVIVAL OF RAT CEREBELLAR GRANULE NEURONS. M. Li, M.P. Allen, T. Laessig, X. Wang, M.E. Wierman, and K.A. Heidenreich. Depts. Pharmacology and Medicine, Univ. Colorado Med. Sch. and Denver VA Med. Ctr., Denver, CO 80262

MEF2 transcription factors play a critical role in the development of skeletal, cardiac, and smooth muscle. MEF2 factors are present in the brain, but less is known about their function in nervous tissue. The MEF2 factors, MEF2A, -B, -C, and –D, bind to DNA as homo-or heterodimers to regulate gene expression. We show that all four MEF2s were present in rat cerebellar granule neurons (RCGN) grown in the presence of serum and 25 mM KCl. Gel mobility shift assays indicated that MEF2A and MEF2D were the major MEF2s bound to a MEF2 consensus oligonucleotide. MEF2A and MEF2D were present as heterodimers as evidenced by coimmunoprecipitation. When RCGN were induced to undergo apoptosis by lowering extracellular KCl to 5mM, MEF2A and MEF2D were phosphorylated and a decrease in the MEF2/DNA binding complex was observed. Transfection of RCGN with a dominant-inactive mutant of MEF2A (pcDNA.MEF2A131) induced apoptosis in the presence of serum and 25 mM KCl, whereas, the dominant-active MEF2 (pcDNA.MEF2VP16) blocked apoptosis induced by lowering KCl. We conclude that MEF2A and MEF2D are critical factors for survival of cerebellar granule neurons. This work was supported by VA Merit and USAMRAA medical research grants.

Key Words: (see instructions p. 4)

1. apoptosis
2. transcription factors
3. depolarization
4. gene expression

Signature of Society for Neuroscience member required below. ***No member may sign more than one abstract. The signing member must be an author on the paper and an asterisk must be placed after the sponsor's (signing member) name on the abstract.***

The signing member certifies that any work with **human or animal subjects** related in this abstract complies with the guiding policies and principles for experime procedures endorsed by the Society. This signature acknowledges that each author on this abstract has seen and approved the final version of the abstract and has g consent to appear as an author. Authors must comply with ethical guidelines for human and animal research, and may be asked to supply added documentation.

Kim A. Heidenreich
Society for Neuroscience member's signature

Kim A. Heidenreich
Printed or typed name

8304
Member ID number (mandatory)

(303) 399-8020 (3
Telephone number

Tear at perforation

Appendix 6

Brain Research
in press
5-30-00

Inhibitors of p38 MAP kinase increase the survival of transplanted dopamine neurons

W. Michael Zawada,[1,3] Mary K. Meintzer, [2,4] Pravin Rao,[2,4] Jonathan Marotti,[1] Xioamin Wang, [2,4] James E. Esplen,[1] Edward D. Clarkson,[1] Curt R. Freed,[1,3] and Kim A. Heidenreich[2,3,4]

[1]Departments of Medicine and Pharmacology, Division of Clinical Pharmacology, [2]Department of Pharmacology, [3]Neuroscience Training Program, University of Colorado School of Medicine, Denver, CO 80262; [4]Denver Veterans Administration Medical Center, Denver, CO 80220

Send correspondence to:
Dr. Kim A. Heidenreich
Department of Pharmacology, C-236
University of Colorado Health Sciences Center
4200 E. 9th Ave.
Denver, CO 80262

Phone: (303) 399-8020 ext. 3891
Fax: (303) 393-5271
email: Kim.Heidenreich@UCHSC.edu

Abstract

Fetal cell transplantation therapies are being developed for the treatment of a number of neurodegenerative disorders including Parkinson's disease [1-8]. Massive apoptotic cell death is a major limiting factor for the success of neurotransplantation. We have explored a novel protein kinase pathway for its role in apoptosis of dopamine neurons. We have discovered that inhibitors of p38 MAP kinase (the pyridinyl imidazole compounds: PD169316, SB203580, and SB202190) improve survival of rat dopamine neurons *in vitro* and after transplantation into hemiparkinsonian rats. In embryonic rat ventral mesencephalic cultures, serum withdrawal led to 80% loss of dopamine neurons due to increased apoptosis. Incubation of the cultures with p38 MAP kinase inhibitors at the time of serum withdrawal prevented dopaminergic cell death by inhibiting apoptosis. In the hemiparkinsonian rat, preincubation of ventral mesencephalic tissue with PD169316 prior to transplantation accelerated behavioral recovery and doubled the survival of transplanted dopamine neurons. We conclude that inhibitors of stress-activated protein kinases improve the outcome of cell transplantation by preventing apoptosis of neurons after grafting.

Key words: pyridinyl imidazole, apoptosis, Parkinson's disease, neurodegeneration, neurotransplantation, dopamine neuron, p38 MAP kinase

1. Introduction

Parkinson's disease is a neurodegenerative disorder characterized by progressive deterioration of motor function resulting from the loss of nigrostriatal dopamine neurons and depletion of striatal dopamine [9]. Because L-dopa [10] therapy loses its effectiveness after 5 to 20 years of treatment, alternative therapeutic strategies such as neurotransplantation of fetal dopamine cells have been sought. Despite the success of neural transplants in some Parkinson patients, other patients improve only slightly or not at all. Data from animal [11] and human post-mortem studies [5] indicate that much of the variability in neurotransplantation results from poor survival of transplanted dopamine cells. Although some cells in the transplants probably die by necrosis from handling and shear forces created during implantation, the majority of the observed cell death is apoptotic [12, 13]. The number of apoptotic cells observed in grafts of ventral mesencephalic tissue in parkinsonian rats is greatest during the first 24 hours after transplantation and is dramatically reduced by the end of the first week [13]. These findings offer the exciting possibility that signaling pathways leading to the initiation and execution of apoptosis can be blocked to prevent or reduce neuronal cell death. We have explored the p38 MAP kinase pathway for its role in apoptosis of dopamine neurons and found that inhibitors of p38 MAP kinase improve survival of dopamine neurons both in culture and after neurotransplantation in parkinsonian rats. These inhibitors offer advantages over other anti-apoptotic approaches because they are small organic molecules that are orally active [14] and cross the blood-brain barrier.

2. Methods

2.1. Culture of mesencephalic neurons and detection of apoptosis. E15 rat ventral mesencephalon was dissected as previously described [15]. Primary cultures of rat ventral mesencephalon were prepared in 1 ml of ice cold Ca^{2+}/Mg^{2+}-free Hanks' balanced salt solution (Mediatech) by mechanically dispersing tissue pieces using a sterile tip of a 1.0 ml Pipetman. Subsequently, cells were centrifuged at 200xg for 5 min and resuspended in F12 medium (Irvine Sci.) with 5 % human placental serum, 2 mM L-glutamine, 100 µg/ml streptomycin, 100 U/ml penicillin, 2.2 µg/ml ascorbic acid. Cells were seeded at a density of 6.0×10^4 viable cells/cm^2 in polyethylenimine-(Sigma) coated [16] 96-well plates in 0.1 ml of media. Cells were grown in a 95 % air/ 5 % CO_2 humidified atmosphere at 37 °C in serum-containing medium for 24 hrs.

At that time, medium was replaced with identical medium or medium lacking serum in the presence or absence of 0.01 - 100 μM PD169316 (4-[5-(4-Fluoro-phenyl)-2-(4-nitro-phenyl)-2H-imidazol-4-yl]-pyridine), obtained from Dr. Alan Saltiel of Parke-Davis Pharmaceuticals, Ann Arbor, MI or SB203580 and SB202190 (0.01-200 μM, commercially available from Calbiochem). Twenty hours after media change cultures were fixed in 4% paraformaldehyde. Dopamine neurons were identified using polyclonal anti-rat TH antibody (1:100; Pel-Freez) followed by ABC staining kit (Vector) as described below. Cultures for the studies of apoptosis were fixed in 1% paraformaldehyde followed by 70% ethanol in glycine buffer 18 hrs after serum withdrawal. These cultures were sequentially incubated with a polyclonal anti-TH antibody (1:100) overnight, anti-rabbit FITC conjugate (1:40; Calbiochem) for two hrs and with 8 μg/ml of Hoechst 33258 DNA dye for 10 min. TH^+ cells (green fluorescence) were counted as apoptotic only if their nuclei (blue) contained one or more lobes of condensed nuclear chromatin. In the entire experiment, a total of 5066 TH^+ neurons were examined for nuclear chromatin condensation. Four groups were tested: 1. +serum (n=2595); 2. –serum (n=269); 3. –serum + 10 μM PD169316 (n=1615); 4. –serum + 10 μM SB203580 (n=587).

2.2. 6-hydroxydopamine lesion and behavioral recovery test. Forty seven male Sprague-Dawley rats (225-250 gm) were anesthetized with equithesin (4 ml/kg) and placed in a stereotaxic frame. Unilateral lesions of the medial forebrain bundle were done by infusing 20 μg of 6-OHDA HBr (RBI), dissolved in 4 μl of sterile saline containing 0.2 % ascorbate at 1 μl/min per site at 2 sites (AP: -2.1 mm posterior to bregma, LAT: 2.0 mm from the midline, VD: -7.8 mm below the dura; and AP: -4.3 mm posterior to bregma, LAT: 1.5 mm from the midline, VD: -7.8 mm below the dura). Animals were tested as previously described [17] for ipsilateral to the lesion turning (90 min) in response to methamphetamine (5.0 mg/kg injected ip) two weeks after receiving lesions. Lesioned animals were assigned to four groups of equal rotational rates: 1. vehicle only, (n = 9, RPM = 7.8 ± 1.0); 2. tissue + vehicle (n = 11, RPM = 8.4 ± 1.5); 3. tissue + PD169316 (n = 14, RPM = 8.2 ± 0.9); 4. tissue + SB203580 (n=13, RPM = 8.2 ± 0.1). Only rats that rotated at three rpm or greater were included in this study. We have previously demonstrated [17] that in our drug-induced circling test performed in flat-bottomed Plexiglas cylinders circling above two rpm correlates with >95% dopamine depletion. In contrast, Ungerstedt and Arbuthnott demonstrated

that, when methamphetamine-induced circling test is performed in hemispherical bowls instead of cylinders, higher circling rates (4-6 rpm) predict >95% dopamine depletion [18].

2.3. Neurotransplantation. E15 rat ventral mesencephalon was dissected according to previously published methods [15]. For transplantation, half of a ventral mesencephalon was shaped into a tissue strand (200 μm in diameter) by extruding tissue through a tapered glass cannula made by heating a commercially available blank (Kimble Kontes, Cat# 663500-0444). Hemiparkinsonian rats received transplants of ventral mesencephalic strands that were incubated for two hours in a 95 % air/ 5 % CO_2 humidified atmosphere at 37 °C in vehicle (Ca^{2+}/Mg^{2+}-free Hanks' balanced salt solution, n=11), in vehicle containing 10 μM PD169316 (n=14), or in vehicle containing 10 μM SB203580 (n=13). Each animal received a transplant of half of a ventral mesencephalon. Another 9 animals received infusion of only vehicle into the transplant site located in the denervated striatum (AP: 0.0 mm from bregma, LAT: 3.0 mm from the midline, VD: -3.5 to -7.5 mm below the dura) in 4.0 μl over 4 min. Animals were tested for response to intreperitoneal methamphetamine (5.0 mg/kg) three and six weeks after receiving transplants. Behavioral recovery was analyzed using mixed-effects analysis of variance appropriate for repeated measures ANOVA.

2.4. Morphological evaluation of grafts. All transplant recipients were sacrificed six weeks after transplantation. Graft-containing areas of each brain were sectioned on a cryotome in the coronal plane at 40 μm thickness and mounted on glass microscope slides. Every third section was stained for TH-immunoreactivity using a polyclonal antibody against rat TH and ABC staining kit (Vector). Endogenous peroxidase was inactivated by a 20 min treatment in methanol containing 20 % hydrogen peroxide (v/v) at room temperature. Nonspecific binding was blocked with 10 % goat serum in PBS containing 1 % BSA and 0.3 % Triton-X for 60 min at room temperature. The primary anti-TH antibody (1:100 dilution) was applied to each slide overnight at 37 °C. Sections were then incubated with a biotinylated goat anti-rabbit IgG antibody and subsequently with avidin/biotinylated horseradish peroxidase complex, each for 2 hrs at room temperature. The peroxidase was visualized with diaminobenzidine dissolved in PBS and 0.03 % hydrogen peroxide.

All TH-positive profiles were counted in each section. Abercrombie's correction [19] assumed cell diameter of 20 μm and was used to generate the final estimate of the number of surviving dopamine neurons in each animal. To assure that treatment with the inhibitors did not alter dopamine neuron cell size, which would render use of Abercrombie's correction inappropriate, one rat was selected from each transplant group for detailed neuron size analysis. The rat selected had closest to the median value of surviving dopamine neurons for each group. In each selected rat, images of all sections containing grafted cells were captured at x400 magnification into SlideBook digital deconvolution software (Intelligent Imaging Innovations). The size of the soma for all dopamine neurons was determined using SlideBook's analysis tools. The total number of TH^+ somas measured was 353 for the animal receiving vehicle pre-treated tissue, 439 for the animal receiving PD169316 pre-treated tissue and 500 for the animals receiving SB203580 pre-treated tissue. For the measurement of the graft size and TH^+ fiber outgrowth, every third section was digitized using a Nikon slide scanner. Using the NIH Image program, area of the graft and area of the fiber outgrowth were manually outlined in each section. The areas were measured by the computer using a calibrated area analysis feature and volumes were calculated from the component areas.

3. Results

3.1. Effects of pyridinyl imidazole compounds on dopamine neuron survival and apoptosis. The survival of embryonic dopaminergic neurons in tissue culture is dependent on the presence of trophic factors contained in serum, and withdrawal of serum results in apoptosis. This model system has been used in the present studies to examine factors that rescue dopaminergic neurons from apoptotic cell death. In each experiment, primary neurons from ventral mesencephalon were grown in the presence of 5% human placental serum for 24 hours. At that time, medium was replaced with identical medium or medium lacking serum in the presence or absence of increasing concentrations of the p38 MAP kinase inhibitors PD169316, SB203580, and SB202190. Twenty hours after the media change, the cultures were fixed and stained with antibodies against tyrosine hydroxylase (TH) to identify surviving dopamine neurons. The structures of the pyridinyl imidazole compounds used in these experiments are shown in Figure 1a. The inhibitors differ only by the para substitution in the phenyl ring that is in the 2-position of the imidazole ring. In control cultures fed with

medium containing serum, there were 835 ± 29 surviving TH^+ neurons/cm^2 (Fig. 1b). Serum withdrawal (20hr) reduced the number of surviving TH^+ neurons/cm^2 to 122 ± 16 ($p<0.001$). All of the tested pyridinyl imidazole compounds, when added at the time of serum withdrawal, improved the survival of TH^+ neurons at concentrations shown to be effective in blocking p38 MAP kinase activity [20]. The survival effects of SB203580 and SB202190 reached their maximum at 100 and 200 μM, respectively. Application of SB203580 (100 μM) and SB202190 (200 μM) resulted in survival of 1321 ± 283 and 1703 ± 188 TH^+ neurons/cm^2, respectively. The highest dose (200 μM) of the SB203580 was toxic to dopamine neurons. The maximum effect of PD169316 was observed at 55 μM, when 1943 ± 240 dopamine neurons survived. Because the inhibitors tested in this study have limited solubility above 10 μM, cultures supplemented with 55 μM imidazole inhibitors contained abundant undissolved inhibitor crystals, which might have contributed to increased variability in cell survival observed in these cultures. Cultures supplemented with 10 μM of SB203580 or SB202190, at which concentration crystal formation was not a problem, had 470 ± 56 and 601 ± 48 surviving TH^+ neurons/cm^2, respectively. By contrast, 10 μM PD169316 protected all of the TH^+ neurons from serum withdrawal-induced death, supporting the survival of 1008 ± 126 TH^+ neurons/cm^2. These experiments have revealed that all three inhibitors can fully protect dopamine cells from serum withdrawal. The order of potency for complete neuroprotection from serum withdrawal was PD169316>SB203580>SB202190. In some cases, high concentrations of the inhibitors augmented TH^+ cell survival above that observed in serum-containing cultures (PD169316 at 55 and 100 μM, SB203580 at 100 μM, and SB202190 at 200 μM, $p<0.01$).

The morphology of TH^+ neurons grown in the absence and presence of serum is shown in Figure 2. Twenty hours after the media change, dopamine neurons cultured in medium containing serum (with or without 10 μM PD169316) appeared healthy and contained long neurites and highly ramified growth cones (Fig. 2a, c). By contrast, dopamine neurons from which serum was withdrawn were fewer in number, had truncated neurites and lacked growth cones (Fig. 2b). Supplementation of the serum-withdrawn cultures with 10 μM PD169316 rescued the TH^+ neurons. Their morphology was indistinguishable from that of the serum-fed neurons (Fig. 2d).

To determine if PD169316 exerted its survival effects on dopamine neurons by reducing the rate of apoptosis, we co-stained rat ventral mesencephalic cultures with TH antibodies to identify surviving dopamine neurons and Hoechst 33258 dye to examine nuclear morphology. Apoptotic

dopamine neurons were defined as TH^+ cells that contained one or more lobes of condensed nuclear chromatin. In the presence of serum, greater than 90% of TH^+ neurons showed normal nuclear morphology with the chromatin uniformly distributed throughout the nucleus (Fig. 3a). The apoptotic dopamine neurons showed marked nuclear condensation and had degenerating neurites (Fig. 3b). Maintenance of cell membrane integrity in the apoptotic dopamine neurons, another characteristic of apoptosis, was demonstrated by retention of TH enzyme within the apoptotic bodies (Fig. 3b). Removal of serum increased the number of adherent apoptotic cells by over 3-fold (Fig. 3c). PD169316 reduced the rate of apoptosis of dopamine neurons to control levels and SB203580 partially reduced the level of apoptosis seen after serum withdrawal.

3.2. Effects of pyridinyl imidazole compounds on dopamine neuron survival and function after transplantation. To determine whether inhibitors of p38 MAP kinase could increase the survival of dopamine neurons and accelerate motor recovery after transplantation, we transplanted rat ventral mesencephalic dopamine neurons obtained from embryonic day 15 rats into the brains of hemiparkinsonian rats. This rat model of Parkinson's disease is created by a unilateral injection of the neurotoxin 6-OHDA into the median forebrain bundle leading to the death of dopamine neurons in substantia nigra and dopamine depletion in striatum [17, 18]. Upon intraperitoneal injection of methamphetamine (5mg/kg), lesioned animals run in circles in a direction ipsilateral to the lesion. This circling behavior can be abolished by transplantation of embryonic rat dopamine neurons into the denervated striatum [21]. Grafted dopamine neurons survive, project neurites, form synapses, and improve behavior [22].

Rats were lesioned and tested for rotational behavior two weeks later. Lesioned rats that showed motor asymmetry (greater than 3 rpm) in response to methamphetamine were transplanted with one of the following: 1. vehicle only, 2. mesencephalic tissue pretreated with vehicle, 3. mesencephalic tissue pretreated with 10 μM PD169316, or 4. mesencephalic tissue pretreated with 10 μM SB203580. For the pretreatment, all tissues were incubated for two hours in a 95 % air/ 5 % CO_2 humidified atmosphere at 37 °C. Inhibitor concentration of 10 μM was chosen for the transplantation experiments, because higher concentrations of the inhibitors result in an unacceptably high crystal formation upon contact with aqueous solutions. Inhibitors of p38 MAP kinase that have much better solubility in aqueous solutions are being developed [23].

Behavioral recovery was tested at three and six weeks following transplantation. Animals that received vehicle without tissue did not reduce their rotational rate over the six-week period. At three weeks, animals that received transplants of tissue pretreated with vehicle alone reduced their circling rate by 60% from the pretransplantation rate (Fig. 4). By contrast, recipients of transplants pretreated with the pyridinyl imidazole compounds had significantly accelerated reduction in their rotational rates when compared to the vehicle pretreated tissue recipients. The PD169316 pretreated group reduced their rotational rate by 90% ($p<0.01$), while the SB203580 pretreated group reduced their circling by 74% ($p<0.01$). At six weeks after transplantation, behavioral improvement continued (Fig. 4). The vehicle pretreated group showed a 77% reduction in circling. The PD169316 pretreated group showed the greatest reduction in circling (99%) and was significantly different from the control group ($p<0.01$). The SB203580 pretreated group reduced their rotational rate by 82%, a value not statistically different from the vehicle group. Thus, animals receiving mesencephalic tissue that was pretreated with PD169316 completely stopped circling at six weeks after transplantation.

To determine if behavioral improvement coincided with increased survival of dopamine neurons in the graft, animals were sacrificed and their brains processed for tyrosine hydroxylase immunocytochemistry. Examples of coronal sections through grafts stained for TH are shown in Figure 5a. Cell counting of TH^+ neurons in these coronal sections revealed that 1550 ± 294 dopamine neurons survived in grafts pretreated with vehicle (Fig. 5b). The number of surviving TH^+ neurons doubled to 3023 ± 518 when the tissue was pretreated with PD169316 ($p<0.05$). Although pretreatment of tissue with SB203580 increased the number of surviving dopamine neurons to 2321 ± 394, the increase was not statistically significant. Analysis of the graft size (Fig.5c) and TH^+ fiber outgrowth (Fig.5d) using the NIH Image program revealed that pretreatment of mesencephalic tissue with PD169316 prior to transplantation increased the graft size by 140% ($p<0.01$), while pretreatment of the tissue with SB203580 increased the graft size by 100% ($p<0.05$). Preincubation with either PD169316 or SB203580 also augmented the TH^+ fiber outgrowth by 130% ($p<0.01$).

To assure that treatment with the inhibitors did not alter dopamine neuron cell size, which would render use of Abercrombie's correction inappropriate, one rat was selected from each transplant group for detailed neuron size analysis. The rat selected had closest to the median value of surviving dopamine neurons for each group. Measurement of soma size of TH^+ neurons

from images captured at x400 magnification into SlideBook digital deconvolution software revealed that average area of TH^+ cell soma was not changed by the *ex vivo* inhibitor treatment (Fig. 6). Specifically, average area of TH^+ cell soma of cells in tissue treated with the vehicle was 177 ± 4 μm^2, 180 ± 3 μm^2 in tissue treated with PD169316, and 172 ± 3 μm^2 in tissue treated with SB203580.

4. Discussion

Results from these studies indicate that pyridinyl imidazole inhibitors of p38 MAP kinase improve survival of dopamine neurons both in tissue culture and after neurotransplantation in hemiparkinsonian rats. The improved survival of grafts treated with the p38 MAP kinase inhibitors correlated with more rapid improvement in motor behavior. These data suggest that apoptotic programmed cell death occurring *in vivo* after transplantation results from activation of p38 MAP kinase. This outcome is consistent with *in vitro* experiments showing that inhibitors of p38 MAP kinase block apoptosis of neurons [24, 25]. Despite the rescue of many of the transplanted dopamine neurons by p38 MAP kinase inhibitors, the majority of dopamine neurons did not survive transplantation. Further improvement in grafting may come from short-term systemic administration of the inhibitors to sustain higher inhibitor concentration during the first week after grafting when neuronal apoptosis is greatest [13]. More potent and more soluble p38 MAP kinase inhibitors are being developed [23]. It is also possible that use of the p38 MAP kinase inhibitors in combination with growth factors [13, 26], antioxidants [27, 28], or other antiapoptotic agents such as caspase inhibitors [29] would provide additive benefits in cell survival and transplant outcome. The advantages that the pyridinyl compounds have over growth factors and caspase inhibitors for preventing apoptosis *in vivo* include their low molecular weight, acceptable systemic toxicity [14] and ability to cross the blood-brain barrier. These characteristics make the pyridinyl imidazole compounds promising candidate drugs for improving survival of dopamine neurons following transplantation into humans.

Acknowledgements

We thank Cindy Hutt and Pat Bell for their technical work, Dr. Kim Bjugstad for help with statistical analysis, Dr. Jenifer Monks for help with computer imaging, Dr. Joe Gal for constructive comments, and Dr. Alan Saltiel of Parke-Davis Pharmaceuticals for providing PD169316. This research was supported by U.S. Public Health Grants NS18639, NIGMS GM07063, M01 RR00069 (C.R.F), NS38619 (K.A.H. and W.M.Z.) and VA Merit and VA Research Enhancement Award (K.A.H.).

Figure Legends

Fig.1. The effects of pyridinyl imidazole compounds on the survival of embryonic dopamine neurons. (**a**) Structures of PD169316, SB203580, and SB202190. Note that the differences between the compounds exist in the para substitution in the phenyl ring that is in the 2-position of the imidazole ring. (**b**) Protection of dopamine neurons from serum withdrawal-induced death with pyridinyl imidazole compounds. Mesencephalic cultures were initially grown for 24 hrs in 5% human placental serum. At that time, medium was replaced with an identical medium (leftmost solid bar) or medium lacking serum in the presence (0.01-100/200 μM) or absence (open bar) of PD169316, SB203580 and SB202190 for 20 hrs. All inhibitors tested at 10 μM provided protection to dopamine neurons. At 10 μM, PD169316 was most potent inhibitor providing complete protection from death by serum withdrawal. Data are mean ± S.E.M. (n = 4-43) from up to five independent experiments. Statistical significance was determined using one-way ANOVA ($p<0.0001$; $F_{(21, 230)} = 22.7$). Means were considered different from –serum cultures when Newman-Keuls post hoc test revealed $p<0.05$ (asterisks).

Fig. 2. PD169316 protects dopamine neurons from degeneration *in vitro*. (**a-d**) Micrographs of dopamine neurons 20 hours following media change. Cells were immunostained using anti-TH antibody. (**a**) 5% serum only; (**b**) no serum; (**c**) 5% serum plus 10 μM PD169316; (**d**) no serum plus 10 μM PD169316. In these experiments, PD169316 acted as serum replacement. 10 μM PD169316 (**d**) restored both dopamine neuron survival and neurite outgrowth to that observed in serum-containing cultures (***a***). Note that addition of PD169316 to cultures supplemented with

serum (*c*) did not further increase dopamine cell survival or neurite outgrowth. Scale bar = 100 μm.

Fig. 3. Pyridinyl imidazole inhibitors rescue dopamine neurons from apoptosis. (**a** and **b**), Micrographs showing dopamine neurons (green) identified using anti-TH primary antibody followed by FITC-conjugated secondary antibody and nuclei (blue) stained with Hoechst 33258. All cells were cultured in 5% human placental serum for 24 hours. At that time, medium was replaced with an identical medium or medium lacking serum in the presence or absence of 10μM PD169316 or 10μM SB203580. All cultures were fixed 18 hours following media change. (**a**) Micrograph showing a healthy dopamine neuron among several healthy non-dopaminergic nuclei in serum supplemented culture. (**b**) An apoptotic dopamine neuron containing two lobes of condensed chromatin. Note degeneration of the neurites and retention of TH within the apoptotic body. Scale bar = 25 μm. (**c**) Quantitation of the percent of adhering TH^+ neurons that are apoptotic. In the presence of serum, 8.8% of dopamine neurons were apoptotic. Serum withdrawal for 18 hours raised apoptosis in dopamine neurons to 32.3%. Addition of 10μM PD169316 completely prevented the increase in apoptosis induced by serum withdrawal (7.8% dopamine neurons were apoptotic). SB203580 reduced apoptosis to 16.5%. Data are mean ± S.E.M. In this experiment, a total of 5066 TH^+ neurons were examined for apoptotic morphology. Statistical significance was determined using one-way ANOVA ($p<0.001$; $F_{(3, 23)} = 34.5$). Asterisks signify $p<0.001$ (compared to –serum) based on Newman-Keuls post hoc test.

Fig. 4. Reduction in circling behavior following neurotransplantation. All animals were injected with methamphetamine (5mg/kg; ip) to test motor asymmetry after a unilateral 6-OHDA lesion. High rotations indicate dopamine imbalance (lesion severe), while low rotations indicate dopamine level normalization (lesion corrected). Net ipsilateral rotation scores are shown for four experimental groups that received intrastriatal transplants: 1. vehicle only, (n = 9); 2. tissue + vehicle (n = 11); 3. tissue + 10 μM PD169316 (n = 14) and 4. tissue + 10 μM SB203580 (n=13). Rats were tested prior to transplantation (two weeks after lesioning) and three and six weeks after transplantation. At three weeks, groups transplanted with tissues treated with both PD and SB compounds had significantly lower rotational scores than controls receiving vehicle-pretreated tissue ($p<0.01$). PD169316 treated group was the only group to stop rotating at six

weeks after transplantation ($p<0.01$ vs tissue + vehicle). Data are mean ± S.E.M. Significance was determined using two-way ANOVA ($p<0.001$; $F_{(6, 86)} = 4.7$) followed by a Fisher LSD post hoc test.

Fig. 5. Morphological and histological graft assessment. **(a)** Coronal sections showing tyrosine hydoxylase (TH) immunostaining of the representative grafts transplanted into denervated adult rat striatum. Note that even under gross examination, both graft size and TH^+ fiber outgrowth are greatest in the graft pretreated with PD169316 (middle section). Scale bar = 1mm. **(b)** Number of surviving transplanted TH^+ neurons per animal. PD169316 doubled TH^+ neuron survival ($p<0.01$; t-test). **(c)** Graft size was also significantly increased ($p<0.01$; $F_{(2,37)} = 7.0$) by PD199316 ($p<0.01$) and SB203580 ($p<0.05$). **(d)** The imidazole inhibitors significantly extended fiber outgrowth ($p<0.01$; $F_{(2,37)} = 7.4$). Data are mean ± S.E.M. (n = 9-14). Statistical analysis was done using one-way ANOVA followed by a Newman-Keuls post hoc test.

Figure. 6. Preincubation of ventral mesencephalic tissue strands with pyridinyl inhibitors of p38 MAP kinase does not alter the size of transplanted dopamine neurons. TH-immunoreactive cells from **(a)** transplant of ventral mesencephalic tissue pretreated with vehicle, **(b)** transplant pretreated with 10 μM PD169316, and **(c)** transplant pretreated with 10 μM SB203580. Scale bar = 20 μm. **(d)** Mean soma area of TH^+ neurons found in three different experimental groups six weeks after grafting.

References

[1] C.R. Freed, R.E. Breeze, N.L. Rosenberg, S.A. Schneck, T.H.Wells, J.N. Barrett, S.T. Grafton, S.C. Huang, D. Eidelberg, D.A. Rottenberg, Transplantation of human fetal dopamine cells for Parkinson's disease. Arch. Neurol. 47 (1990) 505-512.

[2] O. Lindvall, P. Brundin, H. Widner, S. Rehncrona, B. Gustavii, R. Frackowiak, K.L. Leenders, G. Sawle, J.C. Rothwell, C.D. Marsden, A. Björklund, Grafts of fetal dopamine neurons survive and improve motor function in Parkinson's disease. Science 247 (1990) 574-577.

[3] C.R. Freed, R.E. Breeze, N.L. Rosenberg, S.A. Schneck, E. Kriek, J.X. Qi, T. Lone, Y.B. Zhang, J.A. Synder, T.H. Wells, L.O. Ramig, L. Thompson, J.C. Mazziotta, S.C. Huang, S.T. Grafton, D. Brooks, G. Sawle, G. Schroter, A.A. Ansari. Survival of implanted fetal dopamine cells and neurologic improvement 12 to 46 months after transplantation for Parkinson's disease. N. Engl. J. Med. 327 (1992) 1549-1555.

[4] M. Peschanski, G. Defer, J.P. N'Guyen, F. Ricolfi, J.C. Monfort, P. Remy, C. Geny, Y. Samson, P. Hantraye, R. Jeny, A. Gaston, Y. Kéravel, J.D. Degos, P. Cesaro, Bilateral motor improvement and alteration of L-dopa effect in two patients with Parkinson's disease following intrastriatal transplantation of foetal ventral mesencephalon. Brain 117 (1994) 487-499.

[5] J.H. Kordower, T.B. Freeman, B.J. Snow, F.J. Vingerhoets, E.J. Mufson, P.R. Sanberg, R.A. Hauser, D.A. Smith, G.M. Nauert, D.P. Perl, C.W. Olanow, Neuropathological evidence of graft survival and striatal reinnervation after the transplantation of fetal mesencephalic tissue in a patient with Parkinson's disease. N. Engl. J. Med. 332 (1995) 1118-1124.

[6] T.B. Freeman, C.W. Olanow, R.A. Hauser, G.M. Nauert, D.A. Smith, C.V. Borlongan, P.R. Sanberg, D.A. Holt, J.H. Kordower, F.J. Vingerhoets, B.J. Snow, D. Calne, L.L. Gauger, Bilateral fetal nigral transplantation into the postcommissural putamen in Parkinson's disease. Ann. Neurol. 38 (1995) 379-388.

[7] O.V. Kopyov, D. Jacques, A. Lieberman, C.M. Duma, R.L. Rogers, Clinical study of fetal mesencephalic intracerebral transplants for the treatment of Parkinson's disease. Cell Transplantation 5 (1996) 327-337.

[8] G.K. Wenning, P. Odin, P. Morrish, S. Rehcrona, H. Widner, P. Brundin, J.C. Rothwell, R. Brown, B. Gustavii, P. Hagell, M. Jahanshahi, G. Sawle, A. Björklund, D.J. Brooks, C.D. Marsden, N.P. Quinn, O. Lindvall, Short- and long-term survival and function of unilateral intrastriatal dopaminergic grafts in Parkinson's disease. Ann. Neurol. 42 (1997) 95-107.

[9] H. Ehringer, O. Hornykiewicz, Verteilung von noradrenalin and dopamin (3-hydroxytyramin) im gehirn des menschen und ihr verhalten bei erkrankungen des extrapyramidalen systems. Klin. Wochenschr. 38 (1960) 1236-1239.

[10] G.C. Cotzias, M.H. Van Woert, L.M. Schiffer, Aromatic amino acids and modification of parkinsonism. N. Engl. J. Med. 276 (1967) 374-379.

[11] P. Brundin, G. Barbin, O. Isacson, M. Mallat, B. Chamak, A. Prochiantz, F.H. Gage, A. Björklund, Survival of intracerebrally grafted rat dopamine neurons previously cultured *in vitro*. Neurosci. Lett. 61 (1985) 79-84.

[12] T.J. Mahalik, W.E. Hahn, G.H. Clayton, G.P. Owens, Programmed cell death in developing grafts of fetal substantia nigra. Exp. Neurol. 129 (1994) 27-36.

[13] W.M. Zawada, D.J. Zastrow, E.D. Clarkson, F.S. Adams, K.P. Bell, C.R. Freed, Growth factors improve immediate survival of embryonic dopamine neurons after transplantation into rats. Brain Res. 786 (1998) 96-103.

[14] A.M. Badger, J. N. Bradbeer, B. Votta, J.C. Lee, J.L. Adams, D.E. Griswold, Pharmacological profile of SB 203580, a selective inhibitor of cytokine suppressive binding protein/p38 kinase, in animal models of arthritis, bone resorption, endotoxin shock and immune function. J. Pharmacol. Exp. Therap. 279 (1996) 1453-1461.

[15] S.B. Dunnett, A. Björklund, Staging and dissection of rat embryos. In Neural Transplantation: A Practical Approach. S.B. Dunnett and Björklund, A., editors (Oxford University Press, New York. (1992) 1-19.

[16] K.D. Beck, B. Knüsel, F. Hefti, The nature of the trophic action of brain-derived neurotrophic factor, des(1-3)-insulin-like growth factor-1, and basic fibroblast growth factor on mesencephalic dopaminergic neurons developing in culture. Neuroscience 52 (1992) 855-866.

[17] J.B. Richards, K.E. Sabol, C.R. Freed, Unilateral dopamine depletion causes bilateral deficits in conditioned rotation in rats. Pharmacol. Biochem. Behav. 36 (1990) 217-223.

[18] U. Ungerdstedt, G.W. Aurbuthnott, Quantative recording of rotational behavior in rats after 6-hydroxydopamine lesions of the nigrostriatal dopamine system. Brain Res. 24 (1970) 485-493.

[19] M. Abercrombie, Estimation of nuclear population from microtome sections. The Anatomical Record 94 (1946) 239-247.

[20] A. Cuenda, J. Rouse, Y.N. Doza, R. Meier, P. Cohen, T.F. Gallagher, P.R. Young, J.C. Lee, SB203580 is a specific inhibitor of a MAP kinase homologue which is stimulated by cellular stresses and interleukin 1. FEBS Lett. 364 (1995) 229-233.

[21] E.D. Clarkson, W.M. Zawada, F.S. Adams, K.P. Bell, C.R. Freed, Strands of mesencephalic tissue show greater dopamine neuron survival and better behavioral improvement than cell suspensions after transplantation in parkinsonian rats. Brain Res. 806 (1998) 60-68.

[22] T.J. Mahalik, T.E. Finger, I. Strömberg, L. Olson, Substantia nigra transplants into denervated striatum of the rat: ultrastructure of graft and host interconnections. J. Comp. Neurol. 240 (1985) 60-70.

[23] J.N. Liverton, J.W. Butcher, C.F. Claiborne, D.A. Claremon, B.E. Libby, K.T. Nguyen, S.M. Pitzenberger, H.G. Selnick, G.R. Smith, A. Tebben, J.P. Vacca, S.L. Varga, L. Agarwal, K. Dancheck, A.J. Forsyth, D.S. Fletcher, B. Frantz, W.A. Hanlon, C.F. Harper, S.J. Hofsess, M. Kostura, J. Lin, S. Luell, E.A. O'Neill, C.J. Orevillo, M. Pang, J. Parsons, A. Rolando, Y. Sahly, D.M. Visco, S.J. O'Keefe, Design and synthesis of potent, selective, and orally bioavailable tetrasubstituted imidazole inhibitors of p38 mitogen-activated protein kinase. J. Med. Chem. 42 (1999) 2180-2190.

[24] J.L. Kummer, P.K. Rao, K.A. Heidenreich, p38 MAP kinase mediates apoptosis induced by withdrawal of trophic factors. J. Biol. Chem. 272 (1997) 20490-20494.

[25] H. Kawasaki, T. Morooka, S. Shimohama, J. Kimura, T. Hirano, Y. Gotoh, E. Nishida, Activation and involvement of p38 mitogen-activated protein kinase in glutamate-induced apoptosis in rat cerebellar granule cells. J. Biol. Chem. 272 (1997) 18518-1852.

[26] H. Takayama, J. Ray, H.K. Raymon, A. Baird, J. Hogg, L.J. Fisher, F.H. Gage, Basic fibroblast growth factor increases dopaminergic graft survival and function in a rat model of Parkinson's disease. Nature Med. 1 (1995) 53-58.

[27] N. Nakao, E.M. Frodl, W.-M. Duan, H. Widner, P. Brundin, Lazaroids improve the survival of grafted rat embryonic dopamine neurons. Proc. Natl. Acad. Sci. USA 91 (1994) 12408-12412.

[28] N. Nakao, E.M. Frodl, H. Widner, E. Carlson, F.A. Eggerding, C.J. Epstein, P. Brundin, Overexpressing Cu/Zu superoxide dismutase enhancs survival of transplanted neurons in a rat model of Parkinson's disease. Nature Med. 1 (1995) 226-231.

[29] G.S. Schierle, O. Hansson, M. Leist, P. Nicotera, H. Widner, P. Brundin, Caspase inhibition reduces apoptosis and increases survival of nigral transplants. Nature Med. 5 (1999) 97-100.

a

b

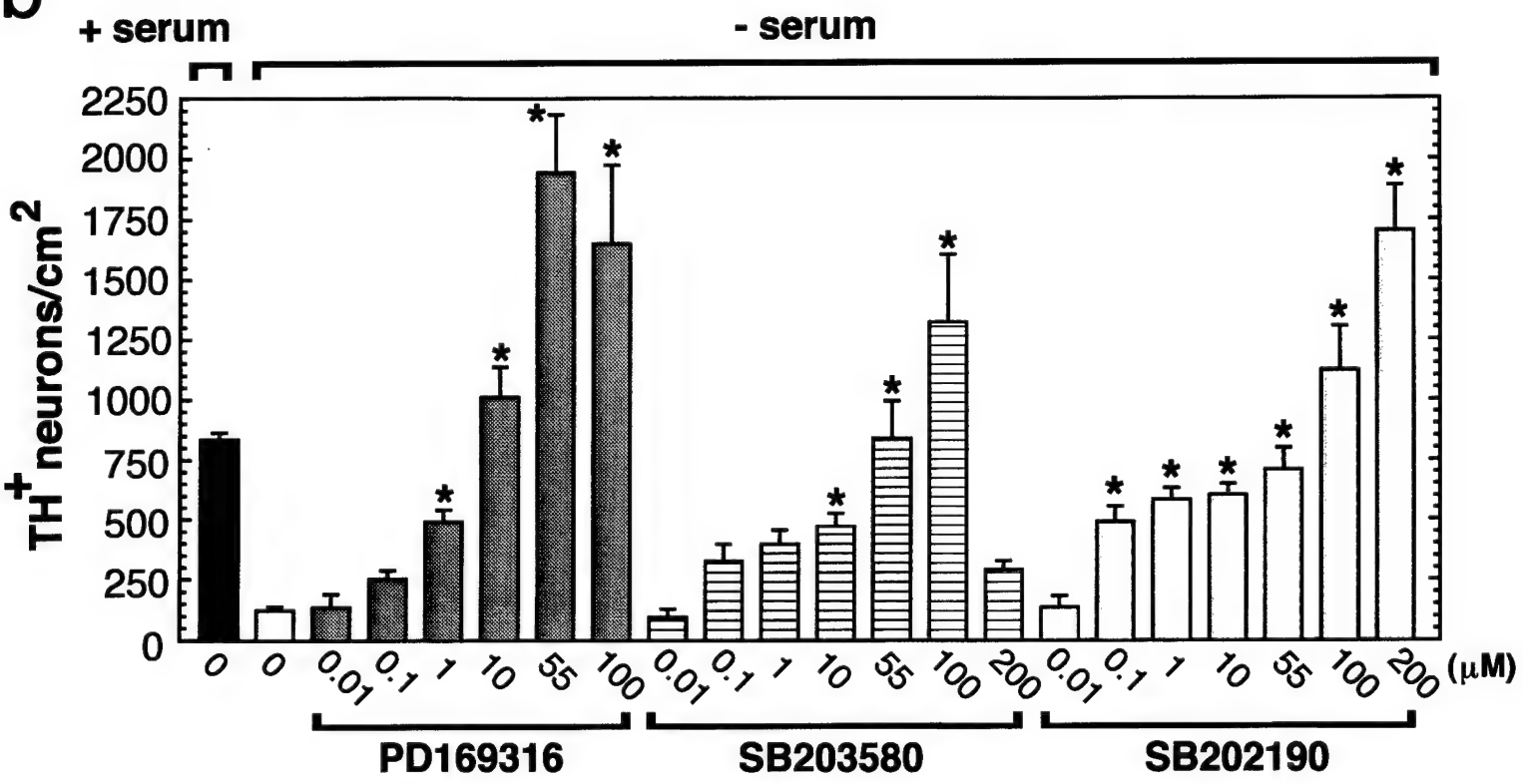

Figure 1
The effects of pyridinyl imidazole compounds on the survival of embryonic dopamine neurons.
Zawada et al., 2000

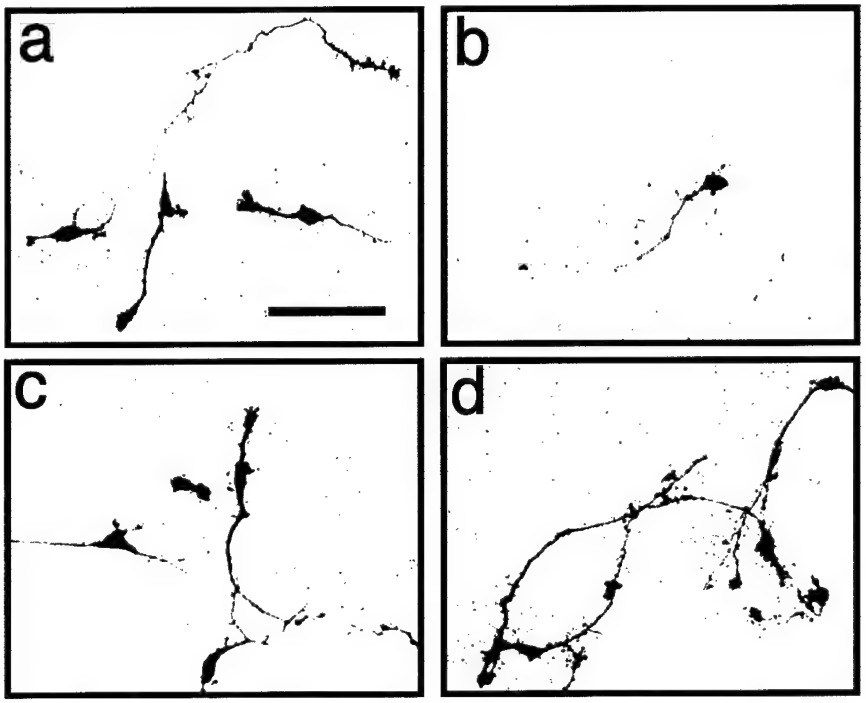

Figure 2
PD169316 protects dopamine neurons from degeneration *in vitro*.
Zawada et al., 2000

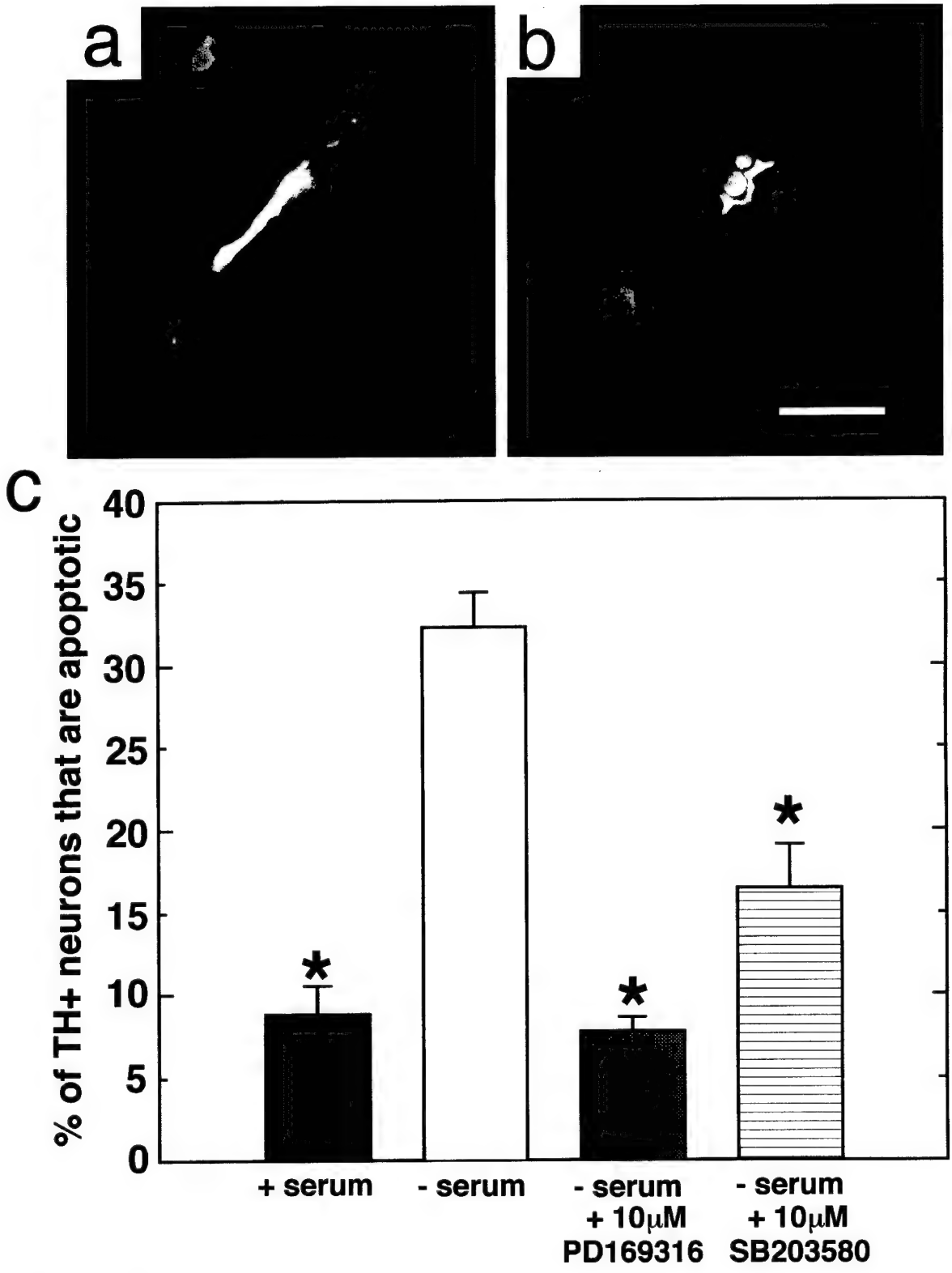

Figure 3
Pyridinyl imidazole inhibitors rescue dopamine neurons from apoptosis.
Zawada et al., 2000

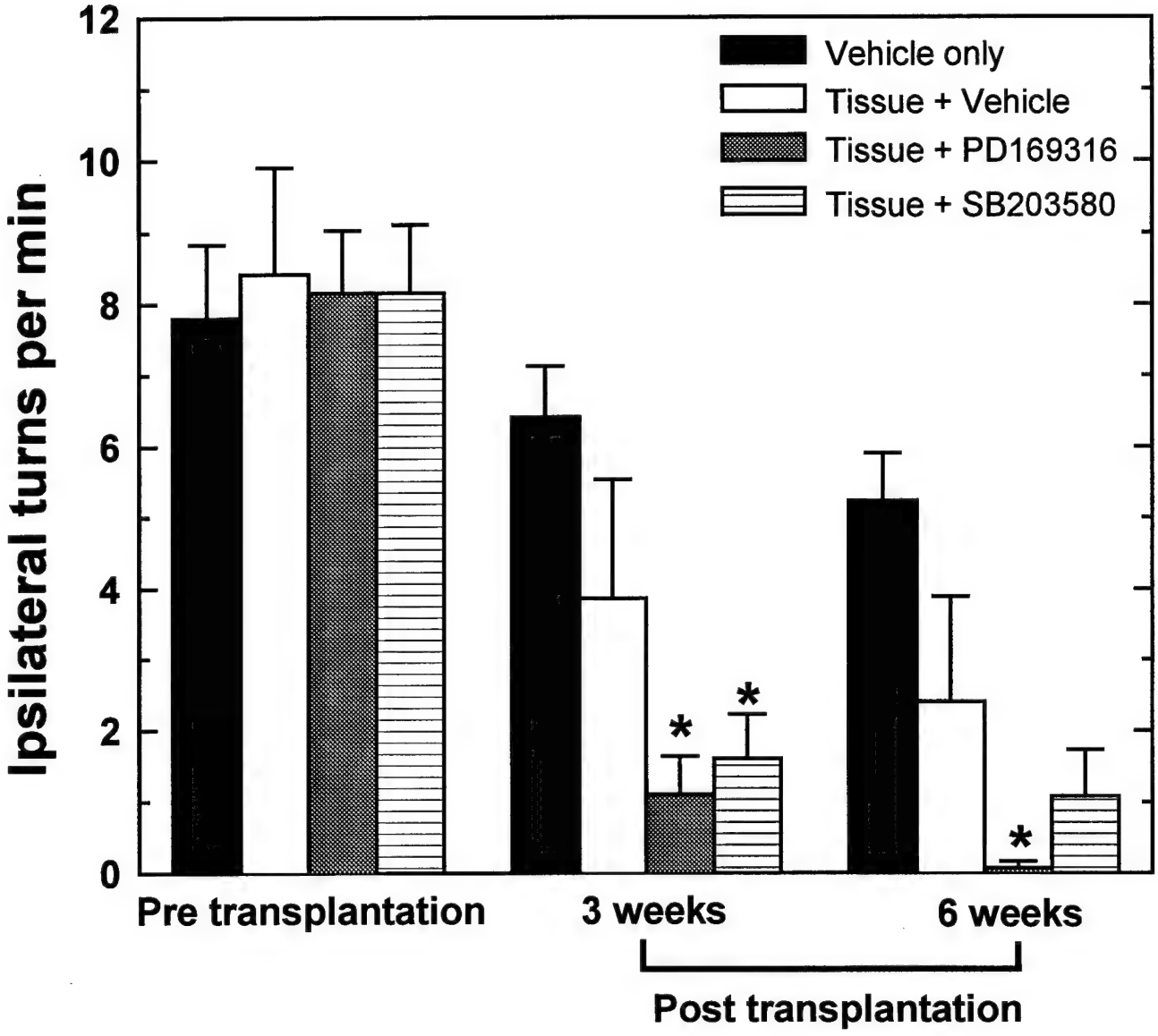

Figure 4
Reduction in circling behavior following neurotransplantation.
Zawada et al., 2000

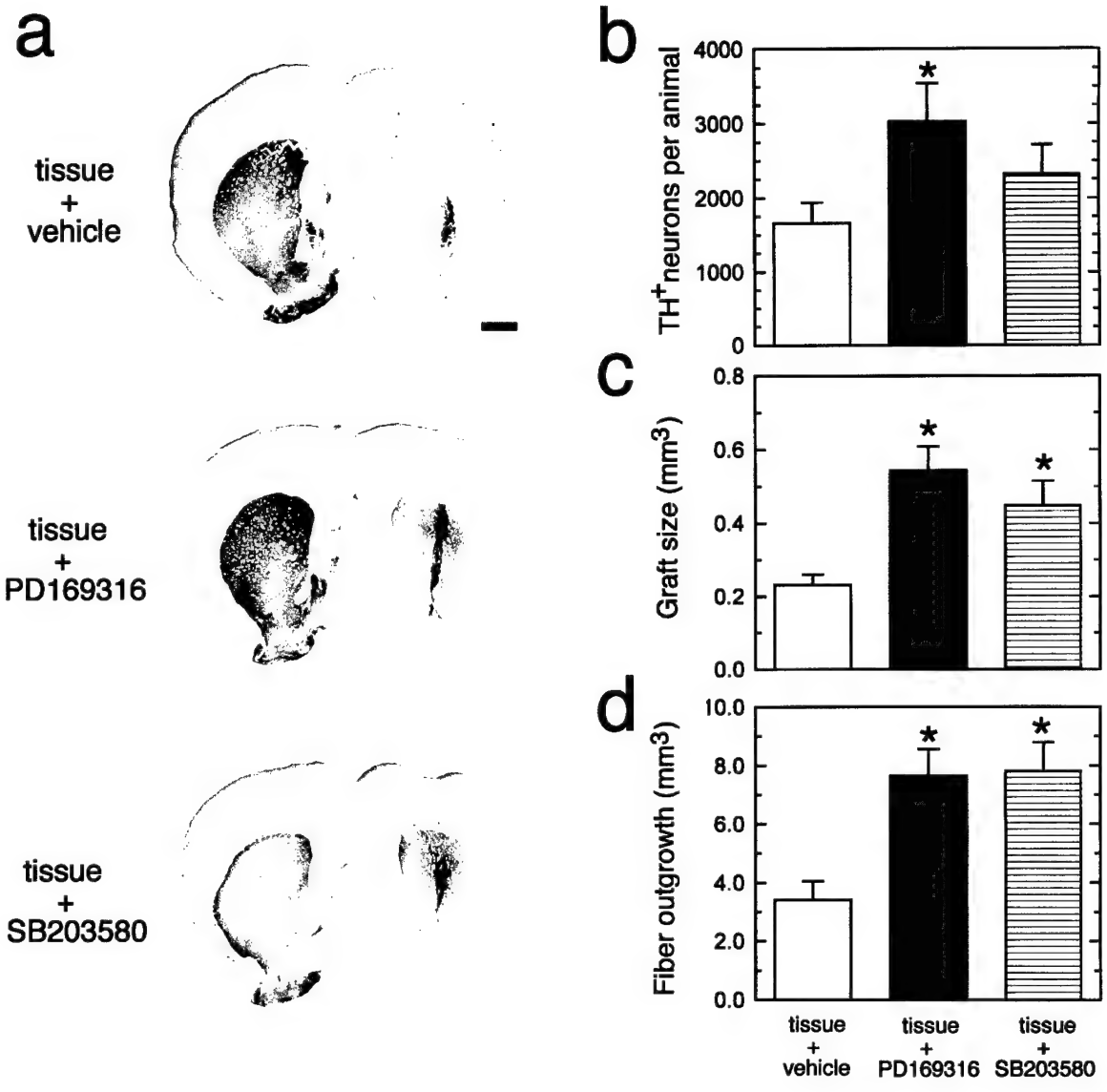

Figure 5
Morphological and histological graft assessment.
Zawada et al., 2000

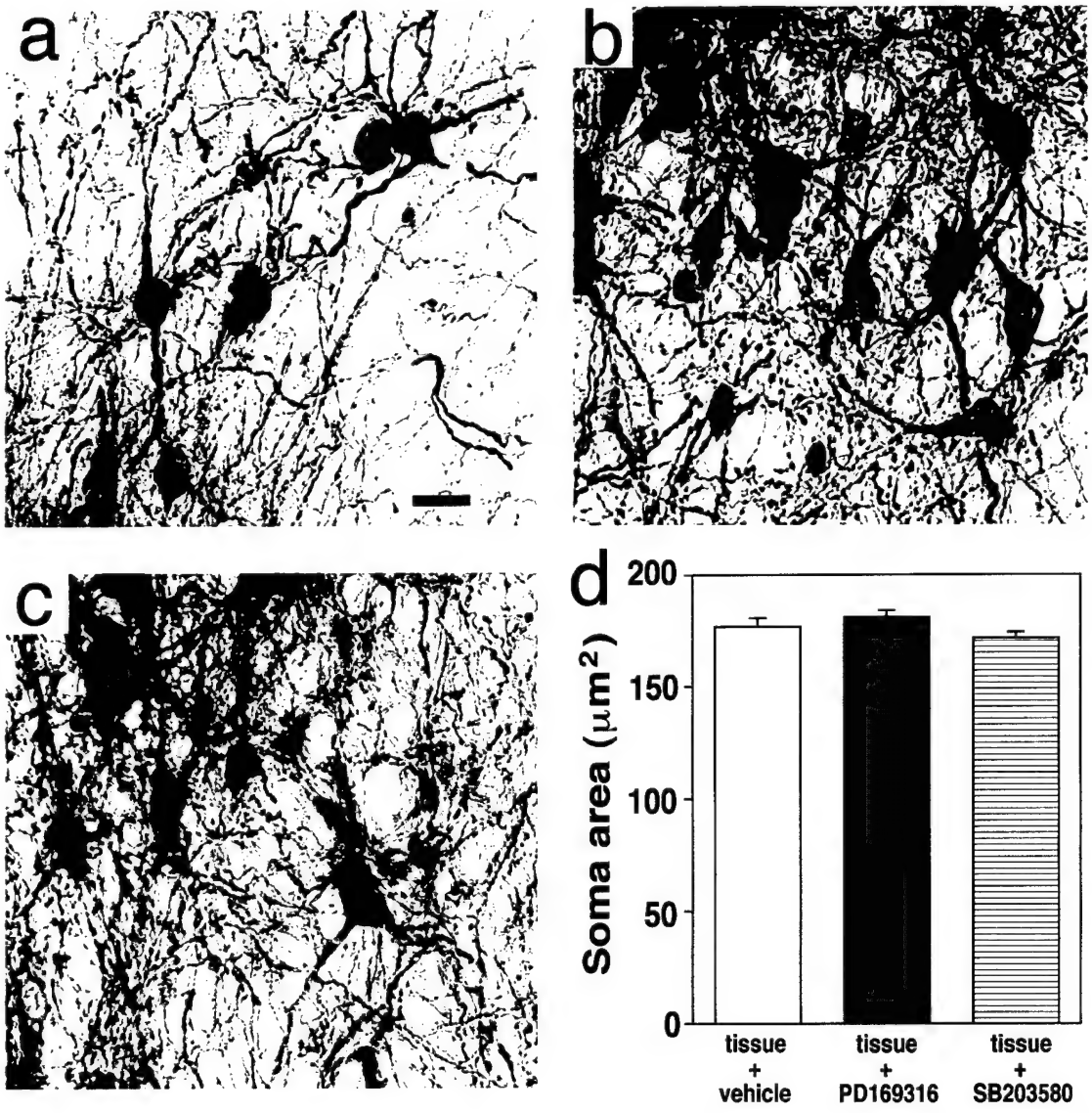

Figure 6
Preincubation of ventral mesencephalic tissue strands with pyridiny inhibitors of p38 MAP kinase does not alter the size of dopamine neurons following transplantation.
Zawada et al., 2000

Appendix 7

Exp. Neurology (in press)

Clarkson et al., 2000

IGF-I and bFGF Improve Dopamine Neuron Survival and Behavioral Outcome in Parkinsonian Rats Receiving Cultured Human Fetal Tissue Strands

Edward D. Clarkson[1], W. Michael Zawada[2, 4, 5],

K. Pat Bell[4], James E. Esplen[4], Paul K. Choi[4], Kim A. Heidenreich[3, 5, 6] and Curt R. Freed[2, 3, 4, 5]

[1]US Army Medical Research Institute of Chemical Defense, 3100 Ricketts Point Road, MCMR-UV-DB, Aberdeen Proving Grounds, MD 21010-5400; [2]Departments of Medicine and [3]Pharmacology, [4]Division of Clinical Pharmacology, [5]Neuroscience Program, University of Colorado School of Medicine, 4200 East Ninth Avenue, Denver, CO 80262; [6] Denver Veterans Administration Medical Center, Denver, CO 80220

Send correspondence to:

Curt R. Freed, MD
Division of Clinical Pharmacology, C-237
University of Colorado School of Medicine
4200 East Ninth Avenue
Denver, CO 80262
Phone (303) 315-8455
FAX (303) 315-3272

Keywords: Parkinson's Disease, Human Fetal Tissue, 6-OHDA, Transplantation, IGF-I, bFGF.

Proposed Running Head: IGF-I/bFGF improve outcome of transplanted human fetal tissue.

ABSTRACT

To promote dopamine cell survival in human fetal tissue strands transplanted into immunosuppressed 6-OHDA lesioned rats, we have preincubated tissue in insulin-like growth factor-I (IGF-I, 150 ng/ml) and basic fibroblast growth factor (bFGF, 15 ng/ml) *in vitro* for two weeks. Growth factor treatment did not affect the rate of homovanillic acid production *in vitro* but increased overall dopamine neuron survival in animals after transplant from 1240 ± 250 to 2380 ± 440 neurons ($p<0.05$). Animals in the growth factor-treated group had a significantly greater reduction in methamphetamine-induced rotation (66%) compared to control transplants (30%, $p<0.05$). We conclude that *in vitro* preincubation of human fetal tissue strands with IGF-I and bFGF improves dopamine cell survival and the behavioral outcome of transplants.

INTRODUCTION

In Parkinson's disease, progressive deterioration of motor function results from the loss of nigrostriatal dopamine neurons and consequent dopamine depletion in the caudate and putamen (17). Among neurological disorders, Parkinson's disease is a prime candidate for a new strategy for treatment because drug therapy loses its effectiveness after 5 to 10 years. In 1979, Björklund and Stenevi (5) and Perlow *et al.* (43) demonstrated the potential benefits of mesencephalic grafts in parkinsonian rats. Since then, fetal tissue transplantation has been developed as a treatment for Parkinson's disease in humans (19-26, 32, 35, 59). Decisions about the appropriate age of human fetal donor tissue and its preparation have been based on extrapolation from the embryonic development of rodents as well as direct transplantation of human fetal tissue into parkinsonian rats (11, 26, 31, 49-52, 55-58).

A major problem with neurotransplantation is that up to 95% of embryonic dopamine neurons die after transplantation (7, 33). Since cells in transplants of embryonic mesencephalon have been shown to undergo apoptotic cell death *in vivo* (36, 62), we and others are examining possible uses of neurotrophic factors to reduce apoptosis (12, 13, 28, 37, 38, 47, 48, 61, 62). Two of the growth factors being examined are insulin-like growth factor-I (IGF-I) and basic fibroblast growth factor (bFGF) which improve dopamine neuron survival *in vitro* (30) and *in vivo* (53). We have recently shown that dopamine neuron survival can be improved by a two-hour pre-incubation of transplanted tissue with the growth factor combination of glial cell line-derived neurotrophic factor (GDNF), IGF-I and bFGF (62). We have also shown that a combination of IGF-I and bFGF reduces

the rate at which dopamine neurons undergo apoptosis *in vitro* (61). The growth factors may be acting indirectly through stimulation of trophic factor production by astrocytes (18), since the neuroprotective effect can be blocked by inhibition of astrocyte proliferation with cytosine arabinoside (61). We have found that most dopamine cell death occurs in the first day to the first week after transplant (62). This result indicates that short-term induction of astrocytes by IGF-I and bFGF *in vivo* may be sufficient to protect transplanted dopamine neurons from programmed cell death.

To provide time for quality control of tissue prior to transplantation, we have developed methods for maintaining human embryonic cells in culture for extended periods of one to four weeks prior to transplant (21). In a further effort to improve survival of cells after transplant, we have now tested whether long term (14 day) *in vitro* incubation of human fetal tissue with the combination of IGF-I and bFGF will promote the subsequent survival of these cells after transplantation into hemiparkinsonian rats.

Currently in our laboratory, strands of human fetal tissue placed in tissue culture are tested for dopamine production by measuring the concentration of the dopamine metabolite homovanillic acid (HVA) in tissue culture supernatant. The *in vitro* storage method is also critical for accumulating a sufficient quantity of tissue for transplantation and for demonstrating that the tissue is not infected with bacteria, viruses or fungus. The *in vitro* environment provides an opportunity to treat tissue with trophic factors in an effort to improve transplant survival of cells following transplantation.

MATERIALS AND METHODS

Preparation of Fetal Tissue

Postmitotic embryonic dopamine cells from early in development, 13 to 15 days after conception in the rat and 45 to 55 days after conception in the human (40), are able to survive and develop when implanted in the adult Parkinsonian brain (9, 10, 50). Only tissue from human embryos in this developmental range was used in this study.

Fetal tissue was obtained after elective abortion by standard clinical methods and with the use of sterile collection apparatus. Women donating tissue signed specific informed consent for experimental use of tissue. The consent and all collection methods complied with state and federal laws and were approved by the Colorado Combined Institutional Review Board. The rostral half of ventral mesencephalon containing dopamine cells was dissected as a block about 2 by 4 by 1 mm. This block was then cut in half down the midline to generate two identical pieces of mesencephalon. These pieces are referred to subsequently as a "matched pair". The tissue was washed in 3 petri dishes each containing ~20 ml of cold calcium and magnesium-free Hanks' balanced salt solution (HBSS).

Tissues strands were created by extruding one half of a mesencephalon through a glass cannula with a luer adaptor at one end and a taper to a 0.2 mm bore at the other (14, 21). These extruders were made by heating and drawing a commercially available blank (Kimble Kontes, Cat #

663500-0444, Vineland, NJ). Mesencephalic tissue was aspirated into the hub of a 1 ml tuberculin syringe in HBSS, then slowly ejected through the buffer-filled glass extruder. Care was taken to avoid excess pressure during extrusion, which could cause compression/decompression damage to the tissue. Strands were extruded into 4 ml culture medium in one well of a 6-well plastic tissue culture plate (Corning Inc, Corning, NY). Medium was F12 containing 5% dialyzed human placental serum (heat inactivated at 55°C for 30 min), heparin (1 $\mu g\ ml^{-1}$) to bind bFGF (63), 2.2 $\mu g\ ml^{-1}$ ascorbic acid, 10 $\mu g\ ml^{-1}$ vancomycin (Eli Lilly & Co., Indianapolis, IN), 2 $\mu g\ ml^{-1}$ gentamicin (Elkins-Sinn Inc., Cherry Hill, NJ) and 2 mM L-glutamine (Sigma, St. Louis, MO).

Human recombinant IGF-I (150 ng/ml; Cephalon Inc., Philadelphia, PA) and human recombinant bFGF (15 ng/ml; Scios Inc., Mountain View, CA) were added to the medium immediately after strands were placed in culture. Medium was changed at 3, 6, 9, 12 and 14 days after strands were placed in culture. This was done by removing and freezing 2 ml of medium for later HVA analysis, then adding 2 ml of fresh medium together with fresh IGF-I and bFGF.

High-Performance Liquid Chromatography (HPLC) Analysis

Testing for the content of HVA in tissue culture extracts used HPLC with electrochemical detection (Bioanalytical Systems) as previously described (3, 29). Separation was achieved on a Spherisorb ODSA microbore column (1 x 100 mm, Keystone Scientific) using a mobile phase containing per liter: 13.7 ml phosphoric acid, 4.1 g trichloroacetic acid, 0.5 g sodium EDTA, 0.4 g octyl sodium sulfate, and 8% methanol (pH 3.0). Any detectable HVA in the media blank was

subtracted from each sample.

Unilateral 6-OHDA Injections

Male Sprague Dawley rats (250-350 g) were anesthetized with equithesin (4 ml/kg) and placed in a stereotaxic frame. A 30 ga. cannula was then lowered into the medial forebrain bundle at the following coordinates: AP: -4.3 mm posterior to bregma, L: 1.5 mm from the midline, VD: -7.5 mm from the dura (42). Ten μg of 6-OHDA HBr (RBI, Natick, MA), dissolved in 5 μl sterile saline containing 0.2% ascorbate, was infused at 1 μl/min over 5 min (55). The cannula was left in place an additional 2 min with no infusion. Then the pump was started and the cannula was withdrawn while infusing saline. Lesions were tested behaviorally as noted below and confirmed histologically post-mortem by the unilateral loss of TH immunoreactive dopamine neurons in the substantia nigra.

Methamphetamine and Apomorphine-Induced Rotation

Two weeks after surgery the completeness of the lesion was assessed, by measuring turning behavior in response to methamphetamine HCl (5.0 mg/kg, i.p., Sigma, St. Louis, MO) and apomorphine (0.05 mg/kg, s.c., Sigma) in a flat-bottomed rotometer. Methamphetamine circling was selected as the primary behavioral variable. Briefly, the rotometer consisted of a plexiglass cylinder 20 cm in diameter. The rat was tethered to a counter with a harness fastened around its chest. Rats that circled ipsilateral to the lesion more than 3.0 rpm during the period of 30 to 120 minutes after

methamphetamine injection were used for transplantation and further rotational testing. Average ipsilateral rotation of animals chosen for the experiments was 8.3 rpm for controls and 7.2 rpm for IGF-I/bFGF treated group. We have previously demonstrated (45) that in our methamphetamine-induced circling test performed in flat-bottomed Plexiglas cylinders circling above two rpm correlates with >95% dopamine depletion. In contrast, Ungerstedt and Arbuthnott demonstrated that, when methamphetamine-induced circling test is performed in hemispherical bowls instead of cylinders, higher circling rates (4-6 rpm) predict >95% dopamine depletion (55).

Circling after apomorphine was also addressed. Rats that showed apomorphine-induced turning contralateral to the lesion of greater than 3.0 rpm during the period of 0 to 30 minutes after injection were considered to be positive for an apomorphine effect and had apomorphine data collected. Average apomorphine-induced rotation of animals chosen for the experiments was 8.1 rpm for controls and 6.1 rpm for IGF-I/bFGF treated group. Of the 6 pairs of rats that were positive for methamphetamine-induced rotation, only 5 pairs were positive for apomorphine-induced rotation. Methamphetamine and apomorphine-induced turning were measured 4, 8 and 10.5 weeks after transplantation to test the behavioral effect of developing neural grafts. To prevent possible confounding of drug test effects, methamphetamine-induced turning was measured 48 hr after apomorphine testing.

Transplantation of Embryonic Tissue

Recipient animals were anesthetized with equithesin (4 ml/kg). Three burr-holes were made through the skull and a 20 ga. guide cannula supported by a motorized stereotaxic arm (Narishige, Tokyo) was used for transplantation. The cannula was lowered into the brain to 3.0 or 3.5 mm below the dura. Three transplant sites were required to accommodate all of the tissue present in one-half of a human mesencephalon. Transplant coordinates were: 1) AP: 0.0 mm from bregma, L: 2.0 mm from midline, VD: -7.0 to –3.0 mm below dura; 2) AP: 0.0 mm from bregma, L: 3.5 mm from midline, VD: -7.5 to –3.5 mm below dura; 3) AP: 1.0 mm anterior to bregma, L: 3.5 mm from midline, VD: -7.0 to –3.0 mm below dura. Animals were paired based on whether they received growth factor-treated or non-treated tissue from the same human mesencephalon.

Matched pair tissue strands representing half-mesencephalons were removed from tissue culture, re-extruded as described above, and then drawn up into a 24 ga. stainless steel transplantation cannula in a volume between 4 and 8 μL. The transplantation cannula (which protruded 4 mm beyond the guide) was then inserted through the guide cannula to a final depth of 7 or 7.5 mm below the dura. The tissue was ejected with the aid of a syringe pump over 4 min. For each transplant, the pump was switched on and allowed to run for 15 seconds and then the cannula was withdrawn at a rate of 1 mm/min with the pump running. At the top of the tract (after 4 min) the pump and guide cannula were stopped for 2 min to allow the pressure to equilibrate. Afterwards, withdrawal was continued while about 4 μl of HBSS was pumped through the cannula. No sham transplants were done since in our previous work we found that shams had no improvement in

amphetamine- (44) and methamphetamine-induced rotation (15, 60). All transplanted rats were immunosuppressed 24 hrs prior to transplantation with cyclosporine A (Sandimmune; 10 mg/kg; sc; Sandoz) and daily thereafter for the duration of the experiment.

Tyrosine Hydroxylase Immunohistochemistry

At 10.5 weeks after transplant, following behavioral testing, animals were killed by chloral hydrate overdose (2 g/kg, i.p.) and intracardially perfused with heparinized saline (30 units/ml) followed by 4% phosphate-buffered paraformaldehyde. The brains were post-fixed for two days in the same fixative and cryoprotected in 30% sucrose. 40 μm sections were cut on a freezing microtome and each section was processed for TH immunohistochemistry.

The staining procedure supplied by the manufacturer was used. After blocking for one hour with 10% goat serum, 1% BSA and 0.3% Triton-X at 37°C, the slices were incubated in polyclonal, affinity-purified rabbit anti-rat TH antibody 1:200 (Pel-Freez, Rogers, AR) for 16 hours at 37°C. Sections were then incubated with a secondary biotinylated, affinity-purified, goat anti-rabbit IgG antibody and subsequently with avidin/biotinylated horseradish peroxidase complex, each for 4 hours at room temperature (Vector Lab, Burlingame, CA). The peroxidase was visualized with diaminobenzidine dissolved in PBS and 0.03% hydrogen peroxide.

Anatomical Analysis

The total number of dopamine neurons within the transplant tracts was estimated by counting all TH-positive cells in every third section of the tissue block. Abercrombie's correction (1) with an assumed cell diameter of 20 μm was used to generate the final estimate of the number of surviving dopamine neurons in each animal. Work previously done in our laboratory has shown that treatment with a combination of IGF-I and bFGF does not affect transplanted dopamine neuron size (14). Sequential section stereological counting (16) was not possible since the 40 μm sections were collected six sections per single well of a 24-well plate and were thus randomized per well. To assure that treatment with IGF-I and bFGF did not alter dopamine neuron cell size, which would render use of Abercrombie's correction inappropriate, one rat was selected from each transplant group for detailed neuron size analysis. The rat selected had closest to the median value of surviving dopamine neurons for each group. In each selected rat, images of all sections containing grafted cells were captured at x400 magnification into SlideBook digital deconvolution software (Intelligent Imaging Innovations). The size of the soma for all dopamine neurons was determined using SlideBook's analysis tools. The total number of TH^+ somas measured was 197 for the control and 408 for the animal receiving IGF-I/bFGF treatment.

Statistical Analysis

The behavioral data were analyzed via SAS Procedures GLM and Mixed (SAS Institute, Cary, NC) using a mixed effects model appropriate for repeated measures data (34). This method accounts for variability between rats as well as between multiple measurements on the same rat. The TH^+ neuron survival and TH^+ neuron soma size data were analyzed using Student's t-test and InStat statistical software (GraphPad, San Diego, CA).

RESULTS

Measurement of the stable dopamine metabolite HVA in the media of cultured fetal strands provides evidence for ongoing production of dopamine in the tissue culture (Fig. 1). Levels of HVA production per day appeared to be lower in fetal strands treated with the combination of IGF-I and bFGF, though these differences did not reach statistical significance ($n=6$, $p>0.2$). The same trend was seen in cumulative HVA levels, with IGF-I/bFGF treated strands producing a total of 320 ± 130 pmol after 14 days *in vitro* and untreated control strands producing 490 ± 130 pmol after 14 days *in vitro* (data not shown). This difference was not statistically significant.

Figure 2 shows that animals receiving growth factor-treated human fetal mesencephalon, had a significantly greater behavioral improvement than animals transplanted with human mesencephalon not treated with growth factors. Transplants of growth factor-treated strands led to a significant

reduction in methamphetamine-induced rotation at 10.5 weeks post-transplant when compared to control strands ($p<0.05$; Fig. 2A). Growth factor-treated strands appeared to cause a more rapid improvement in apomorphine circling when compared to control strands (Fig. 2B). However, these apparent differences did not reach statistical significance ($p>0.05$). By 10.5 weeks, both groups had nearly stopped circling to apomorphine, indicating that enough human dopamine cells survived to eliminate apomorphine circling.

The number of surviving dopamine neurons in grafts of animals sacrificed 10.5 weeks after transplant is shown in figure 3A. Transplants of fetal tissue strands treated with the combination of IGF-I/bFGF had better dopamine neuron survival than untreated control grafts. In animals receiving one-half a human mesencephalon treated with growth factors, a total of 2380 ± 440 dopamine neurons survived (Fig. 3A). By contrast, animals receiving the non-growth factor-treated half mesencephalon had only 1240 ± 250 surviving dopamine neurons ($p<0.05$; Fig. 3A).

To assure that growth factor treatment did not alter dopamine neuron cell size, which would render use of Abercrombie's correction inappropriate, one rat was selected from each transplant group for detailed neuron size analysis. The rat selected had closest to the median value of surviving dopamine neurons for each group. Measurement of soma size of TH^+ neurons from images captured at x400 magnification into SlideBook digital deconvolution software revealed that average area of TH^+ cell soma was not changed by the *ex vivo* growth factor treatment (Fig. 4A). Specifically, average area of TH^+ cell soma of control cells was $193 \pm 3\ \mu m^2$ and $187 \pm 2\ \mu m^2$ in tissue treated with IGF-I and bFGF.

DISCUSSION

Our study demonstrates that treating individual fragments of human fetal ventral mesencephalon with a combination of IGF-I/bFGF for two weeks in tissue culture leads to better survival of dopamine neurons after transplant into immunosuppressed hemiparkinsonian rats. Previous work in our laboratory has shown that combinations of IGF-I and bFGF reduce the rate of apoptotic death in rat dopamine neurons *in vitro* (61), and pretreatment with a combination of GDNF, IGF-I and bFGF improves cell survival after transplant (62). Co-transplantation of bFGF-expressing fibroblasts with rat mesencephalic dopamine neurons greatly enhanced survival of transplanted cells and accelerated behavioral recovery (53). We hypothesize that treatment of human fetal tissue with IGF-I/bFGF reduces the rate of apoptotic death that occurs while the strands are in culture. Because these growth factors appear to work indirectly by stimulating astrocyte proliferation and neurotrophic factor production (18, 53, 61), the beneficial effect of growth factor treatment may also carry over for a few days after transplantation.

In addition to anti-apoptotic properties of some growth factors, treatment with inhibitors of specific pro-apoptotic pathways has proven to be neuroprotective (8). Specifically, 2-hour preincubation of rat ventral mesencephalic cell suspension with a caspase inhibitor, Ac-YVAD-cmk, tripled survival of transplanted dopamine neurons (47). By contrast, transplantation of mouse ventral mesencephalon overexpressing the anti-apoptotic protein Bcl-2 did not affect dopamine neuron survival, although fiber outgrowth was improved in such grafts (48). Other neuroprotective

treatments attempt to reduce free radical damage to transplanted cells. An approach, that has shown promise in protecting transplanted dopamine neurons has treated cell suspensions with antioxidants such as lazaroids (37, 41). The lazaroid, trilazad mesylate, improves survival of cultured human embryonic dopamine neurons (41). A second effective strategy is transplantation of mesencephalic tissue overexpressing Cu/Zn superoxide dismutase (38).

Storing dopamine neurons prior to transplantation is critically important for accumulation of enough specimens for a transplant operation and to test tissue for infection. To store dopamine neurons prior to transplantation, freshly dissected ventral mesencephalon can be placed in hibernation medium at 10°C for up to several days (46, 54). In our study, human embryonic brain tissue was stored at 10°C for up to several hours prior to dissection and was then placed in tissue culture for two weeks. We have found that dopamine cells in culture medium containing 5% human placental serum and a combination of IGF-I and bFGF have nearly 100% increased survival in transplants compared to cells cultured without growth factors. Others have shown that supplementation of hibernating cells with a combination of 8% human placental cord serum, GDNF and brain-derived neurotrophic factor (BDNF) improved TH-immunoreactive cell survival by 40% (54). Rat ventral mesencephalic tissue hibernated for six days in GDNF-containing medium enhanced six-week survival of transplanted dopamine neurons by 30% (2). Cryopreservation would be desirable for long term storage of cells. Unfortunately, cryopreservation methods lead to unacceptable losses of rat and human mesencephalic cells, regardless if the cells are cryopreserved as tissue fragments or cell suspension (46). Transplantation of cryopreserved human embryonic dopamine neurons reduced survival of dopamine neurons to only 9% of fresh tissue control grafts (27).

Since bFGF can expand the progenitor population for dopamine neurons in embryonic rat cultures (6), it is possible that the IGF-I/bFGF combination may lead to more surviving dopamine neurons by promoting progenitor cell division in human fetal tissue strands. The observed increase in dopamine neuron survival in animals receiving IGF-I/bFGF treated fetal tissue correlates with the greater improvement in behavioral deficits seen in animals receiving growth factor-treated fetal tissue compared to control tissue. Although treatment with the IGF-I/bFGF combination led to faster recovery of methamphetamine-induced circling, complete behavioral recovery was not achieved due to the slow maturation of human dopamine grafts in the rat host (4, 50).

For the past ten years, we have prepared embryonic tissue as strands for transplantation into patients with Parkinson's disease (19, 20). Since we have shown that treatment of these strands with the combination of IGF-I and bFGF can nearly double the survival of dopamine neurons in transplants as well as significantly improve behavioral effects of transplants, growth factor pretreatment may prove useful for improving dopamine neuron survival after transplantation in Parkinson's disease patients.

ACKNOWLEDGEMENTS

Authors thank Dr. J.A. Abraham from Scios Inc., Mountain View, CA for providing bFGF and Dr. J. M. Farah from Cephalon Inc., West Chester, PA for providing IGF-I for these studies. This work was supported by USPHS R01 NS29982, R01 NS35348, and R01 NS18639; the General Clinical Research Centers Program National Centers for Research Resources, NIH (M01 RR00069) and from the Program to End Parkinson's Disease (C.R.F.) and R01 NS38619 (K.A.H. & W.M.Z.).

REFERENCES

1. ABERCROMBIE, M. 1946. Estimation of nuclear population from microtome sections. *The Anatomical Record* **94**, 239-247.

2. APOSTOLIDES, C., SANFORD, E., HONG, M., AND MENDEZ, I. 1998. Glial cell line-derived neurotrophic factor improves intrastriatal graft survival of stored dopaminergic cells. *Neuroscience* **83,** 363-372.

3. AMUS, P.A., AND FREED, C.R. 1979. Reversed-phase high-performance liquid chromatography of catecholamines and their congeners with simple acids as ion-pairing reagents. *J. Chromatography* **169**, 303-311.

4. BELKADI, A.M., GÉNY, C., NAIMI, S., JENY, R., PESCHANKI, M., AND RICHE, D. 1997. Maturation of fetal human neural xenografts in the adult rat brain. *Exp. Neurol.* **144,** 369-380.

5. BJÖRKLUND, A., AND STENEVI, U. 1979. Reconstruction of the nigrostriatal dopamine pathway by intracerebral nigral transplants. *Brain Res.* **177**, 555-560.

6. BOUVIER, M.M., AND MYTILINEOU, C. 1995. Basic fibroblast growth factor increases division and delays differentiation of dopamine precursors in vitro, *J. Neurosci.* **15**, 7141-7149.

7. BRUNDIN, P., ISACSON, O., AND BJÖRKLUND, A. 1985. Monitoring of cell viability in suspensions of embryonic CNS tissue and its use as a criterion for intracerebral graft survival.

Brain Res. **331**, 251-259.

8. BRUNDIN, P., KARLSSON, J., EMGRAD, M., SCHIERLE, G.S., HANSSON, O., PETERSEN, A., AND CASTILHO, R.F. 2000. Improving the survival of grafted dopaminergic neurons: a review over current approaches. *Cell Transplantation* **9,** 179-195.

9. BRUNDIN, P., NILSSON, O.G., STRECKER, R.E., LINDVALL, O., ASTED, B. AND BJÖRKLUND, A. 1986. Behavioral effects of human fetal dopamine neurons grafted in a rat model of Parkinson's disease. *Exp. Brain Res.* **65**, 235-240.

10. BRUNDIN, P., STRECKER, R.E., WIDNER, H., CLARKE, D.J., NILSSON, O.G., ASTEDT, B., LINDVALL, O., AND BJÖRKLUND, A. 1988. Human fetal dopamine neurons grafted in a rat model of Parkinson's disease: Immunological aspects, spontaneous and drug-induced behavior, and dopamine release. *Exp. Brain Res.* **70**, 192-208.

11. CLARKE, D.J., BRUNDIN, P., STRECKER, R.E., NILSSON, O.G., BJÖRKLUND, A., AND LINDVALL, O. 1998. Human fetal dopamine neurons grafted in a rat model of Parkinson's disease: ultrastructural evidence for synapse formation using tyrosine hydroxylase immunocytochemistry. *Exp. Brain Res.* **73**, 115-126.

12. CLARKSON, E.D., ZAWADA, W.M., AND FREED, C.R. 1995. GDNF reduces apoptosis in dopaminergic neurons *in vitro. NeuroReport* **7,** 145-149.

13. CLARKSON, E.D., ZAWADA, W.M., AND FREED, C.R. 1997. GDNF improves survival and reduces apoptotic cell death in human embryonic dopaminergic neurons *in vitro. Cell & Tissue Res.* **289**, 207-210.

14. CLARKSON, E.D., ZAWADA, W.M., ADAMS, F.S., BELL, P.K. AND FREED, C.R.

1998. Embryonic mesencephalic tissue strands show greater dopamine neuron survival and better behavioral outcome than cell suspensions after transplantation in parkinsonian rats. *Brain Res.* **806**, 60-68.

15. CLARKSON, E.D., LA ROSA, F.G., EDWARDS-PRASAD, J., WEILAND, D.A., WITTA, S.E., FREED, C.R. AND PRASAD, K.N. 1998. Improvement of neurological deficits in 6-hydroxydopamine-lesioned rats after transplantation with allogeneic simian virus 40 large tumor antigen gene-induced immortalized dopamine cells. *Proc. Natl. Acad. Sci. USA* **95,** 1265-1270.

16. COGGESHALL, R.E., AND LEKAN, H.A. 1996. Methods for determining numbers of cells and synapses: A case for more uniform standards of review. *J. Comp. Neurol.* **364,** 6-15.

17. EHRINGER, H., AND HORNYKIEWICZ, O. 1960. Verteilung von noradrenalin and dopamin (3-hydroxytyramin) im gehirn des menschen und ihr verhalten bei erkrankungen des extrapyramidalen systems. *Klin. Wochenschr.* **38**, 1236-1239.

18. ENGELE, J., AND BOHN, M.C. 1991. The neurotrophic effects of fibroblast growth factors on dopaminergic neurons *in vitro* are mediated by mesencephalic glia. *J. Neurosci.* **11,** 3070-3078.

19. FREED, C.R., BREEZE, R.E., ROSENBERG, N.L., SCHNECK, S.A., WELLS, T.H., BARRETT, J.N., GRAFTON, S.T., HUANG, S.C., EIDELBERG, D. AND ROTENBERG, D.A. 1990. Transplantation of human fetal dopamine cells for Parkinson's disease. Results at 1 year. *Arch. Neurol.* **47**, 505-512.

20. FREED, C.R., BREEZE, R.E., ROSENBERG, N.L., SCHNECK, S.A., *et al.* 1991. Fetal

neural implants for Parkinson's disease: results at 15 months. In: *Restorative Neurology, Intracerebral Transplantation in Movement Disorders,* Elsevier Publishers, Amsterdam, Netherlands, vol. 4, pp. 69-77.

21. FREED, C.R., BREEZE, R.E., ROSENBERG, N.L., SCHNECK, S.A., KRIEK, E., QI, J.X., LONE, T., ZHANG, Y.B., SNYDER, J.A., WELLS, T.H, RAMIG, L.O., THOMPSON, L., MAZZIOTTA, J.C., HUANG, S.C., GRAFTON, S.T., BROOKS, D., SAWLE, G., SCHROTER, G., AND ANSARI, A.A. 1992. Survival of implanted fetal dopamine cells and neurologic improvement 12 to 46 months after transplant for Parkinson's disease. *N. Engl. J. Med.* **327,** 1549-1555.

22. FREED, C.R., BREEZE, R.E., ROSENBERG, N.L., AND SCHNECK, S.A. 1992. Embryonic dopamine cell implants as a treatment for the second phase of Parkinson's disease: Replacing failed nerve terminals. In: *Advances in Neurology*, H. Narabayashi, T. Nagatsu, N. Yanagisawa, and Y. Mizuno, eds., Raven Press, New York, vol 60, pp. 721-728.

23. FREED, C.R., BREEZE, R.E., SCHNECK, S.A., BAKAY, R.A.E., AND ANSARI, A.A. 1995. Fetal neural transplantation for Parkinson disease. In: *Clinical Immunology: Principles and Practice,* Rich, R.R., eds., Mosby-Year Book, Inc. St. Louis, MO, pp. 1677-1687.

24. FREEMAN, T.B., SPENCE, M.S., BOSS, B.D., SPECTOR, D.H., STRECKER, R.E., OLANOW, C.W., AND KORDOWER, J.H. 1991. Development of dopaminergic neurons in the human substantia nigra. *Exp. Neurol.* **113,** 344-353.

25. FREEMAN, T.B., OLANOW, C.W., HAUSER, R.A., NAUERT, G.M., SMITH, D.A., BORLONGAN, C.V., SANBERG, P.R., HOLT, D.A., KORDOWER, J.H.,

VINGERHOETS, F.J.G., SNOW, B.J., CALNE, D., AND GAUGER, L. 1995. Bilateral fetal nigral transplantation into the postcommissural putamen in Parkinson's disease. *Ann. Neurol.* **38,** 379-388.

26. FREEMAN, T.B., SANBERG, P.R., NAUERT, G.M., BORLONGAN, C.V., LIU, E.-Z., BOSS, B.D., SPECTOR D., OLANOW, C.W., AND KORDOWER, J.H. 1995. The influence of donor age on the survival of solid and suspension intraparenchymal human embryonic nigral grafts. *Cell Transplantation* **4**, 141-154.

27. FRODL, E.M., DUAN, W.M., SAUER, H., KUPSCH, A., AND BRUNDIN, P. 1994. Human embryonic neurons xenografted to the rat: effects of cryopreservation and varying regional source of donor cells on transplant survival, morphology and function. *Brain Res.* **647,** 286-298.

28. HEFTI, F. 1997. Neurotrophic factor therapy- Keeping score. *Nature Med.* **3**, 497-498.

29. HERREGODTS, P., AND MICHOTTE, Y. 1987. Combined ion-pair extraction and high-performance liquid chromatography for the determination of the biogenic amines and their major metabolites in single brain tissue samples. *J. Chromatography* **421**, 51-60.

30. KNUSEL, B., MICHEL, P.P., SCHWABER, J.S., AND HEFTI, F. 1990. Selective and nonselective stimulation of central cholinergic and dopaminergic development *in vitro* by nerve growth factor, basic fibroblast growth factor, epidermal growth factor, insulin and insulin-like growth factors I and II. *J. Neurosci.* **10**, 558-570.

31. KONDOH, T., PUNDT, L.L., AND LOW, W.C. 1995. Development of human fetal ventral mesencephalic grafts in rats with 6-OHDA lesions of the nigrostriatal pathway. *Neurosci.*

Res. **21**, 223-233.

32. KOPYOV, O.V., JACQUES, D., LIEBERMAN, A., DUMA, C.M., AND ROGERS, R.L. 1996. Clinical study of fetal mesencephalic intracerebral transplants for the treatment of Parkinson's disease. *Cell Transplantation* **5**, 327-337.

33. KORDOWER, J.H., FREEMAN, T.B., SNOW, B.J., VINGERHOETS, F.J.G., MUFSON, E.J., SANBERG, P.R., HAUSER, R.A., SMITH, D.A., NAUERT, M., PERL, D.P., AND OLANOW, C.W. 1995. Neuropathological evidence of graft survival and striatal reinnervation after the transplantation of fetal mesencephalic tissue in a patient with Parkinson's disease. *N. Eng. J. Med.* **322**, 1118-1124.

34. LAIRD, N.M., AND WARE, J.H. 1982. Random effects for longitudinal data. *Biometrics* **38**, 963-974.

35. LINDVALL, O., BRUNDIN, P., WIDNER, H., REHNCRONA, S., GUSTAVII, B., FRACKOWIAK, R., LEENDERS, K.L., SAWLE, G., ROTHWELL, J.C., MARSDEN, C.D., AND BJÖRKLUND, A. 1990. Grafts of fetal dopamine neurons survive and improve motor function in Parkinson's disease. *Science* **247**, 574-577.

36. MAHALIK, T.J., HAHN, W.E., CLAYTON, G.H., AND OWENS, G.P. 1994. Programmed cell death in developing grafts of fetal substantia nigra. *Exp. Neurol.* **129**, 27-36.

37. NAKAO, N., FRODL, E.M, DUAN, W.-M., WIDNER, H., AND BRUNDIN, P. 1994. Lazaroids improve the survival of grafted rat embryonic dopamine neurons. *Proc. Natl. Acad. Sci. USA* **91,** 12408-12412.

38. NAKAO, N., FRODL, E.M., WIDNER, H., CARLSON, E., EGGERDING, F.A.,

EPSTEIN, C.J., AND BRUNDIN, P. 1995. Overexpressing Cu/Zu superoxide dismutase enhances survival of transplanted neurons in a rat model of Parkinson's disease. *Nature Med.* **1,** 226-231.

39. OLANOW, C.W., KORDOWER, J.H., AND FREEMAN, T.B. 1996. Fetal nigral transplantation as a therapy for Parkinson's disease. *Trends Neurosci.* **19**, 102-109.

40. O'RAHILLY, R., AND MULLER, F. 1987. Developmental stages in human embryos. Carnegie Institution of Washington publication 637. Meriden, Conn.: Meriden-Stinehour Press.

41. OTHBERG, A., KEEP, M., BRUNDIN, P., AND LINDVALL, O. 1997. Trilazad mesylate improves survival of rat and human embryonic mesencephalic neurons *in vitro*. *Exp. Neurol.* **147,** 498-502.

42. PAXINOS, G., AND WATSON, C. 1986. The Rat Brain in Stereotaxic Coordinates. Academic Press, New York.

43. PERLOW, M.J., FREED, W.J., HOFFER, B.J., SEIGER, A., OLSON, L., AND WYATT, R.J. 1979. Brain grafts reduce motor abnormalities produced by destruction of nigrostriatal dopamine system. *Science* **204**, 643-647.

44. RICHARDS, J.B., SABOL, K.E., AND FREED, C.R. 1990 Unilateral dopamine depletion causes bilateral deficits in conditioned rotation in rats. *Pharmacol. Biochem. Behav.* **36**, 217-223.

45. RICHARDS, J.B., SABOL, K.E., KRIEK, E.H., AND FREED, C.R. 1993. Trained and amphetamine-induced circling behavior in lesioned, transplanted rats. *J. Neural Trans. &*

Plasticity, **4**, 157-166.

46. SAUER, H. 2000. Pregraft tissue storage methods for intracerebral transplantation. In: *Neuromethods: Neural transplantation methods,* Dunnet, S.B., Boulton, A.A., and Baker, G.B. eds. Humana Press Inc., Totowa, NJ, vol. 36, pp. 27-40.

47. SCHIERLE, G.S., HANSSON, O., LEIST, M., NICOTERA, P., WIDNER, H., AND BRUNDIN, P. 1999. Caspase inhibition reduces apoptosis and increases survival of nigral transplants. *Nature Med.* **5,** 97-100.

48. SCHIERLE, G.S., LEIST, M., MARTINOU, J.C., WIDNER, H., NICOTERA, P., AND BRUNDIN, P. 1999. Differential effects of Bcl-2 overexpression on fibre outgrowth and survival of embryonic dopaminergic neurons in intracerebral transplants. *Eur. J. Neurosci.* **11,** 3073-3081.

49. SPENGER, C., HAQUE, N.S., STUDER, L., EVTOUCHENKO, L., WAGNER, B., BUHLER, B., LENDAHL, U., AND SEILER, R.W. 1996. Fetal ventral mesencephalon of human and rat origin maintained in vitro and transplanted to 6-hydroxydopamine-lesioned rats gives raise to grafts rich in dopaminergic neurons. *Exp. Brain Res.* **112**, 47-57.

50. STRÖMBERG, I., BYGDEMAN, M., GOLDSTEIN, M., SEIGER, A., AND OLSON, L. 1986. Human fetal substantia nigra grafted to the dopamine-denervated striatum of immunosuppressed rats: evidence for functional reinnervation. *Neurosci. Lett.* **71**, 271-276.

51. STRÖMBERG, I., ALMQVIST, P., BYGDEMAN, M., FINGER, T.E., GERHARDT, G., GRANHOLM, A.C., MAHALIK, T.J., SEIGER, A., HOFFER, B., AND OLSON, L. 1988. Intracerebral xenografts of human mesencephalic tissue into athymic rats: Immunochemical

and *in vivo* electrochemical studies. *Proc. Natl. Acad. Sci. USA* **85**, 8331-8334.

52. STRÖMBERG, I., BYGDEMAN, M., GOLDSTEIN, M., SEIGER, A., AND OLSON, L. 1988. Human fetal substantia nigra grafted to the dopamine-denervated striatum of immunosuppressed rats: evidence for functional reinnervation. *Neurosci. Lett.* **71**, 271-276.

53. TAKAYAMA, H., RAY, J., RAYMON, H.K., BAIRD, A., FISHER, L.J., AND GAGE, F.H. 1995. Basic fibroblast growth factor increases dopaminergic graft survival and function in a rat model of Parkinson's disease. *Nature Med.* **1**, 53-58.

54. THAJEB, P., LING, Z.D., POTTER, E.D., AND CARVEY, P.M. 1997. The effects of storage conditions and trophic supplementation on the survival of fetal mesencephalic cells. *Cell Transplantation* **6**, 297-307.

55. UNGERSTEDT, U. AND ARBUTHNOTT, G.W. 1970 Quantitative recording of rotational behavior in rats after 6-hydroxydopamine lesions of the nigrostriatal dopamine system. *Brain Res.* **24**, 485-490.

56. VAN HORNE, C.G., MAHALIK, T., HOFFER, B., BYGDEMAN, M., ALMQVIST, P., STIEG, P., SEIGER, A., OLSON, L., AND STRÖMBERG, I. 1990 Behavioral and electrophysiological correlates of human mesencephalic dopaminergic xenograft function in the rat striatum. *Brain Res. Bull.* **25**, 325-334.

57. WALTERS, A.M., CLARKE, D.J., BRADFORD, H.F. AND STERN, G.H. 1992. The properties of cultured fetal human and rat brain tissue and its use as grafts for the relief of the parkinsonian syndrome. *Neurochem. Res.* **17**, 893-900.

58. WANG, Y., LIN, J.C., CHIOU, A.L., LIU, J.Y. AND ZHOU, F.C. 1995. Human ventromesencephalic grafts restore dopamine release and clearance in hemiparkinsonian rats. *Exp. Neurol.* **136**, 98-106.

59. WIDNER, H., TETRUD, J., REHNCRONA, S., SNOW, B., BRUNDIN, P., GUSTAVII, B., AND LANGSTON, J.W. 1992. Bilateral fetal mesencephalic grafting in two patients with Parkinsonism induced by 1-methyl-4-phenyl-1,2,3,6-tetrahydropyridine (MPTP). *N. Eng. J. Med.* **327**, 1556-1563.

60. ZAWADA, W.M., CIBELLI, J.B., CHOI, P.K., CLARKSON, E.D., GOLUEKE, P.J., WITTA, S.E., BELL, K.P., KANE, J., PONCE DE LEON, A.P., JERRY, D.J., ROBL, J.M., FREED, C.R., AND STICE, S.L. 1998. Somatic cell cloned transgenic bovine neurons for transplantation in parkinsonian rats, *Nature Med.* **4**, 569-574.

61. ZAWADA, W.M., KIRSCHMAN, D.L., COHEN, J.J., HEIDENREICH, K.A. AND FREED, C.R. 1996. Growth factors rescue embryonic dopamine neurons from programmed cell death. *Exp. Neurol.* **140**, 60-67.

62. ZAWADA, W.M., ZASTROW, D.J., CLARKSON, E.D., ADAMS, F.S., BELL, K.P., AND FREED, C.R. 1998. Growth factors improve immediate survival of embryonic dopamine neurons after transplantation into rats. *Brain Res.* **786**, 96-103.

63. YAYON, A., KLAGSBRUN, M., ESKO, J.D., LEDER, P., AND ORNITZ, D.M. 1991. Cell surface, heparin-like molecules are required for binding of basic fibroblast growth factor to its affinity receptor. *Cell* **64,** 841-848.

FIGURE LEGENDS

Fig. 1. Effects of growth factor treatment on HVA production in human fetal tissue. Matched pairs of mesencephalon strands were made by bisecting fragments of human fetal ventral mesencephalon, extruding through a 0.2 mm diameter cannula and treating for two weeks either with IGF-I (150 ng/ml) + bFGF (15 ng/ml) in F12 media supplemented with 5% human placental serum (*open triangles*) or with F12 supplemented with serum alone (*solid squares*). Testing for the content of HVA in tissue culture extracts was done by HPLC with electrochemical detection (2, 32). All data represent the mean ± SEM (n=6 pairs).

Fig. 2. Effects of transplanted human fetal tissue on behavioral deficits in 6-OHDA-lesioned rats. Matched pairs of mesencephalon strands were treated either with IGF-I + bFGF (*open triangles*), or with no growth factors (control, *solid squares*). Tissue was transplanted into striatum of 6-OHDA-lesioned rats. A) rotational rate induced by methamphetamine (5 mg/kg, i.p.). Animals receiving growth factor-treated strands had an improvement at 10.5 weeks post-transplant compared to controls. Asterisk represents statistical significance at $p<0.05$ compared to controls using a mixed effects analyses of variance (29) (n=6 pairs) and B) rotational rate induced by apomorphine (0.05 mg/kg, s.c.). Animals receiving growth factor treated strands had their rotational rate induced by apomorphine measured at 4, 8 and 10.5 weeks after transplantation. Although the growth factor treated animals had a greater reduction in apomorphine-induced circling, this rate of reduction was not significantly greater when compared to controls.

Fig. 3. Effects of treatment with IGF-I + bFGF on human dopamine neurons transplanted into 6-OHDA-lesioned rats. A) Matched pairs of mesencephalon strands treated with IGF-I + bFGF (*solid bar*) and control tissue (*open bar*) were transplanted into 6-OHDA-lesioned rats. At 10.5 weeks post-transplant the rats were sacrificed, brain sections made at 40 μm, sections were stained for TH immunoreactivity and all TH^+ neurons counted. Estimates are for the whole brain using Abercrombie's correction (1). Data are presented as the means ± SEM. Significance was shown by the Student's t-test. Dopamine neuron survival was significantly enhanced by IGF-I and bFGF (* = $p<0.05$, n=6). B) Micrograph showing TH^+ neurons in a representative control graft. C) Micrograph showing TH^+ neurons in a representative graft treated with a combination of IGF-I and bFGF. Scale bar in B and C = 500 μm..

Fig. 4. Dopamine neuron cell size analysis. A) Mean soma area of TH^+ neurons found in two different experimental groups 10.5 weeks after grafting. Student's t-test confirmed that the IGF-I and bFGF treatment had no significant effect on the mean soma area of transplanted dopamine neurons. B) Transplant of control ventral mesencephalic tissue showing TH^+ neurons. C) Transplant of growth factor combination-treated tissue. Scale bar in B and C = 20 μm..

FIGURE 1

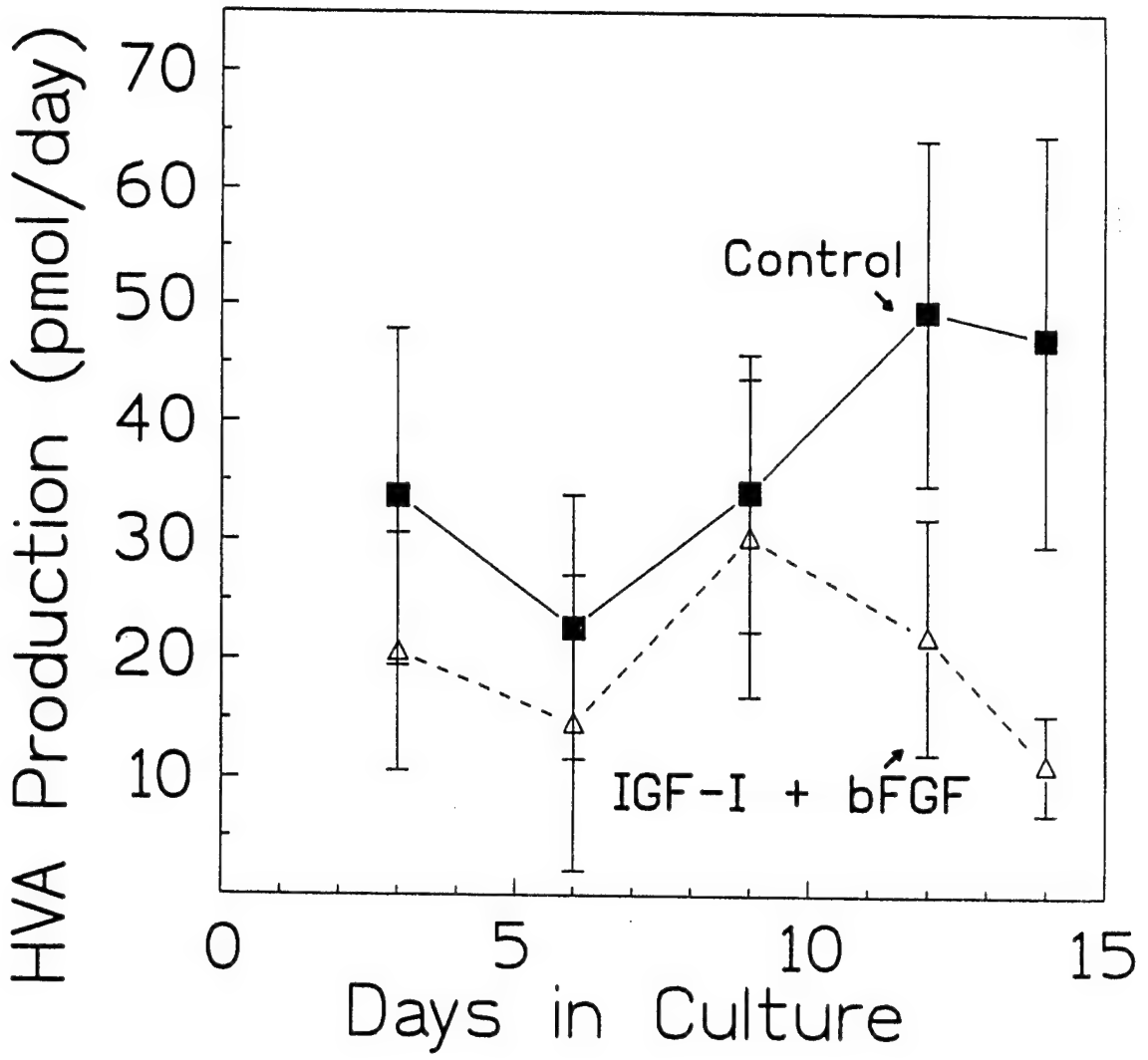
HVA Production (pmol/day)
70
60
50
40
30
20
10
0
5
10
15
Days in Culture
Control
IGF-I + bFGF

FIGURE 2A

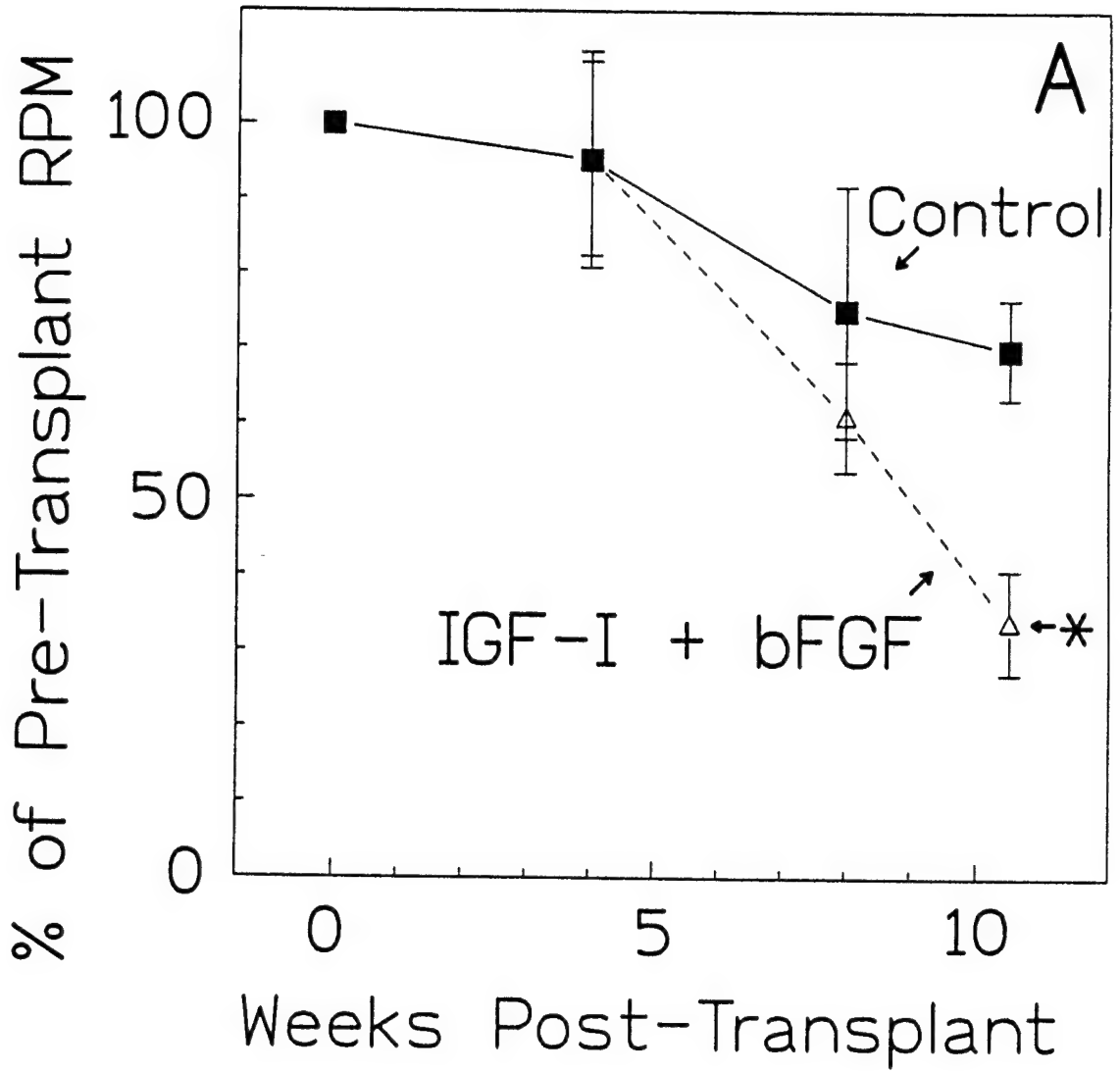
A
100
50
0
% of Pre-Transplant RPM
Control
IGF-I + bFGF
*
0
5
10
Weeks Post-Transplant

FIGURE 2B

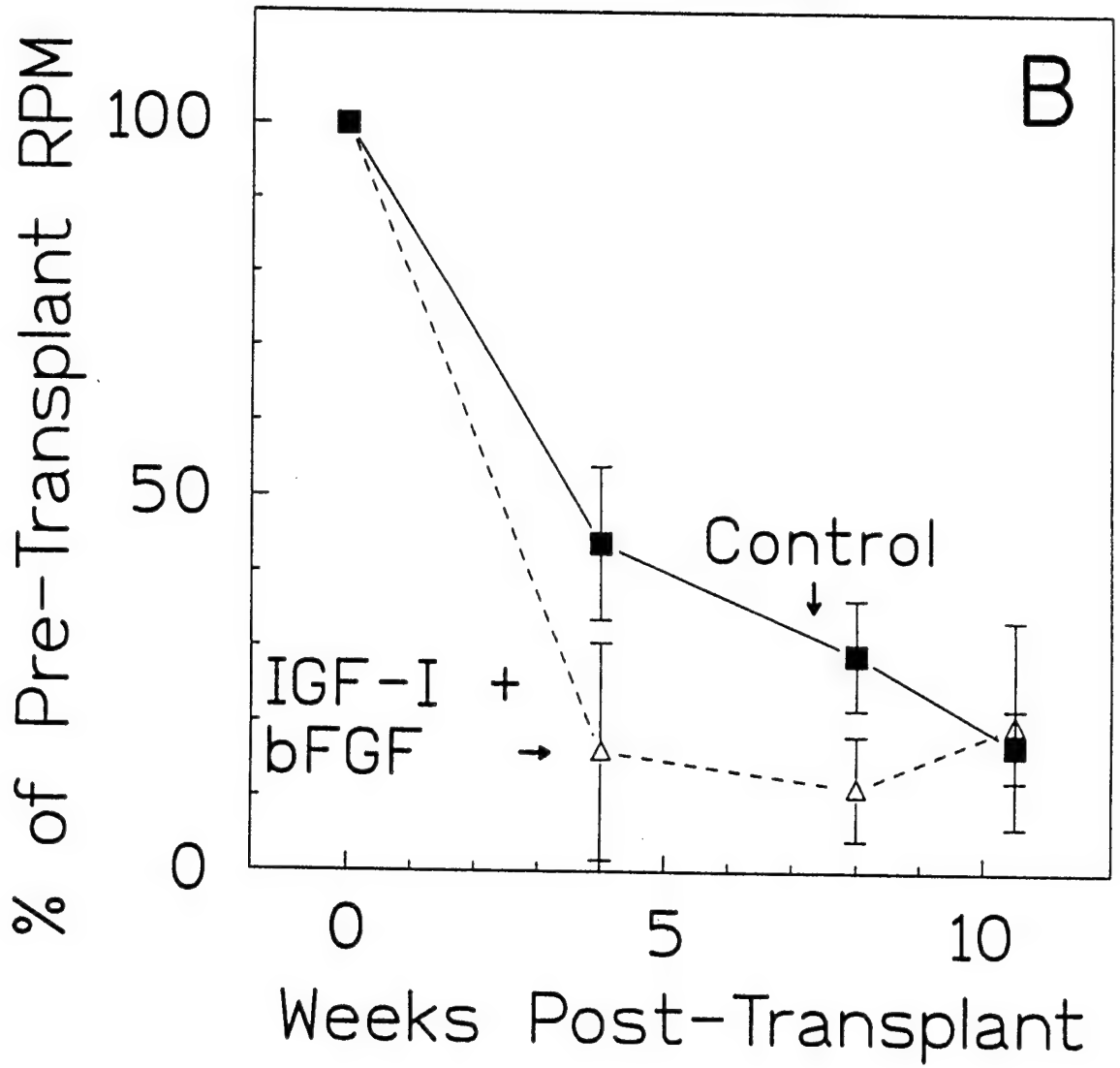
B
100
50
0
% of Pre-Transplant RPM
Control
IGF-I +
bFGF
0
5
10
Weeks Post-Transplant

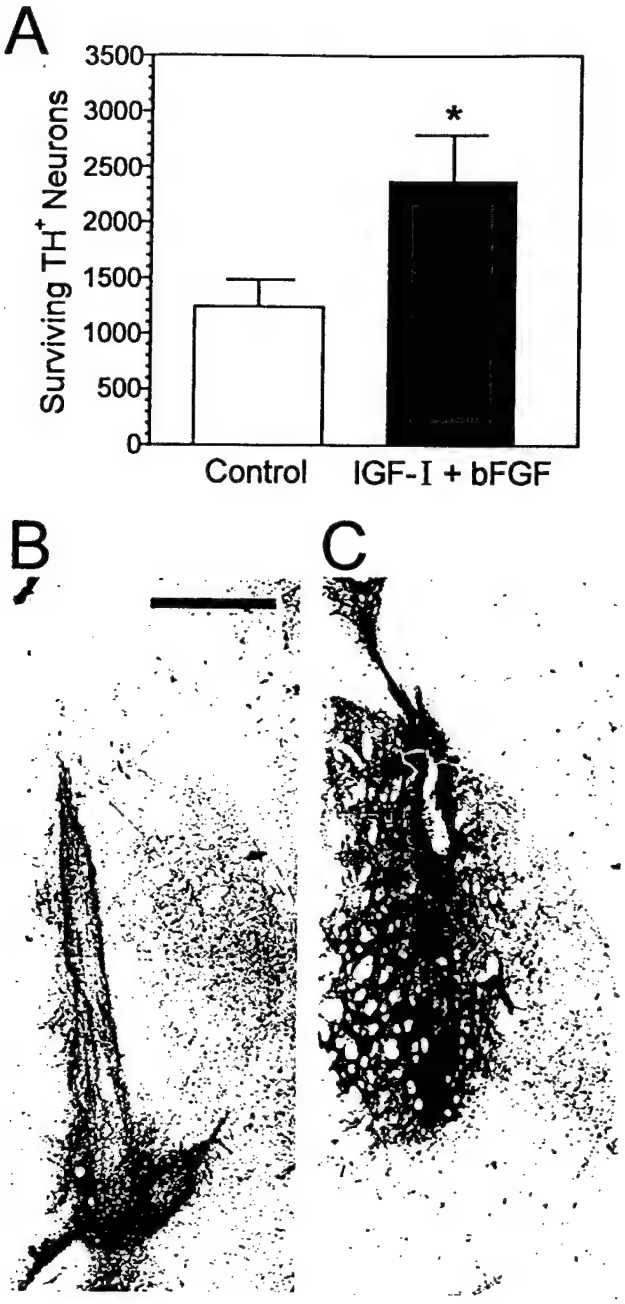
A
3500
3000
2500
2000
1500
1000
500
0
Surviving TH+ Neurons
*
Control
IGF-I + bFGF
B
C

FIGURE 3

FIGURE 4

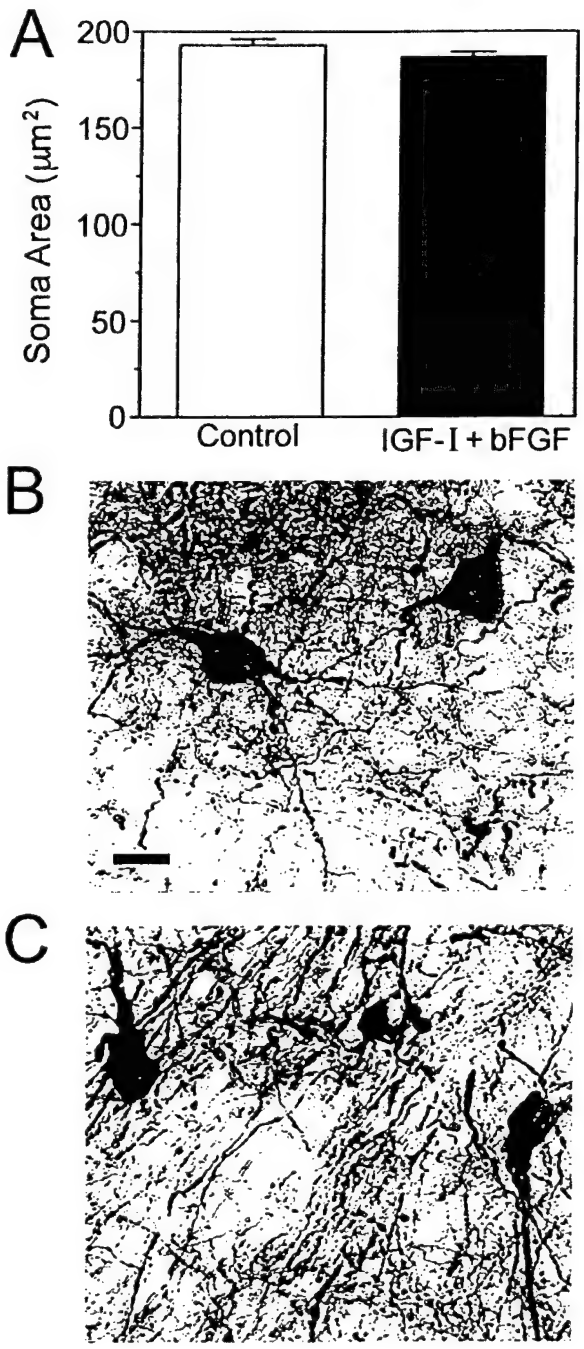

Neuroscience Abstract 1999

PYRIDINYL IMIDAZOLE COMPOUNDS RESCUE DOPAMINERGIC NEURONS FROM APOPTOTIC CELL DEATH. W.M. Zawada,[1]* M.K. Meintzer,[3] C. Sable,[2] C.R. Freed,[1] and K.A. Heidenreich[2,3]. [1]Div. Clin. Pharmacol., Depts. Med. & [2]Pharmacol., Univ. Colorado School of Medicine, [3]Denver Veterans Administration Medical Center, Denver, CO 80262.

Parkinson's disease is marked by a progressive loss of dopamine neurons occurring, in part, by an apoptotic mechanism. To examine the role of p38 MAP kinase in apoptosis of dopamine neurons we studied the effects of pyridinyl imidazole compounds (PD169316, SB203580, and SB202190), putative p38 MAP kinase inhibitors, on apoptosis induced by serum withdrawal in E15 rat ventral mesencephalic cultures. Serum withdrawal reduced the number of surviving dopamine neurons to 10% of serum controls and PD169316 (10 μM) completely prevented dopaminergic cell death. The number of attached apoptotic cells increased from 1.4% to 14% following serum withdrawal. PD169316 blocked the increment in apoptosis by ~90%. Protective effects of the SB compounds were less than than those of PD169316. Under basal conditions in the presence of serum, p38 MAP kinase activity was very low although kinase levels were present as detected by Western blotting. Serum withdrawal had no detectable acute effect on p38 activity but lead to upregulation of the enzyme after 16-20 hrs. Upregulation of p38α was completely blocked by PD169316. In contrast, JNK activity was high under basal conditions and serum withdrawal had no effect on the activity or levels of this enzyme. PD169316, and to as lesser extent SB203580, markedly blocked endogenous JNK activity. These data suggest that the pyridinyl imidazole compounds block apoptosis in dopamine neurons by inhibiting endogenous JNK activity and preventing p38 upregulation. We conclude that simultaneous inhibition of p38 MAP kinase and JNK signaling is highly effective in protecting dopamine neurons from apoptosis. Inhibitors of stress-activated protein kinases may be beneficial in preventing apoptosis during brain transplantation and in the treatment of neurodegenerative diseases involving enhanced apoptosis. Supported by NS18639, NIGMS GM07063, the NPF and VA Merit.

Appendix 8

Sable 851081

Category: Basic Science: 14. Intracellular Signaling

81st Annual Meeting of The Endocrine Society 1999 Abstract Form

Corresponding Author: Carol L Sable
Address: 1055 Clermont St. 111H , Denver, CO, 80220
Phone: (303) 399-8020 ext 5264 **Fax:** (303) 393-5271 **E-Mail:** sablec@den-res.org
Format Preference: Poster presentation only
Award: Travel Grant Award
Keywords: apoptosis, Akt, p38 MAPK,
Disclosure: I have nothing to disclose.

REGULATION OF APOPTOSIS IN RAT CEREBELLAR GRANULE NEURONS C L Sable[1, 2]*, M K Meintzer[1, 2], and K A Heidenreich[1, 2]. [1]Pharmacology, University of Colorado Health Sciences Center, Denver, CO, and [2]Endocrinology, Veterans Administration Medical Center, Denver, CO.

Apoptosis of neuronal cells contributes to neurodegenerative diseases, therefore elucidating mechanisms which regulate neuronal apoptosis is important for preventing or slowing progression of these diseases. We have been studying the role of various protein kinase pathways in regulating apoptosis of rat cerebellar granule neurons (RCG neurons). RCG neurons require depolarizing concentrations of potassium (25 mM), in addition to serum, to maintain them in culture. Removal of serum and lowering potassium concentrations to 5 mM increased the extent of apoptosis 4-5 fold. This increase in apoptosis was accompanied by a decrease in activity of the antiapoptotic kinase Akt with no changes in the level of Akt.protein. The downregulation of Akt required at least one hour in deprivation media and continued over 8 hours. Akt downregulation, like apoptosis, required both the removal of serum and reduction of potassium. To further determine whether Akt protects RCG neurons from apoptosis in the presence of high potassium and serum, we examined the effect of wortmannin (an inhibitor of phosphatidyl inositol-3 kinase which is an upstream activator of Akt) on apoptosis in complete media. Although wortmannin (100 nM) was able to induce apoptosis under these conditions, the extent of apoptosis was much lower than that induced by serum withdrawal in low potassium. This implies that the protective effects of serum and high potassium are mediated through additional signaling pathways. Therefore, we examined the involvement of the stress-activated protein kinases, p38 MAP kinase and c-Jun N-terminal protein kinase (JNK), in mediating apoptosis in RCG neurons. The pyridinyl imidazole inhibitors of p38 MAP kinase (PD169316 and SB203580) blocked the apoptotic response to serum withdrawal in low potassium by 83% and 64% respectively. These compounds (10 μM), in addition to their known inhibitory actions on p38 MAP kinase, decreased endogenous JNK activity in RCG neurons. PD169316 and SB203580 had no effect on either the activation of Akt by growth factors or on the downregulation of Akt indicating the target of the pyridinyl imidazole compounds it either downstream or independent of Akt. In conclusion, apoptosis of RCG neurons is controlled by multiple signaling pathways, including Akt and the stress-activated protein kinases. The balance of activity between these protein kinase pathways determines neuronal cell fate.

Kris A. Heidenreich

Sponsoring Member Signature (K A Heidenreich)

If you are paying by check or money order don't forget to print a payment form.

Please have your browser font settings set to the smallest font to avoid multiple pages when printing.

Appendix 9

Please select Print from the file menu to print your Abstract.

ENDO 2000 The Endocrine Society 82nd Annual Meeting

Invited Speaker Submission

Filename: 9844
Corresponding Author: Margaret E. Wierman
Department/Institution: 111 H Endocrinology,VA Med Ctr, University of Colorado School of Med.
Address: 1055 Clermont St., Denver, CO, 80220-3808
Phone: 303-399-8020 ext 3150 **Fax:** 303-393-5271 **E-Mail:** margaret.wierman@uchsc.edu
Keywords: neuronal migration, GnRH, adhesion related kinase

Factors Regulating GnRH Neurons.

Margaret E Wierman [1], Melissa P Allen [1], Zhaoqin Fang [1], Mei Xu [1], Chan Zeng [1], Kim Heidenreich [2] and Stuart Tobet [3]. [1]Dept Med and Res Service, VA Med Ctr and UCHSC, Denver, CO, 80220; [2]Res Service and Dept Pharmacology, VA Med Ctr and UCHSC, Denver, CO, 80220; and [3]Biomedical Sciences, Shriver Center, Waltham, MA.

Gonadotropin releasing hormone (GnRH) is the hypothalamic releasing hormone that controls gonadotropin gene expression and reproductive competence. The GnRH neuronal population is small,consisting of only 800-1000 neurons in the rodent. The neurons are born in the olfactory placode and migrate across the cribiform plate into the forebrain to form a complex neuronal network in the hypothalamus. The signals required for this precisely-timed neuronal migration are poorly understood, but defects in GnRH neuronal migration in the human may result in hypogonadotropic hypogonadism. We recently used differential display on two GnRH producing cell lines derived during specific windows of GnRH neuronal migration to identify novel factors involved in the process. Gn10 cells, created by Radovick and coworkers, were isolated from an olfactory tumor during GnRH neuronal migration and make little GnRH. GT1-7 cells, cloned by Mellon and colleagues are from a forebrain tumor of postmigratory cells and make abundant GnRH. Our screen identified Adhesion related kinase (Ark) in Gn10 but not GT1-7 cells. Ark is a member of a new family of growth factor receptors, unique in that their amino termini have fibronectin and immunoglobulin repeats characteristic of cell adhesion molecules, and an intracellular domain that encodes a tyrosine kinase. In vivo, Ark and GnRH mRNA were detected by Northern analysis in total RNA isolated from the cribiform plate region at day 13 (the time when the GnRH population is concentrated in this location). These data strongly suggest that Ark is expressed in GnRH neurons during migration. We have studied three potential physiologic functions of Ark in GnRH neuronal cells. First, Ark signaling via its ligand, growth arrest specific gene 6 (Gas-6), rescues neurons from growth factor withdrawal-induced apoptosis. We showed that the ERK1,2 MAP kinase and the PI3-kinase/Akt pathways are critical for this inhibition of programed cell death. We postulate this protective function is used during GnRH neuronal migration to ensure an adequate number of neurons reach their ultimate destination in the hypothalamus. Secondly, Ark may be one of the factors regulating GnRH neuronal migration. In vitro migration studies using a Boyden chamber assay demonstrated that Gn10 (Ark+)neurons migrate at a higher basal

rate than GT1-7(Ark-)neurons. In addition, Gas-6 augments migration only in Gn10 cells. The signaling pathways involved in this process are under study. This function may be critical in targeting GnRH neurons to the forebrain. Thirdly, the GnRH promoter is the first identified downstream nuclear target of Ark signaling. Ark repression of neuronal GnRH expression requires activation of the ERK1,2 pathway. Inhibition is mediated by proximal GnRH promoter elements that bind myocyte enhancer factor 2-B and 2-C proteins, and a homeodomain protein. Ark control of GnRH expression may play a role in limiting GnRH transcription until the GnRH neuronal population has reached its final destination in the forebrain. Together these studies show the relevance of using novel strategies to identify factors important in GnRH neuronal migration. Newly discovered molecules may serve as candidates for defects resulting in hypogonadism and new targets for pro or antifertility agents. (Supported by Lalor Fellowship to MPA, VA Merit Review and NIH HD32017 to MEW)

Disclosure: There is no disclosure information to present

Presenting Author Signature: (Margaret E Wierman) **Date:**

Return To Thank You

Note: Use the buttons on the left to move between screens or the "Reload" button if you encounter an error message.

Appendix 10

SFN Support Team
sfn-support@cjp.com
1.888.348.2065 (24 hr
Click here for support
Forgot your ID numbe

2000

Abstract Proof

Edit Menu (Click on these to edit the data in your abstract.)

Contact Info
Details
Themes and Topics
Institutions
Authors
Title
Key Words
Body
Disclaimers
Back to Menu

To see a sample of what an abstract will look like in the abstract book, click here.

(Note: You need Adobe Acrobat Reader to see it.)

- Total characters left: **180**
- When you are satisfied that all the information below is complete and accurate, press the *Finished Revising/Submit* button and enter your credit card information. You must pay the submission fee for your abstract to be considered.
- Submission of this abstract is final, like putting a paper abstract into the mailbox. Once you have submitted and paid for your abstract, you will not be able to revise it without submitting a replacement abstract and paying the replacement abstract fee of $50.00 USD.
- If you want to continue revising your abstract, you may do so by pressing the *Save Abstract* button below. Remember that you must submit by the deadline for your abstract to be considered.
- If you are going to submit this abstract, be sure to print this page for your records.
- After you have submitted your abstract, and received your control number, you must contact the SFN Program Department if you wish to have your abstract withdrawn.

Contact Info	W Michael Zawada Univ Colorado HSC Denver CO USA 303-315-8455 303-315-3272 mike.zawada@uchsc.edu
Presentation Type:	Slide/Poster
Theme 1:	A. Development and Regeneration
Topic 1:	23. Transplantation
Theme 2:	J. Disorders of the Nervous System and Aging
Topic 2:	131. Degenerative disease: Parkinson's
Abstract Title:	INHIBITORS OF p38 MAP KINASE INCREASE THE SURVIVAL OF TRANSPLANTED DOPAMINE NEURONS
Contributing Authors:	1. W.M. Zawada[1,3*] 2. M.K. Meintzer[2,4]

3. P. Rao[2,4]
4. J. Marotti[1]
5. X. Wang[2,4]
6. J.E. Esplen[1,2]
7. E.D. Clarkson[1]
8. C.R. Freed[1,3]
9. K.A. Heidenreich[2,4]

Institutions:

1. Clinical Pharmacology, 2. Pharmacology, 3. Neuroscience Program, University of Colorado Health Sciences Center, Denver, CO, USA

4. Denver Veterans Administration Medical Center, Denver, CO, USA

Key words: PARKINSON, MIDBRAIN, PROTEIN KINASE, TRANSPLANT*

Abstract:

Fetal cell transplantation therapies are being developed for the treatment of a number of neurodegenerative disorders including Parkinson's disease. Massive apoptotic cell death is a major limiting factor for the success of neurotransplantation. We have explored a novel protein kinase pathway for its role in apoptosis of dopamine neurons. We have discovered that inhibitors of p38 MAP kinase (the pyridinyl imidazole compounds: PD169316, SB203580, and SB202190) improve survival of rat dopamine neurons in vitro and after transplantation into hemiparkinsonian rats. In embryonic rat ventral mesencephalic cultures, serum withdrawal led to 80% loss of dopamine neurons due to increased apoptosis. Incubation of the cultures with p38 MAP kinase inhibitors at the time of serum withdrawal prevented dopaminergic cell death by inhibiting apoptosis. In the hemiparkinsonian rat, preincubation of ventral mesencephalic tissue with PD169316 prior to transplantation accelerated behavioral recovery and doubled the survival of transplanted dopamine neurons. We conclude that inhibitors of stress-activated protein kinases improve the outcome of cell transplantation by preventing apoptosis of neurons after grafting.
Supported by: NS18639, NIGMS GM07063, M01 RR00069 (C.R.F.), R01 NS386119 (K.A.H. & W.M.Z.) and VA Merit and VA Research Enhancement Award (K.A.H.)